Feedering Method Analysis for 20 MW Offshore Wind Turbine Installation in the U.S.

MSc Thesis

Rick van Wilsem

TU Delft

Thesis for the degree of MSc in Marine Technology in the specialization of Ship Design

Feedering Method Analysis for 20 MW Offshore Wind Turbine Installation in the U.S.

MSc Thesis

by

Rick van Wilsem

Performed at

Temporary Works Design

This thesis (MT.23/24.014.M.) is classified as confidential in accordance with the general conditions for projects performed by the TUDelft

to be defended publicly on Friday December 15, 2023 at 14:00.

Student number:	4696867	
Contact:	Rick van Wilsem	
Project duration:	March 6, 2023 – December 15, 2023	
Graduation committee:	Dr. A.A. Kana,	TU Delft, chairman & supervisor
	Dr. Ir. A.J. Laguna,	TU Delft, committee member
	Dr. Sc. M. Khosravi,	TU Delft, committee member
	Ir. S. van den Munckhof,	TWD, daily supervisor

Cover: Vineyard feedering barge provided by TWD

TUDelft

Preface

This thesis marks the culmination of my Master's in Marine Technology at Delft University of Technology, shedding light on an emerging market within the offshore wind energy sector. The emerging United States (U.S.) offshore wind market is characterized by protective laws and infrastructure gaps that demand complex engineering solutions. The thesis navigates through this market and provides a framework including solutions answering the demand of the U.S. market. This thesis is commissioned by Delft University of Technology in collaboration with Temporary Works Design (TWD) and aims to contribute practical insights to the ever-growing offshore wind sector.

TWD is an engineering company specialized in method engineering and equipment design. TWD's vision is to strive for a level of simplicity that accelerates the creation of a better world. Through this simplicity, TWD aims to increase project safety, reduce project costs and make construction easier. TWD's mission is to make challenging engineering projects a success - from tender to execution.

This thesis would not have been possible without the help and support of several people. First of all, I would like to thank Austin Kana from Delft University of Technology for the supervision and guidance throughout the project. I enjoyed the structured way of working with you and also getting to know you on a personal level. Thanks for your invested time and for elevating my project. Secondly, I would like to thank TWD for offering me a graduation intern position and for the co-creation and collaboration on my thesis topic. In particular, I would like to thank Sven van den Munckhof for the daily supervision. You helped me to visualize the next steps, find the right information, connected me with the right people and gave me your critical opinion. To everyone at TWD, thanks for your invested time, knowledge and for introducing me to the industry.

Finally, I would like to thank my friends, family, roommates and band for the support and necessary non-academic distraction I needed every now and then.

Rick van Wilsem

Rotterdam, 7 December 2023

Executive summary

Due to the Jones Act and limited port facilities in the U.S., challenges associated with the installation of U.S. offshore wind farms emerge. The Jones Act prohibits the use of foreign vessels to transport wind turbine components from U.S. ports to installation sites, necessitating the use of American-built, flagged, and owned installation vessels. This fleet is non-existent at the moment of writing and will remain slim. The U.S. aims to install 30 GW of offshore wind power by 2030, which would require the installation of 2,000 offshore wind turbine generators within the next seven years, assuming a 15 MW nominal turbine capacity. With only one vessel under construction and no additional installation vessels ordered, alternative methods are necessary to achieve the ambitious renewable energy goals. Limited East Coast port facilities add an extra dimension to the problem as these limit installation vessels from accessing the port and picking up Wind Turbine Generator (WTG) components.

A solution to these challenges is to use the feedering method. In this method, the installation vessel remains stationed at the installation site, while the components are transported from the port to the installation site using Jones Act compliant feedering vessels. This approach enables the utilization of foreign installation vessels for the actual installation of the wind turbine generators, bypassing the restrictions imposed by both the Jones Act and the limiting port facilities thereby allowing progress towards the '30 by 30' offshore wind power target in the U.S. This research aims to obtain the characteristics of an optimized Jones Act compliant feedering method for the transportation and installation of 20 MW WTG components. The study takes the Vineyard Offshore Wind Farm (OWF) project as a reference for the operational area and OWF size.

To measure the performance of the feedering method, three Key Performance Indicators (KPI) are identified: contractor's costs, total project duration, and the variability of the total duration across simulations. Project duration is also seen as the main cost driver and comprises both net duration and downtime. For complex operations such as WTG feedering, weather windows influence the operation's downtime. Therefore, a downtime analysis considering weather windows and event sequences is crucial for accurately simulating the total project duration. A Discrete-Event Simulation (DES) is used to simulate the operation and determine the performance of the feedering method.

Five cost drivers are identified. Project duration, vessels costs, equipment costs, Voyage Expenses (VOYEX) and mobilization costs. These can be deduced to twelve influencing factors, with vessel type and number, equipment type and quantity, and installation strategy being changeable through design modifications. The remaining factors are the number of WTGs, distance to the marshaling port, inner array distance, WTG characteristics, mobilization distance, insurance costs and environmental conditions. These are external and determine the operational settings.

This study identifies the lack of characteristics for commercial 20 MW WTG components and obtains these by means of a scaling analysis. These characteristics are important as they influence installation strategies, feeder vessel selection, and equipment requirements. Wind Turbine Installation Vessel (WTIV)s are preferred for WTG installation. Future designs and concepts are anticipated to align with next-generation WTGs and potentially reduce daily vessel costs, VOYEX, improve workability but will not impact the feedering operation itself for this thesis.

This study presents a method that fuses the systems engineering framework with set-based design and DES to capture the effects of design modifications of vessels, equipment and installation strategies on the performance of the feedering method. This methodology is capable of generating insight into the characteristics of an optimized Jones Act compliant feedering method for 20 MW WTG installation.

Equipment is limited to motion compensation platforms and a quick lift Active Heave Compensator (AHC). The motion compensation platform characteristics are identified as a direct result of the installation strategy. The influence of the quick lift AHC on performance is not taken into account and is limited to a sensitivity study on operating limits due to the lack of costs and characteristics of future systems. The design variables are therefore reduced to the general barge dimensions and installation strategy. This study reveals the effect of the design variables on the operating limits for transit and transfer operations, the daily costs, VOYEX and operational characteristics.

A DES shows how the operating limits and operational characteristics translate to operational performance in a specified environment. The simulation shows that it is crucial to remove bottleneck operations and that large improvements regarding operational performance can be attained by increasing the limits for mooring the feeder vessel to the WTIV. The results of the simulation identify an optimized feedering method that will feature a 400 ft barge, similar to the Memphis Bridge barge, where the WTG tower is transported, transferred and installed in a single piece. This configuration is the best-performing configuration for the Vineyard environment within the considered design space.

In conclusion, this study provides valuable insights into the characteristics of an optimized Jones Act compliant feedering method for the transportation and installation of 20 MW WTG components. It can aid in optimizing project duration, costs, and operational efficiency for future OWF developments. The research shows that the framework has a lot of potential to optimize feedering method WTG installations or other sequenced operations and can easily be adapted for different environments. This research is a first step, but more steps are required to further exploit the potential of this method. Future work should include a seafastening and vessel strength assessment to further determine the feasibility and detailed characteristics of the optimized feedering methods. Additional research should also be carried out regarding the performance of the feedering methods for different operational areas. This work should identify an optimized method for each environment and an optimum overall solution. This would help the industry in decision-making regarding new investments and academia by identifying the area in which future research should be conducted.

Glossary

H_s	significant wave height.
AHC	Active Heave Compensator.
BOEM	Bureau of Ocean Energy Management.
CAPEX	Capital Expenditures.
COG	Center of Gravity.
DES	Discrete-Event Simulation.
DNV	Det Norske Veritas.
DP	Dynamic Positioning.
DSM	Design Structure Matrix.
ECN	Energy research Centre of the Netherlands.
GAO	Government Accountability Office.
GE	General Electric.
KPI	Key Performance Indicators.
LCOE	Levelized Cost Of Energy.
LSW	Light Ship Weight.
MDO	Multidisciplinary Design Optimization.
MPM	Most Probable Maximum.
NREL	National Renewable Energy Laboratory.
NYSERDA	New York State Energy Research & Development Authority.
OPEX	Operating Expenditures.
OWF	Offshore Wind Farm.
PFD	Process Flow Diagram.
RAO	Response Amplitude Operator.
RNA	Rotor Nacelle Assembly.
SBD	Set-Based Design.
TWD	Temporary Works Design.
U.S.	United States.
VCG	Vertical Center of Gravity.
VOYEX	Voyage Expenses.
WTG	Wind Turbine Generator.

WTIV	Wind Turbine Installation Vessel.

Contents

1 Introduction

1.1. Problem Background

Together with the planned and first installments of offshore wind farms in the U.S. arise new problems. In a conventional situation, an installation ship will pick up WTG components at the port, sail to the installation site and install the WTG. Due to the Jones Act, difficulties arise in constructing U.S. wind farms with the conventional method. The Jones Act states that;

“A vessel may not provide any part of the transportation of merchandise by water, or by land and water, between points in the United States to which the coastwise laws apply, either directly or via a foreign port, unless the vessel;

1. *is wholly owned by citizens of the United States for purposes of engaging in the coastwise trade; and*
2. *has been issued a certificate of documentation with a coastwise endorsement under chapter 121 or is exempt from documentation but would otherwise be eligible for such a certificate and endorsement” [1]*

This holds, among others, that foreign (not built in the U.S., not sailing under U.S. flag and not owned by U.S. citizens) vessels are not allowed to install foundations and tower components at a U.S.. offshore wind farm if these components are picked up by the vessel from a U.S. port [2]. Installing WTGs with a conventional method therefore requires American built, flagged and owned installation vessels when picking up components from U.S. ports.

American built, flagged and owned installation vessels do not exist at this moment, with the first, and currently only vessel, planned to be delivered at the end of 2024 [3]. Furthermore, Jones Act compliant installation vessels will remain in low quantity due to reasons including uncertainty regarding vessel contracting, high dayrates and low US-shipyard capacity and expertise as indicated by the United States Government Accountability Office (GAO) [4].

By 2030, the U.S. aims to have 30 GW of installed offshore wind power [5]. With a nominal turbine size of 15 MW, this equates to installing 2000 offshore WTGs within the next 7 years. Given a yearly capacity of 60 turbines, meeting this target would require 33 years of vessel capacity [6]. With only one U.S. WTIV scheduled for delivery at the end of 2024 and no other U.S. WTIVs ordered, the U.S. must exploit alternative installation methods to even come close to their ’30 by 30’ goal [7].

A solution to realizing an offshore wind farm in the U.S. is using a feedering method for the installation of the WTGs. For the feedering method, the installation vessel remains at the wind farm and the components are transported by barges or feedering vessels from the port to the wind farm construction site. In a Jones Act situation, these barges or feedering vessels will have to be built in the United States, sail under U.S. flag and have to be owned by U.S. citizens. This way, foreign installation vessels can

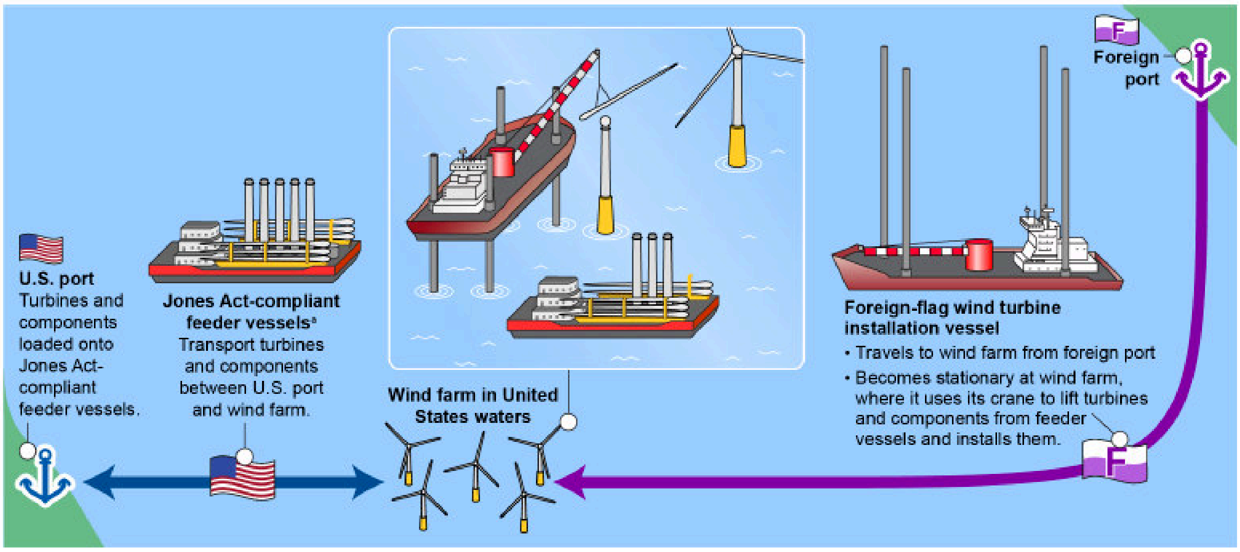

Figure 1.1: Visualization of feedering by GAO [4].

be used to carry out the WTG installation. Figure 1.1 visualizes this method.

1.1.1. Offshore WTG installation

Offshore Wind projects generally consist of five main phases: planning and production, production and acquisition, installation and commissioning, operation and maintenance, and decommissioning and re-powering. Each of these phases requires specific vessels. For this research, only the construction phase will be discussed. The construction phase of a WTG can again be divided into separate phases, each requiring its own set of vessels. The main phases are: foundation installation, cable laying and superstructure installation [8]. Figure 1.2 shows the division of a WTG into its parts. The foundation installation phase ends with the placement of the transition piece. From this point, the superstructure can be installed, which is considered as all WTG components above the transition piece. This research only focuses on the installation and transportation, from the base port to the installation site, of super-structure WTG components.

Accomplishing superstructure installation for current WTGs requires vessels capable of mechanically lifting components of over 800 tons at 150 m meters above the water surface while mitigating the effects of a dynamic sea state. Adding to that, the vessel and crane must also be capable of completing the delicate process of blade installation. In order to achieve this stability, Jack-up vessels are used for the superstructure installation. These jack-up vessels are often referred to as WTIV. By jacking up, the vessel raises the hull above the water, resulting in a bottom fixed structure that is above the waves and able to handle weather and sea state changes more effective while performing heavy lift operations. By becoming a static bottom fixed structure, the jack-up vessel avoids the heeling moment, ballast management and dynamic first order responses to wave loads associated with conventional heavy lift operations while still providing high hoisting capabilities [10]. This research will therefore only focus on superstructure installation conducted by Jack-up vessels.

The Levelized Cost Of Energy (LCOE) is a measure of the average net present cost of electricity generation for a generator over its lifetime. LCOE is used for investment planning and comparing different methods of generation on a consistent basis. For a U.S. offshore wind farm, the LCOE is currently high, ranging from 77 \$/MWh for 8.0 MW WTGs [11] and 89\$/MWh for 5,5 MW WTGs [10]. However, these costs are estimated to drop between \$53 and \$70 per MWh by 2032 for bottom fixed offshore WTGs. For reference, the U.S. National Renewable Energy Laboratory (NREL) estimates the LCOE of onshore wind as 34\$/MWh [11] and the LCOE of a combined cycle gas-turbine is estimated as 42 \$/MWh by the U.S. Energy Information Administration (EIA) [10]. The installation phase makes up 28,5

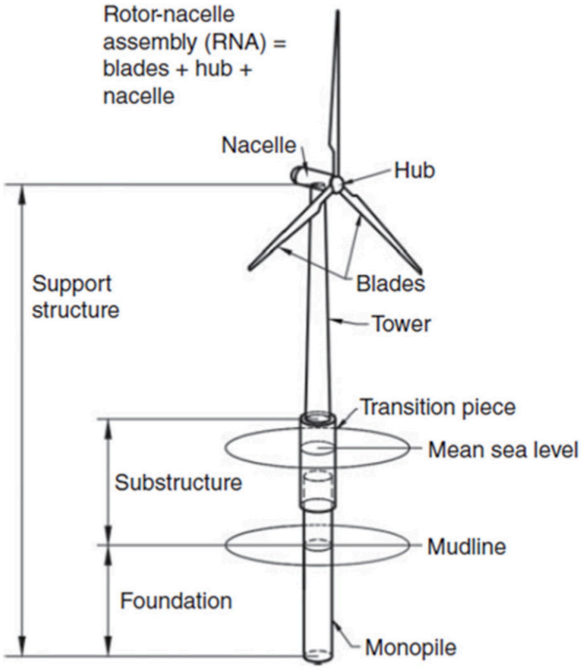

Figure 1.2: Components of an offshore WTG [9].

% of the LCOE of an offshore wind farm. From this part, 6,9 % can be assigned to superstructure installation. Translated to the capital cost of an offshore wind farm, Superstructure installation makes for 10,4 % of the Capital Expenditures (CAPEX). This LCOE and CAPEX division is displayed in figures 1.3 and 1.4 respectively.

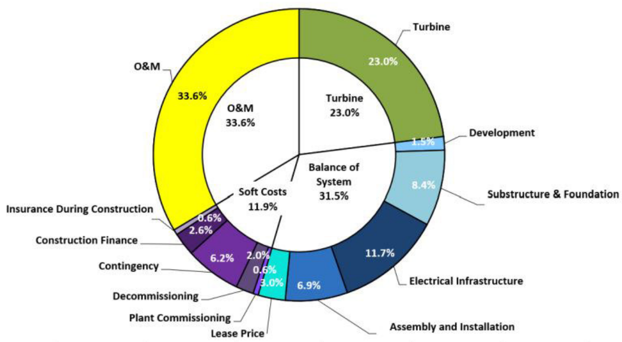

Figure 1.3: OWF LCOE division.

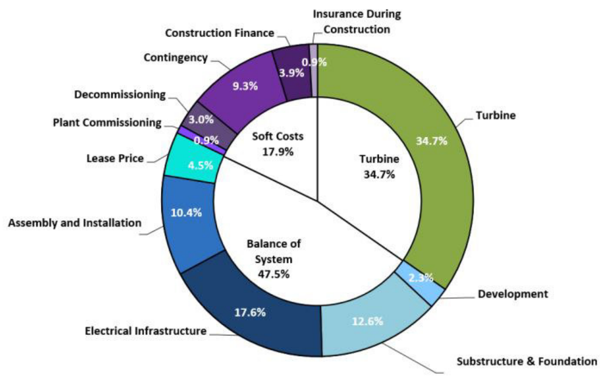

Figure 1.4: OWF CAPEX division.

Assuming that the turbine, substructure & foundation and electrical infrastructure leave limited room for improvement by project management, the next substantial cost category, aside from operation & maintenance, is assembly & installation. This component can be improved by optimizing the supply chain performance [12]. Adding to that, any risk-reducing improvements during transportation and installation will also positively affect the project contingency. More predictable performance will limit the required headroom for overruns, further lowering LCOE and CAPEX.

1.1.2. U.S. market

The East Coast has bathymetry favorable for traditional foundation installation methods used in the European Wind Market. Combined with planning advancing at the state and federal level, the east coast is poised for significant offshore growth in the next decade [10]. This growth is underlined by the expansion of wind energy projects of the coasts of New York, Rhode island and Massachussets and the 30 lease areas indicated by the Bureau of Ocean Energy Management (BOEM), indicating a high level of interest on this coast [13].

As indicated earlier, due to the limited availability of Jones Act compliant WTIVs, alternative installation methods must be used to construct the planned wind farms in the U.S. However, not only the Jones Act forces contractors to use alternative installation methods. Due to limited port facilities, which are further elaborated in section 1.1.3.1, next-generation WTIVs cannot access the majority of east-coast ports due to draft or breadth restrictions [14]. This forces contractors to use a feedering strategy due to the lower draft and breadth of feedering vessels.

Vineyard OWF, located southeast off the coast of Martha's Vineyard and Nantucket Massachussets, will be the first commercial U.S. offshore wind farm and is constructed using a feedering strategy conducted with feeder barges. Throughout this research, the Vineyard OWF project is used to serve as a baseline for the installation methodology and operational area.

The development of a U.S. OWF includes a multitude of stakeholders. These can, depending on their influence, play a significant role in the development and decisions made for the project. Understanding the stakeholders helps to understand the market situation and the desired characteristics of an optimized feedering method. Appendix B introduces and maps the stakeholders.

1.1.3. Operational area

This study is limited to the future wind farms located near Martha's Vineyard. Figure 1.5 maps these future wind farms. Lease area 9 represents the Vineyard site. This section covers the operational area in which the 20 MW WTGs are to be installed, thus the lease areas surrounding area 9. First, the potential marshaling ports are discussed after which the environmental conditions are highlighted.

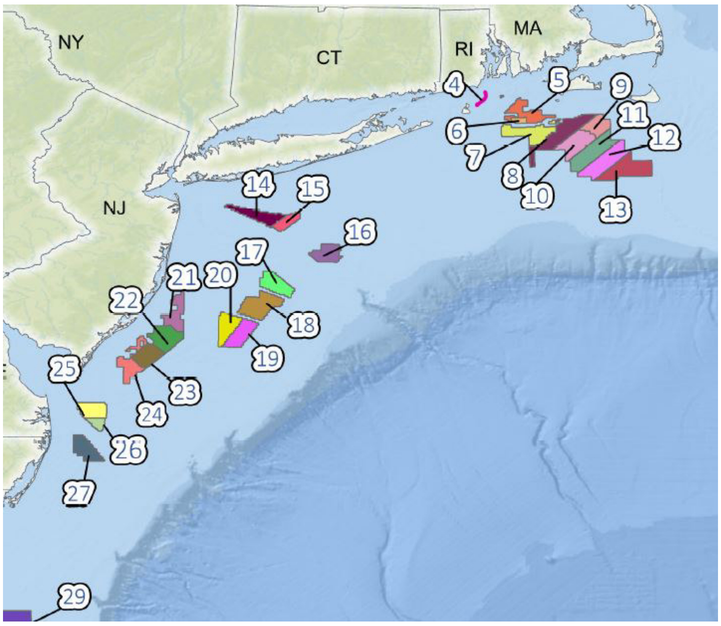

Figure 1.5: Wind energy lease areas as indicated by BOEM [13].

1.1.3.1. Ports

The United States Government Accountability Office (GOA) and NREL state that the ports and their infrastructure are a core part of the logistical problem for installing WTGs in the United States [4] [14]. The number of ideal offshore wind ports on the east coast is limited. Even dedicated offshore wind ports cannot provide access to next generation WTIVs due to draft limitations. For WTIVs, a minimal channel and berth depth of 12 m is considered adequate by NREL. Ports could increase the access draft, but are unlikely to do so as dredging and port upgrades are expensive and require additional permitting processes. This forces some states to use the feedering method, even if Jones Act compliant WTIVs exist and are available. Feeder vessels or barges are less limited by their draft, but height or breadth limitations could play an important factor in the trade-offs that have to be made for developing an optimal feedering method.

NREL identified several potential marshalling ports in the U.S. and reported their current and planned facilities and their deficits. For the Vineyard area, four potential marshalling ports are identified. Figure 1.6 maps these ports. The numbers represent the respective ports and the pin represents the Vineyard site. The characteristics and limiting factors of these ports are listed in table 1.1. The breadth limit of the New Bedford Marine commerce terminal is 24,4 m for vessels equipped with a bow thruster according to Massachussets clean energy center [15]. However, the Marmac 400 Barge as used for the installation of Vineyard OWF has a breadth of 30,5 m [16]. Therefore the 30,5 m breadth of the Marmac 400 Barge is used as the breadth limit. This breadth limit could be critical, as contractors are forced to move to a further port in case their feeder vessels exceed the limit.

Table 1.1: Potential marshalling port characteristics [14].

Port	Unit	New Bedford	Brayton Point	Port of Providence	New London State Pier
State	-	MA	MA	RI	CT
Identifier	-	1	2	3	4
Quayside length	m	366	210	1280	1244
Berth depth	m	9,1	10,5	11,5	12,2
Channel depth	m	9,1	10,16	10,67	10
max breadth	m	30,5	32,61	-	-
Air draft limit	m	-	41,2	62,8	-
Bearing capacity	t/m^2	20	9,8	N.A.	>15
Distance	nm	53	69,1	73,2	77,8

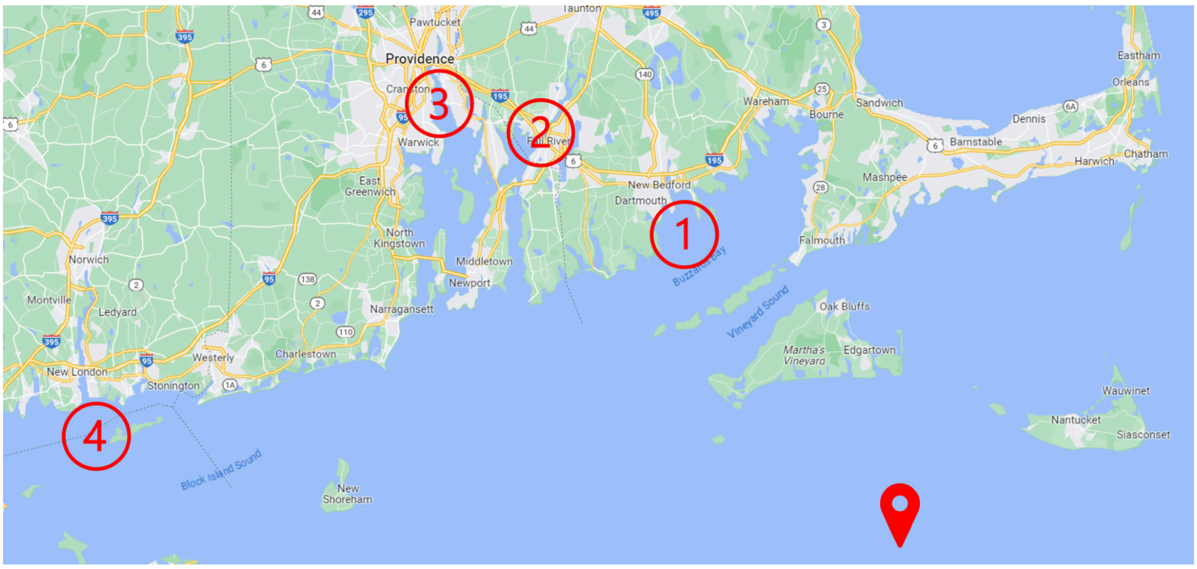

Figure 1.6: Potential marshalling ports.

1.1.3.2. Environment

Wind and waves are environmental factors that influence an offshore operation. The year-round scatter plot provides data regarding the occurrences of waves and can be found in appendix A. The scatter plot holds 40 years of data collected from the Vineyard area. The year-round average significant wave height (H_s) is 1,5 m with the summer average being 1,3 m H_s and a winter average of 1,7 m H_s [17]. This can also be observed in figure 1.9. The figure also shows the maximum H_s and that the extreme values are realized in March and September with the winter maxima being significantly higher than the summer maxima.

Figure 1.7 shows the cumulative, scatter plot based, occurrence of waves and figure 1.8 presents the wave period occurrence at the Vineyard site. From the latter, it can be concluded that 80% of the peak periods occur in the range between 4 and 9 seconds. Vessels with similar natural roll periods can experience significant losses in terms of operational performance when their natural roll periods coincide with these periods.

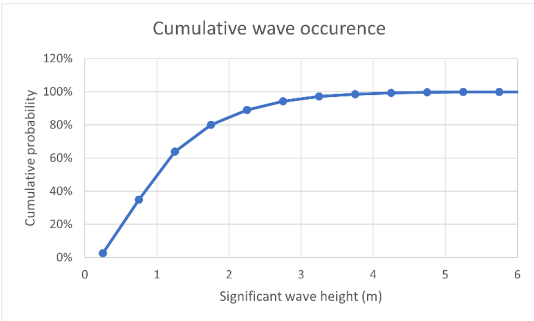

Figure 1.7: Cumulative wave occurrence.

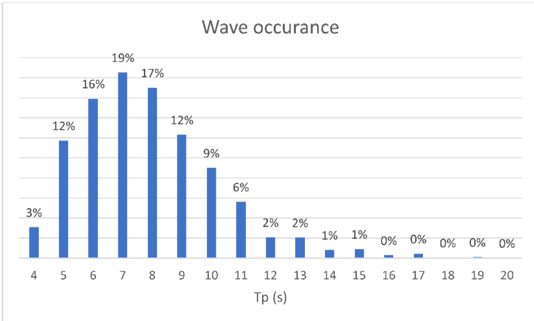

Figure 1.8: Wave period occurrence.

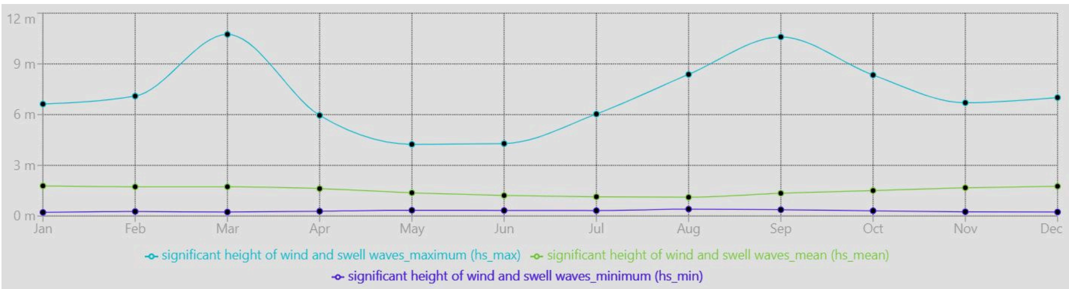

Figure 1.9: Year-round wave variation [17].

Figure 1.10 shows the year-round wind variation at the Vineyard site. It can be observed that the average wind speed is 8 m/s with the maximum wind speed attaining 30 m/s. Strong wind speeds are generally coupled with high waves resulting in situations with unworkable conditions. The limiting environmental conditions are further discussed in section 2.2.

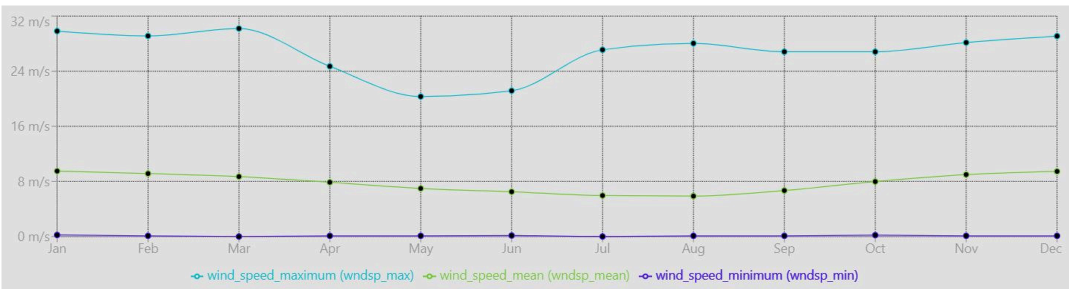

Figure 1.10: Year-round wind variation [17].

1.2. Problem definition

Due to the upcoming of U.S. wind farm projects, the presence of the Jones Act and limited east coast port facilities, the feedering method will be used more often in the future. It is therefore valuable to gain a better understanding of the feedering method and learn how to successfully apply this installation method for future generation wind farm projects. This research will therefore investigate how to successfully apply the feedering method for the installation of 20 MW wind turbine generators in the U.S.

However, little research on the feedering method is available and it is not yet commonly practiced by the industry. In fact, Vineyard Offshore Wind farm, where the start of superstructure installation commenced on September 6th of 2023, is the first commercial-scale U.S. offshore wind project and the first project where all superstructure components are transported and installed with the feedering method. The executed research and industry practices available are further discussed in sections 2.1 and 2.2.

No research has yet been performed on the feedering method for 20 MW WTGs. Adding to that, the effects of vessel characteristics, equipment characteristics and installation methods on the operational performance of the feedering installation method are still unknown. It is crucial to gain insight into these parameters and their effect on operational performance to allow for effective construction of next-generation offshore wind farms. The goal of this research is therefore to obtain an understanding of the Jones Act compliant feedering installation method for future 20 MW WTGs and to optimize the feedering method for this future operation. This allows a contractor to successfully execute feedering method installations in order to realize future offshore wind farms.

1.3. Research questions

In order to obtain the main objective, the following research question is proposed:
'What are the characteristics of an optimized Jones Act compliant feedering method for the installation of future 20MW offshore wind turbine generators?'

To systematically answer this main research question, multiple sub-questions are posed which serve as building blocks. Combined, they provide the answer to the main research question.

- *What are the steps in the U.S. WTG installation process from load-out to installed WTG and related duration, workability and costs, as performed for Vineyard Offshore Wind Farm with a traditional Jack-up vessel and barge?* Sections 2.1, 2.2, 2.3 and 2.4.
- *Which method can be used to measure the performance of a feedering method?* Sections 2.5 and 2.6
- *What are the characteristics of future WTGs and installation vessels?* Chapter 3 and 5
- *Which method can be used to design an optimized feedering method?* Chapter 4
- *What is the effect of vessel characteristics on operability and vessel costs?* Chapter 6
- *What is the effect of equipment characteristics on operability and equipment costs?* Chapter 6
- *What is the effect of the installation method on operability, required vessels and required equipment?* Chapter 6
- *How do the combined operability and required weather windows translate to operational performance?* Chapter 7

This report answers the posed main- and subquestion in order. The thesis is split into three parts. The first part consists of chapters 2, 3 and 4. This part considers the problem analysis and presents the framework to answer the main question. The second part consists of chapters 5, 6 and 7. This part considers the method and describes the elements of the framework in detail. The final part consists of chapters 8 and 9. This part first presents the results of the method. The results are discussed and conclusions are drawn accordingly answering the main question.

2
Feedering

This chapter presents the feedering method as a strategy to transport and install the superstructure of offshore WTGs and elaborates on the specific feedering strategy as used for Vineyard OWF and the costs involved. This chapter further discusses which factors influence the performance of the feedering method, how performance can be measured, and how the performance of the operation can be modeled.

2.1. Feedering method

Feedering is an alternative installation and transportation method for the erection of WTGs. In contrast to the conventional 'shuttling' method where a WTIV transports WTG components from the base port to the installation site itself, transportation is executed by feeder vessels for feedering installation methods. The following feedering concepts are described in the literature: the base-port feeder method [18], the offshore feeder-ship method [19], the practical feeder-ship method [20] and the hybrid feeder method [21]. This thesis focuses on the practical feeder-ship method which is the only feedering method practiced by industry to date. This section describes the practical feeder-ship method and different vessels and installation strategies that can be used to execute the operation. Appendix C describes the remaining methods and their advantages.

2.1.1. Practical feeder-ship method

Smorenberg and Maloney et al. describe the practical feeder-ship method [21] [20]. This is also the considered method by TWD. The method focuses on feedering between the marshaling port and the installation site and WTG installation. The WTG components are stored at the marshaling port, where a feeder vessel picks them up and sequentially transports them to the installation site where an installation vessel is jacked up and ready to receive the set of WTG components. There the WTG components are transferred or directly installed. The feeder vessel sails back to the marshaling port when it is fully unloaded to pick up the next set of WTG components. At the same time the installation vessel constructs the WTG. This method is visualized in figure 2.1. The transportation processes from production sites to the marshaling port are not taken into account. The WTIV does not transport any WTG components and waiting time can be eliminated by using multiple feeder vessels. This makes it suitable for a Jones Act regulated market and allows for an efficient WTIV. However, this method does require an offshore component transfer lift which contains high risks as pointed out by Haselsteiner [22]. Such a lift can only be performed in the right conditions, potentially causing delays for the entire project. This can be counterbalanced by using specialized lifting or motion compensation tools which can increase the range in which a lift can be executed and thus decrease the chance for potential delays.

2.1.2. Feedering vessels

Different vessel types can be used to execute the transport between the base port and the installation site. First of all the feeder vessels can be divided into whole and partial feeders. A whole feeder is defined as a vessel that transports at least all components for one complete WTG. A partial feeder is

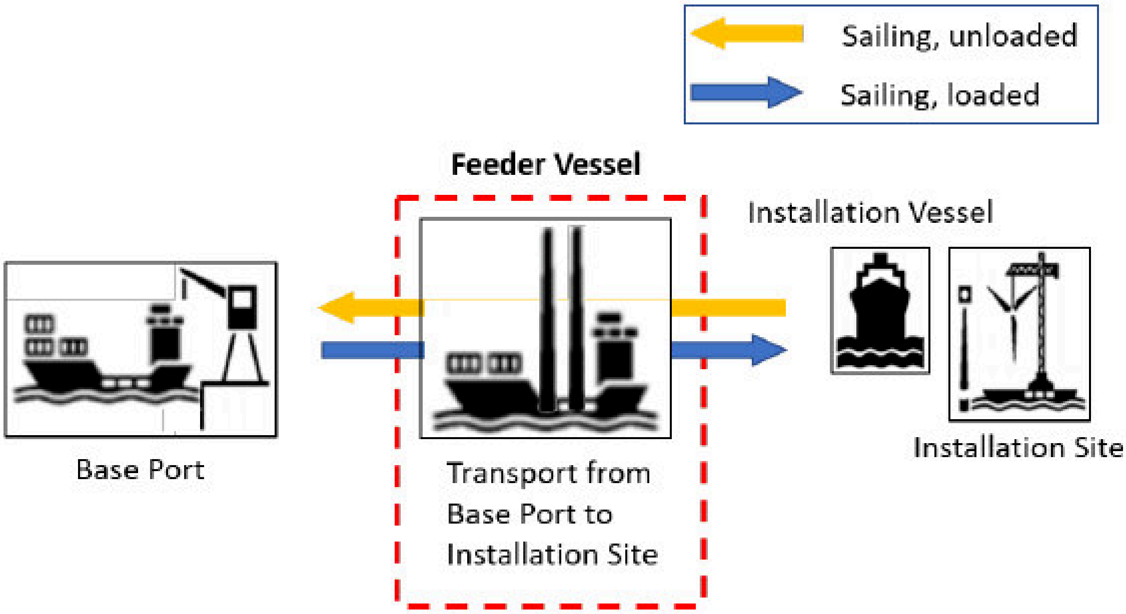

Figure 2.1: Practical feeder-ship method visualized by Smorenberg [21].

generally smaller and defined as a vessel of which multiple are required to deliver the components of one WTG[20].

Transport can take place by means of barges, jack-up barges / liftboats or dynamically positioned feeder vessels. Barges are non-self-propelled and require towing to the installation site. Once at the installation site, they can moor to the installation vessel. Barges could also be equipped with a Dynamic Positioning system, taking away the need for mooring to the installation vessel. Due to the motions a barge will experience, barges are now equipped with motion compensation equipment to allow for a safe and less risky offshore transfer [22]. Liftboats or jack-up barges are vessels that eliminate vessel movement by jacking up and elevating above the water, reducing the risk of an offshore component transfer. Liftboats differentiate themselves from jack-up barges by the fact that they are self-propelled whereas jack-up barges need to be towed to the installation site. Liftboats were also the feeder-vessel of choice for the Block Island pilot wind farm in the U.S.[20]. Although eliminating limitations due to waves during component transfer, the jack-up barge or liftboat still faces environmental limits during the jack-up process. The Dynamic Positioning (DP) feeder vessel is a self-propelled vessel equipped with a dynamic positioning system. This vessel will remain in its geographical position during component transfer by using its thrusters. Just like the barge, the DP vessel needs motion compensation equipment to allow for a safe component transfer. Advantages of the DP vessel over the barge are potentially better seakeeping characteristics, and faster and more efficient transportation of components between the base port and the installation site [21]. Figure 2.2 shows the three types of introduced feeder vessels.

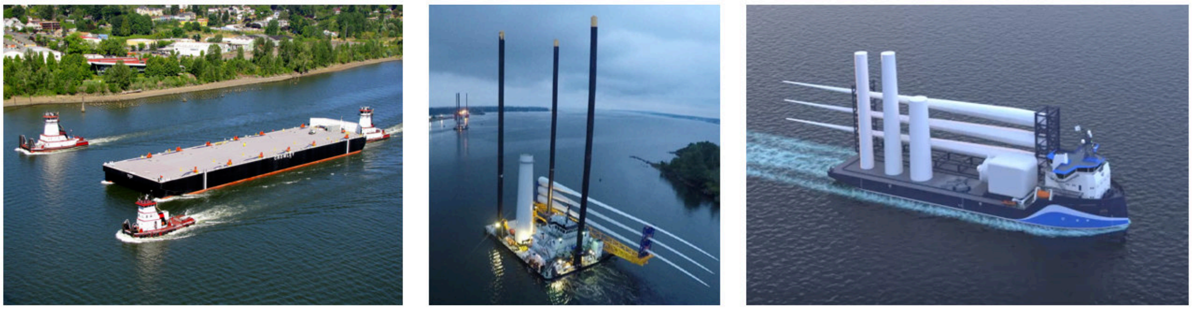

Figure 2.2: (1). A barge by Crowley [23], (2). Liftboat Caitlin loaded with WTG components [20], (3). DP vessel wind feeder concept by C-JOB [24].

2.1.3. Installation methods

Multiple installation strategies can be used to install the WTGs from the feeder vessel. The strategies differ in the number of lifts they require. Figure 2.3 summarizes and visualizes the different strategies as described by Ahn et Al. The amount of lifts is directly related to the installation time, with fewer lifts resulting in less installation time. However, performing fewer lifts means that components have to be pre-assembled onshore and that the lifts performed offshore require heavier equipment and are more susceptible to weather conditions [25].

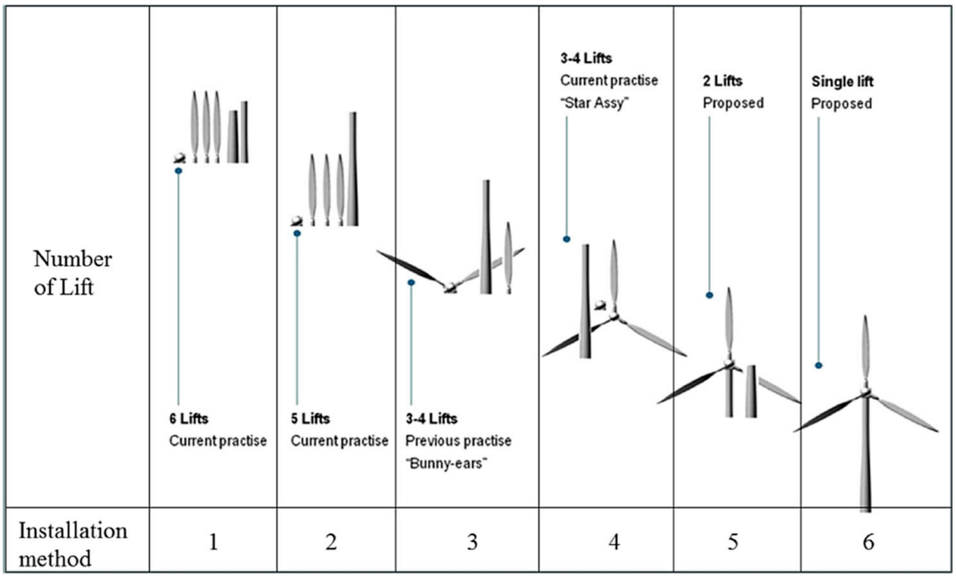

Figure 2.3: Diagrammatic representation of installation strategies [25].

For feedering, every installation strategy can be executed in a direct and indirect way. For indirect installation, the WTIV first transfers all components from the feeder vessel to the WTIV. After loading the components on the WTIV, the feeder vessel leaves and the WTIV installs the WTG. For the direct approach, the components are directly installed from the feeder vessel. A direct installation method leads to a faster installation process due to fewer lifts and fewer changes of lifting tools. The feeder vessel being longer offshore which would require a larger weather window is a downside here. Additionally, the cycle time of a feeder vessel will also be longer. This might require additional feeders for the method to remain operationally efficient and avoid waiting times for the WTIV. Combinations of direct and indirect installation are possible as well. For example, to reduce the cycle time and weather window of the feeder vessel for a direct installation method, it would be beneficial to transfer the complete blade rack to the installation vessel, instead of installing them one by one from the feeder vessel. In this way, the blades are installed indirectly and the feeder vessel can depart from the installation site sooner. The installation strategy as performed for Vineyard is based on the indirect approach of installation method one. The WTG is thus installed in 6 components, where each component is first transferred to the installation vessel. Section 2.2 discusses the feedering installation method as performed for Vineyard in more detail.

2.2. Operation sequence

The complete operation is considered as all the steps necessary to transport all WTGs from the base port to the installation site and all the steps to install the WTGs. The operation sequence can be divided into different phases depending on the level of detail provided. For Vineyard OWF, 12 phases are defined. The phases are listed in table 2.1 and further elaborated in the associated subsections. Each phase has its unique duration and operating limits for which it can proceed. The table shows a range for both the duration and operating limits found in the literature. For a realistic view, it is critical to get these parameters right. Moreover, the maximum allowable seastates are only provided in terms of H_s. In reality, the peak period is a critical factor for operating limits. This limit should be taken into account when assessing the operation. The wind speeds stated in the table are measured at 10 meters above mean sea level. Figure 2.4 shows a graphical representation of the location where each phase is executed. This section provides an overview of the operations and what is known regarding their associated limits and duration according to the literature. Appendix M provides the operational characteristics for the base case simulated operations of this research.

Table 2.1: Operation phases.

Phase number	Phase name	Duration [h]	Maximum seastate [H_s]	Maximum wind speed [m/s]
1	Port transfer	12	-	10 - 18
2	Leaving port	-	2,5	15 - 21
3	Barrier transit	-	2,5	15 - 21
4	Loaded Offshore transit	9,65	2,5	15 - 21
5	Offshore approach	0,67 - 3	1,5 - 2,1	20 - 25
6	Offshore transfer	6-12	1,5 - 2,5	12
7	Offshore departure	0,67 - 1	1,5 - 2,1	20 - 25
8	Unloaded offshore transit	9,65	2-3	15 - 21
9	Barrier arrival	-	2-3	15 - 21
10	Port arrival	-	2-3	15 - 21
11	WTG installation	12 - 28	2,0 - 2,5	8 - 12
12	WTIV relocation	5	1,8 - 3,5	14

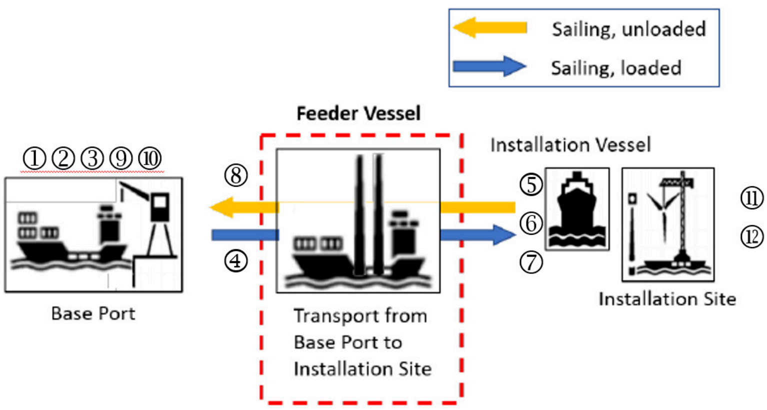

Figure 2.4: Visualization of feedering method including steps.

2.2.1. Port transfer

During the port transfer phase, interface equipment required to transport the WTG components is first unloaded from the feeder vessel. Following the unloading, WTG components, together with their necessary interface components, are loaded onto the feeder vessel. Interface components are defined as components necessary to seafast the WTG components to the seafastening. The only vessel required to complete this operation is the feeder vessel, assuming that a crane is present at the port. This operation takes place in a sheltered port. Therefore, the only limit for this operation is wind speed as it is assumed that there are no waves in port. The wind speed limit used in the literature varies between 10 and 14 m/s depending on the study and the lifted components. The operation as presented by TWD has its windlimit at 16 m/s and takes 12 hours to complete.

2.2.2. Leaving port

In this phase, the feeder vessel leaves the port. In order to leave the port, it will be assisted by a shallow draft tug. In case of using a non-self-propelled barge as is planned for vineyard OWF, a main tug will also attach to the barge in order to leave the port and carry out the rest of the transit operations. For this operation, no weather criteria are given. Therefore the same criteria as for transfer are used. For a barge assisted by tugs, this limit is 2,5 m (H_s) and 15 m/s wind for the Vineyard OWF project.

2.2.3. Barrier transit

The barrier transit is defined as the transit between the port exit and the hurricane barrier. In this phase, the shallow draft tug is replaced by an offshore tug. Depending on the port location, operations will or will not feature an actual transit phase between the port exit and the hurricane barrier. In that case, this phase is only characterized by changing the shallow draft tug for an offshore tug. This operation also features the same limits as the offshore transfer.

2.2.4. Offshore transit

In the offshore transit phase, the loaded feeder sails to the installation site boundary. Different limits for this operation are used throughout the literature, ranging from 2 to 3 m H_s and wind limits ranging from 15 m/s to 21 m/s [18] [21] [19] [26]. The operation carried out for vineyard OWF adheres to a limit of 2.5 m H_s and 15 m/s windspeed. Seafastening and motion-compensating equipment are designed according to this limit. Minimizing accelerations by implementing a different vessel design could increase the design limits. These given limits are the design limits, which are higher than the actual operational limits. Operational limits are acquired by multiplying the design limit with an alpha factor that is determined according to the standards of DNV-GL, and dependent on the type of operation, duration and the presence of weather monitoring [27].

The duration of this operation depends on the vessel speed and sailed distance. For Vineyard OWF the 53 nm transit is performed at 5,5 kts resulting in a 9.65 hour transit duration. During transit, the barge is towed by its main tug and an offshore tug.

2.2.5. Offshore approach

In the offshore approach phase, the vessel sails from the installation site boundary to the exact installation location. 100 Meters before arriving at the foundation, the mooring operation is started. The exact mooring operation is not yet defined, but it should be executed with great care. If the barge or one of the tugs hits the legs of the WTIV, the consequences could be disastrous. Crowley performed a mooring simulation study and concluded that the operating limit is 1,5 m H_s, which is in accordance with the estimation by TWDs engineers, with room at captain's discretion to 2,1 m H_s and a wind limit between 20 and 25 m/s depending on the orientation of the barge [28]. This operation is modeled to take 40 minutes, however engineers from TWD state that it is expected to take around 3 hours before the vessel is securely moored. The vessel can stay moored up to waves between 2 and 3 meters H_s depending on the vessel's orientation [29]. For the approach phase, the WTIV should already be in place and jacked up to the loading airgap. The WTIV is jacked up to the loading airgap and not the installation height to limit the load on the legs. The barge will be positioned by the main and offshore tug.

2.2.6. Offshore transfer

In the offshore transfer phase, the WTG components including interface equipment are lifted from the feeder vessel onto the WTIV. After this, interface components that were positioned on the WTIV vessel from the previous WTG installation will be backloaded on the feeder vessel. Motion compensation platforms that support the tower sections and the quick lift AHC are crucial pieces of equipment for this phase. These pieces of equipment allow contractors to successfully execute the transfer lifts.

Both duration and operating limits vary in the literature depending on the study and the lifted components. The literature study found durations between 6 and 12 hours with maximum H_s ranging from 1,5 to 2,5 m and wind speed limits between 12 and 14 m/s [19] [18] [30]. The total estimated duration by TWD is 10 hours with maximum H_s between 1,5 and 2,5 meters depending on both the component type and wave direction and wind speed limits of 14 m/s for the tower and nacelle and 12 m/s for the blade rack.

2.2.7. Offshore departure

In the offshore departure phase, the backloaded feeder vessel departs from the WTIV and starts its transit back to the base port. For this phase, the same vessels and limits shall be used as in the offshore approach phase as the risk of hitting the legs of the WTIV still exists.

2.2.8. Unloaded offshore transit

In the unloaded offshore transit phase, the feeder vessel sails back to the base port. The duration is based on the transit distance as well as on the vessel speed. Since the vessel is loaded differently than in the offshore transit phase, it could be beneficial to sail at a different vessel speed. The fact that the vessel is unloaded also provides the opportunity to use different operational limits. This could improve the overarching weather window.

2.2.9. Barrier arrival

This phase is the opposite of the barrier transit phase, which is described in section 2.2.3. During this phase, the offshore tug will be replaced by a shallow draft tug. The main tug will stay attached to the barge. Since the vessel is still unloaded, different operational limits could be used than those for the barrier transit.

2.2.10. Port arrival

This phase is opposite to the 'leaving port' phase. A shallow draft tug will assist the feeder vessel during arrival. In the case of a non-self-propelled barge, the main tug will stay attached to the barge. No limits are defined for this stage, but the same limits can be used as the ones used for the unloaded offshore transit and barrier arrival phases.

2.2.11. WTG installation

This phase covers the installation of all the WTG components and takes place parallel to the phases where the feeder vessels are in transit or being loaded at the port. First, the WTIV jacks up from the loading airgap to installation height. The WTG components are then installed in order of lower tower segment, upper tower segment, nacelle assembly and finally the blades.

Duration of WTG installation varies across literature with Ait alla et al. [18] and Rippel et al. [31]. describing an installation time of 14 and 15 hours respectively, the whitepaper of the barge feeder alliance describing 20 hours of installation time [30], and Jalili, Maheri and Ivanovic describing a total installation time of 28 hours [32]. The expected duration by TWD is 22 hours[33].

Wave limits for WTG tower installation regarding significant wave height are congruent, with a limiting height of 2,5 m H_s [18] [31] [32]. Although the installation vessel is jacked up, thereby eliminating vessel movements, limits regarding wave height are still in place. The WTG is excited by waves, causing movements across the whole structure and implying difficulties in the installation process [34]. Blade-hub matching is the most critical operation in conventional WTG installation [35]. The H_s limits for nacelle and blade installation handled by TWD are 2,0 m H_s which contractors prescribe. Wind speed limits vary between 8 and 12 m/s where blades are commonly seen in literature as the most wind-limited lift. The wind limit handled by TWD is 12 m/s for all components.

2.2.12. WTIV relocation

In this phase, the WTIV moves itself to the next foundation where a WTG will be installed. The vessel first jacks down from installation height. The vessel then sails to the next WTG foundation and positions itself to jack up. The vessel will jack-up to the loading airgap. The duration of this operation mainly depends on the water depth and the vessel's jack-up speed. The limiting H_s is 1.8 m for jacking up/down and 2 m for positioning of the vessel according to Rippel et al. [31] and 2,0 m and 3,5 m respectively according to Ait Alla et al. [18]. TWD handles limits of 2,5 m H_s for jacking and relocation. In literature, the duration for jacking up/down and repositioning is 2 and 1 hour respectively. The durations as handled by TWD are 3 hours for jacking up, 1 hour for jacking down and 1 hour for relocation. The complete WTIV relocation phase should take place after the WTG installation phase has been completed, and before the offshore approach phase starts [31].

2.2.13. Parallel and Synchronized processes

The installation sequence as described above is visualized for the installation vessel as well as the feeder vessel in a Process Flow Diagram (PFD). Figure 2.5 shows the simplified feeder vessel PFD and figure 2.6 shows the simplified installation vessel PFD. The processes highlighted in light blue denote the processes that need to be synchronized between the feeder vessel and the WTIV. In order to visualize and provide insight into parallel processes, a possible operation sequence of both the feeder vessel and the WTIV is scheduled on a time horizon in appendix D. In the Gantt chart, the critical path can be identified. In this example, the critical path consists of all operations where the WTIV is involved. In such a case it is only beneficial to improve these operations in terms of duration to obtain a shorter project duration. Decreasing, for instance, the loading time of the feeder vessel in port will only increase the waiting time of the feeder vessel and not benefit the total duration.

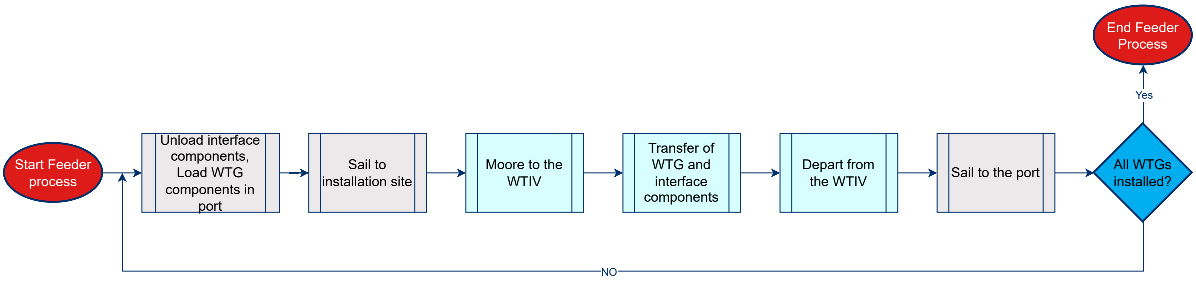

Figure 2.5: Simplified feeder vessel PFD.

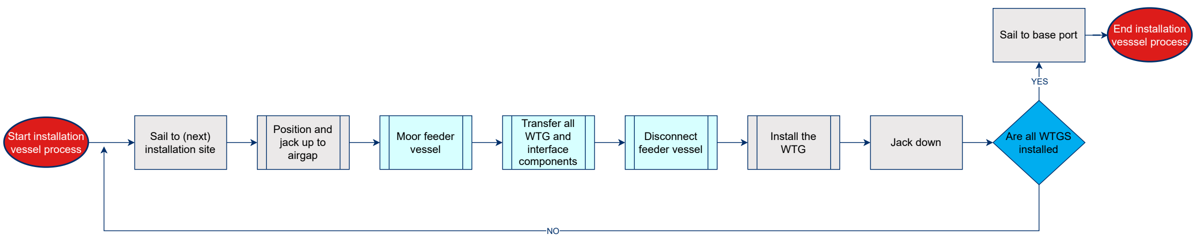

Figure 2.6: Simplified WTIV PFD.

2.2.14. Critical operations

Operations with the most stringent operational limits create bottlenecks in the transport and installation process. Smorenberg [21], New York State Energy Research & Development Authority (NYSERDA) [6] and Barge Feeder Alliance [30] conclude that lifting the blade rack and backloading are the most critical operations. These did not include the phase where the feeder vessel moors to the WTIV which had the same minimal limit as the blade rack lift. This concludes that the limits of the approach phase, departure phase and the blade rack lift must be improved in order to remove the bottlenecks from the operation and increase performance.

2.3. Costs of feedering method WTG installation

There is no standardized way to divide the costs involved in WTG installation [36] [37]. Costs between contractors and developers are divided by means of contract agreements and differ per contract. Also, the way contractors divide and deal with costs internally differs per contractor [37]. Therefore, the costs are first presented for a contractor since this party bears the costs directly. Following, the relationship regarding costs between a contractor and a developer will be explained. Conclusively, the costs are divided on a high level to help identify the main cost drivers.

2.3.1. A contractors perspective

As indicated by Stopford [36], there are multiple methods used in the industry to define costs. For a contractor, the cost to complete an operation consists of the following elements: costs of vessels, costs of tools, voyage expenses (VOYEX) and (de)mobilization costs. Formula 2.1 shows these costs and their dependencies.

$$C_{\text{contractor}} = C_{\text{vessel}}(t) + C_{\text{tool}}(t) + C_{\text{VOYEX}} + C_{\text{mobilisation}} \tag{2.1}$$

Where:
t = Project duration
A = Vessel activity

2.3.1.1. Vessel costs

The vessel costs consist of capital vessel costs (Vessel CAPEX) and operational expenditures Operating Expenditures (OPEX) of a vessel (Vessel OPEX). The combination of these two determines the daily costs for a contractor to operate a vessel. Vessel CAPEX is spread over a whole year and represents the costs made by the contractor for the recoupment of an investment used to acquire a vessel. These costs consist of depreciation and interest [38].

Vessel OPEX represents costs that run all year and are required to keep a vessel operating. OPEX is defined as the costs that a company incurs while performing its normal operational activities. Operational activities are those tasks that must be undertaken from day to day to operate the business and generate revenue [39]. Vessel OPEX consists of personnel costs, maintenance and repair costs, insurance costs and administrative costs. Equation 2.2 represents the vessel costs for a project where t is the project duration in days.

$$C_{\text{vessel}}(t) = \frac{\text{Vessel CAPEX}}{365} * t + \frac{\text{Vessel OPEX}}{365} * t \tag{2.2}$$

2.3.1.2. Tool costs

The second type of costs a contractor encounters are the costs for tools and equipment. Depending on the tool used and the contractor's investment or financial strategy, these costs can be differently categorized. A contractor can decide to buy or lease tools. In case a contractor buys a certain lifting tool, the contractor envisions using the tool for multiple projects. Therefore, it becomes an investment and part of the value of the tool is categorized as CAPEX. Generally 50% of the value of the tool is directly assigned to the actual project. The other 50% will be amortized over the tool's lifetime and thus included in CAPEX for other projects. Another option for a contractor is to lease equipment or tools. In this case, all costs are categorized as OPEX and only assigned to the project for which it is used. The costs are dependent on the time for which the tool is leased and its daily costs. Since this thesis focuses on single projects, tool costs are modeled as if they are leased.

2.3.1.3. VOYEX

VOYEX are the variable costs incurred in undertaking a particular operation. They consist of fuel costs, port dues and tug and pilotage costs. Tug and pilotage costs are the costs of tugs or pilots required to maneuver the feeder vessel in the base port. Unlike the tool and vessel costs, they are not directly related to the project duration. Fuel costs are related to the activity of the vessels whereas port dues and pilotage costs are only related to the time of port operations. Equation 2.3 shows the formula for VOYEX. Smorenberg modeled VOYEX costs as only 3 % of total contractor costs.

$$C_{\text{VOYEX}} = C_{\text{fuel}} + C_{\text{port}} + C_{\text{tugs+pilot}} \tag{2.3}$$

2.3.1.4. Mobilization costs

The final costs a contractor faces are the costs for (de)mobilization. Mobilization is the preparation of the vessels for the project and includes adding the equipment to the vessels and transporting the vessels to the operating region. At the demobilization stage, all equipment is removed from the vessels. Costs for (de)mobilization consist of vessel costs, tool costs, costs for installing and removing seafastening and equipment, transportation costs and insurance costs. Smorenberg modeled these costs as 23 % of the total contractor's costs [21]. These are thus definitely of significance.

Vessel and tool costs are identical as described earlier and represent the daily costs for using a vessel or a tool. Costs for installing and removing seafastening and equipment are determined by equipment and seafastening that needs to be installed and therefore dependent on the installation method. Transportation costs depend on the transportation distance and transportation method. During transportation, it can occur that vessels are insured if they are transported by another vessel to the operating region, which adds to the risk of losing or damaging a vessel. This insurance can be seen as a cargo insurance for the transported vessel [40]. Costs for (de)mobilization are not time or activity-dependent, as they only depend on the initial mobilization time and distance required to prepare the vessels and transport them to the operating region. These costs are therefore seen as a constant. Formula 2.4 shows the costs for mobilization.

$$C_{\text{Mobilization}} = C_{\text{Vessel}}(t_m) + C_{\text{Install/remove}} + C_{\text{Transportation}}(D_m) + C_{\text{Insurance}} \tag{2.4}$$

Where:
t_m = Mobilization time
D_m = Mobilization distance

2.3.2. A developers perspective

Developers often pay a dayrate to a contractor. A dayrate is defined as the charges payable by a company to a contractor (on prorate basis for part of a day) for putting an equipment/tool/set of equipment (provided by contractor) to actual/productive use [41]. Dayrates are primarily determined by supply and demand. Competition between contractors is based on price and quality of their services and reflected in the received dayrate [42]. For a contractor to remain profitable, the dayrate multiplied by the duration should at least cover all expenses made by a contractor over the duration of the project. In general, dayrates therefore at least cover the debt services on the loans used to construct vessels, specialized tools and the labor, overhead and insurance requirements of the company [38]. Since the contractor requires some profit as well, the dayrate also consist of a profit margin. Kaiser and Snyder describe this part as return on investment [40]. Smorenberg describes this as developer costs [21]. This last part is the most susceptible to changes as it depends on market conditions and the level of competition.

2.3.3. Cost drivers

Costs can be divided into time-dependent, time-independent and activity-dependent costs. The cost parameters are vessel costs per day, tool costs per day, VOYEX, (de)mobilization costs and developer costs. Figure 2.7 presents the simplified cost breakdown of the costs involved.

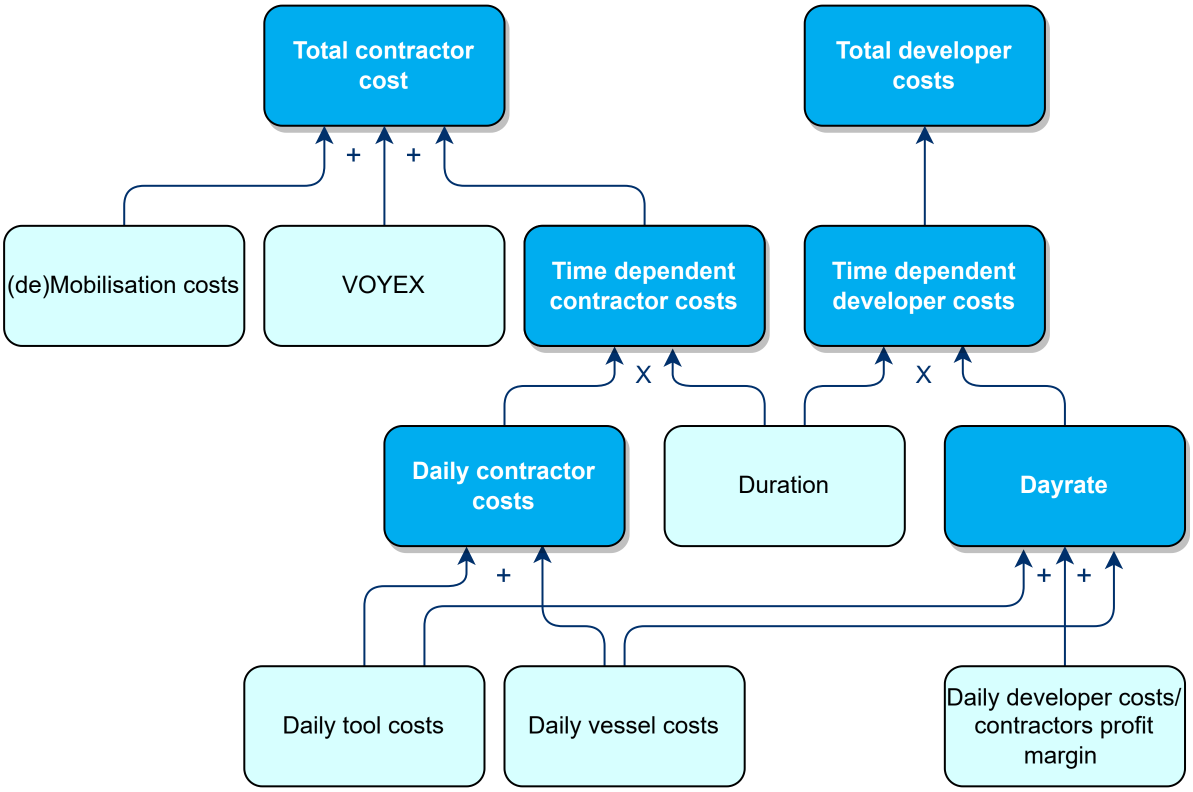

Figure 2.7: Simplified cost breakdown.

The figure shows which factors are additive, and which factors are multiplicative. From this high-level cost division, the following can be concluded. A contractor has daily vessel costs, and daily tool costs and prefers to have a duration as short as possible with as few or least expensive tools and vessels per day to remain cost-competitive. On top of the contractor's daily costs, the developer has daily developer costs which are paid on top of the contractor's daily costs during the entire installation project. Both sides would cost-wise benefit from a shorter installation procedure. On pure costs, the contractor has less advantage for the shorter project duration than the developer since it will earn back fewer 'developer costs' to cover the fixed mobilization costs. However, a shorter project duration makes the contractor more attractive to developers and provides the contractor with an advantage in winning contracts.

The cost parameters are daily vessel costs, daily tool costs, VOYEX, (de)mobilization costs, and developer costs. For the total costs, the daily costs are multiplied by the total installation duration, and the fixed costs and VOYEX are added to this. Smorenberg modeled duration-dependent costs as 74 % of total contractor costs [21]. Figure 2.8 shows the distribution of these daily costs according to an estimation by TWD [33]. The WTIVs dayrate dominates the daily costs and will always be present, regardless of the chosen feeder method. Duration is therefore seen as the main cost driver as it has a direct effect on all time-dependent costs which are dominated by a fixed component. The other cost drivers are vessel costs per day, tool costs per day, VOYEX, and (de)mobilization costs. Developer costs are not regarded as a cost driver as these depend on the desired profit margin by a contractor which can be seen as a constant and not determined by the installation method. The costs for a contractor, developer and their relation, given a profitable situation, are provided by equation 2.5. Given this relation, costs will only be viewed from the contractor's perspective for the remainder of this thesis. In the following section, more detail will be provided on the factors that influence the cost drivers.

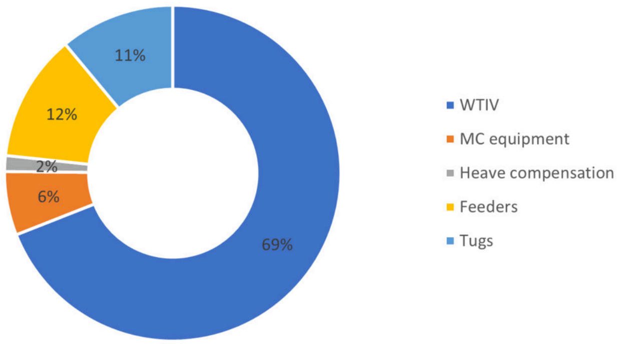

Figure 2.8: Division of Daily costs as estimated by TWD[33].

$$
\begin{aligned}
C_{\text{contractor}} &= (C_{\text{vessel daily}} + C_{\text{tool daily}}) * t + C_{\text{voyex}} + C_{\text{(de)mobilization}} \\
C_{\text{developer}} &= \text{Dayrate} * t \\
C_{\text{developer}} &> C_{\text{contractor}}
\end{aligned}
\tag{2.5}
$$

2.4. Influencing factors

The cost drivers stated in the previous section are all determined by certain factors. This section further elaborates on the factors building up the cost drivers.

2.4.1. Duration

The total duration can be divided into the 'net duration' and downtime. Net duration is the time required for loading, transport and installation of all WTGs from the port to the installation site without any delays. Downtime refers to the time an operation can't proceed. This can be due to weather, equipment failure or maintenance.

2.4.1.1. Net project duration

Net project duration depends on several factors. The evident factor for net project duration is the number of turbines that need to be installed. This factor determines how many times a loading, transportation and installation sequence must be repeated. Additional factors which influence a single loading, transport and installation sequence can be identified by dividing the net project duration of one cycle in smaller blocks. The individual phases as defined in the operation sequence are categorized and used to determine these blocks. The operation phases are categorized in the following blocks: Loading, transportation, transfer, installation and relocation.

Loading time is dependent on the number of lifts that need to be performed to load out the feeder vessel. This is determined by the amount of WTG components or assemblies that need to be lifted onto the feeder vessel and therefore by the installation strategy. Using specialized equipment could speed up the total lifting process. Loading time is thus also dependent on the type of equipment. Transportation time depends on a combination of the vessel's speed and the distance to be sailed. As vessels are sailing predominantly at their cruising speed, transportation time will depend on vessel type and distance. Transfer is similar to loading as it depends on the number of lifts and the time required to execute those lifts. Transfer is therefore subject to the installation strategy and type of equipment. Installation as well depends on the number of lifts and the time required to execute those, thus also dependent on installation strategy and type of equipment. Relocation is dependent on the jack-up/down time and inner-array movement time. It therefore depends on the vessel type and inner array distance [38].

In reality, the duration of all phases will also be determined by crew experience. However, for the remainder of this research, this is assumed constant throughout and across various projects and not seen as an influencing factor. Ultimately, net project duration depends on the number of turbines, the installation strategy, distance to the marshaling port, vessel type, equipment type, inner-array distance and crew experience.

2.4.1.2. Downtime

Downtime is seen as the time that operations can't proceed due to weather, equipment failure or maintenance. Equipment failure can be seen as a random process that happens in time. Regular/preventive maintenance can delay operations but should be scheduled in such a way that it does not cause downtime. In this sense only corrective maintenance which takes place after equipment failure can cause downtime. This will then again be subject to a random process that occurs in time. Therefore this section further only focuses on weather-related downtime. This is achieved by first introducing different marine operations and demonstrating why different methods are required to perform analysis for different categories of marine operations. This then leads to a suitable downtime analysis method for feedering method installation sequences.

An operational limit is a combination of factors above or below which an operation can no longer be (safely) executed. The most common limits are limits on the combination of wave height and wave period. For lifting operations, wind speed is also considered an important limit. The operational limits state in which conditions a vessel can work or an operation can be executed. Figure 2.9 shows the operational limits in terms of significant design wave height for a barge as a function of wave period and direction.

Tp (s) / Heading	0	15	30	45	60	75	90	105	120	135	150	165	180
4	2.50	2.50	2.50	2.50	2.50	2.50	2.50	2.50	2.50	2.50	2.50	2.50	2.50
5	2.50	2.50	2.50	2.50	2.50	2.46	2.17	2.50	2.50	2.50	2.50	2.50	2.50
6	2.50	2.50	2.50	2.50	1.91	1.43	1.31	1.52	2.10	2.50	2.50	2.50	2.50
7	2.50	2.50	2.50	2.35	1.53	1.22	1.18	1.33	1.77	2.50	2.50	2.50	2.50
8	2.50	2.50	2.50	2.05	1.43	1.17	1.14	1.27	1.67	2.50	2.50	2.50	2.50
9	2.50	2.50	2.50	1.91	1.39	1.18	1.18	1.29	1.64	2.39	2.50	2.50	2.50
10	2.50	2.50	2.50	1.87	1.42	1.23	1.24	1.34	1.65	2.31	2.50	2.50	2.50
11	2.50	2.50	2.50	1.90	1.48	1.30	1.33	1.42	1.71	2.31	2.50	2.50	2.50
12	2.50	2.50	2.50	1.96	1.57	1.40	1.44	1.52	1.79	2.34	2.50	2.50	2.50
13	2.50	2.50	2.50	2.04	1.67	1.51	1.56	1.63	1.89	2.41	2.50	2.50	2.50
14	2.50	2.50	2.50	2.14	1.78	1.63	1.69	1.75	2.00	2.49	2.50	2.50	2.50
15	2.50	2.50	2.50	2.25	1.90	1.76	1.83	1.88	2.12	2.50	2.50	2.50	2.50
16	2.50	2.50	2.50	2.36	2.02	1.89	1.98	2.02	2.24	2.50	2.50	2.50	2.50
17	2.50	2.50	2.50	2.48	2.15	2.03	2.13	2.15	2.37	2.50	2.50	2.50	2.50
18	2.50	2.50	2.50	2.50	2.29	2.17	2.29	2.30	2.50	2.50	2.50	2.50	2.50
19	2.50	2.50	2.50	2.50	2.42	2.31	2.45	2.44	2.50	2.50	2.50	2.50	2.50
20	2.50	2.50	2.50	2.50	2.50	2.46	2.50	2.50	2.50	2.50	2.50	2.50	2.50

Figure 2.9: Example of operational limits as a function of wave period and direction [43].

When combining these operational limits with weather data, a workability percentage can be obtained. The workability percentage states the percentage of time in which the operational limits are not exceeded. Equation 2.6 shows the equation for workability percentage. It can be easily seen that the workability percentage refers solely to the weather conditions and doesn't take into account the duration of a project or operation [44]. Therefore, it can not be used to measure downtime for complex operations such as WTG installation where operations require a minimum amount of time and thus a weather window [44].

$$\text{Workability \%} = \frac{\text{\# of workable time steps}}{\text{total length of time series}} * 100\% \tag{2.6}$$

Regarding weather risk, operations can be divided into different categories. Continuous operations, single weather window operations and complex projects.

Continuous operations don't have a fixed 'net duration'. The operation is executed as long as the weather allows it. Examples of these activities are motion compensating or dredging activities[44].

These activities can be paused at any time and don't require a weather window. For these operations, downtime is equal to the time for which the operational limits are exceeded and can be measured with the workability percentage as presented by equation 2.6. Figure 2.10 shows an example of downtime on a time horizon measured for a continuous operation. The green and red workability boxes indicate whether the operational limits are exceeded or not.

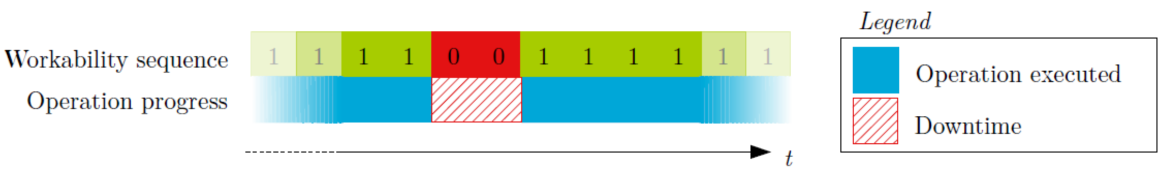

Figure 2.10: Downtime example for a continuous operation [44].

In the case of single or uncoupled operations which require a weather window, downtime is best described as the time to wait before a weather window occurs in which the operation can be executed. These operations have a fixed net duration and cannot be stopped or paused when weather conditions exceed the operating limits. Figure 2.11 presents the downtime on a time horizon for an operation which net duration is 4 time steps [44].

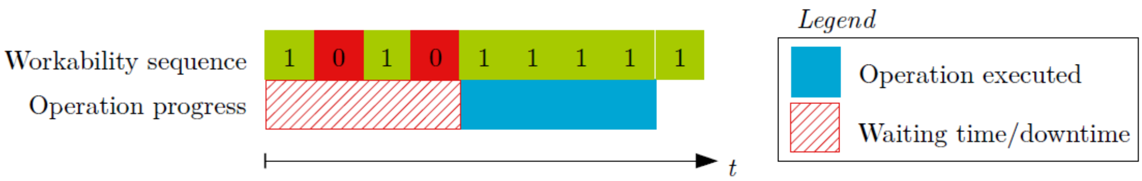

Figure 2.11: Downtime example for an operation requiring a weather window [44].

Complex projects consist of a series of coupled operations that require a weather window. An example is feedering of WTG components. A feeder vessel has to sail to the installation site, moore to the WTIV, transfer components, depart from the WTIV and sail back to the port. Instead of looking at the downtime per individual operation, it is more natural to look at the total downtime of this cycle. However, downtime per operation is still interesting to determine the most weather sensitive operation of a project and thus identifying delay risks. An example of a complex project is presented in figure 2.12. In this example, the net duration of operation 1 is 4 time steps, the duration of operation 2 is 3 time steps and the duration of operation 3 is 3 time steps, but requires a warranty window of 6 time steps. The first two operations are coupled, so operation 2 has to start without any waiting or downtime. This makes that operation 1 cannot start earlier. After operation 2 is finished, the limits for 3 are exceeded causing downtime until a weather window of 6 weeks becomes available [44].

Feedering method installation sequences are complex projects and thus require a similar downtime analysis as presented in figure 2.12. Downtime is affected by the weather, operational limits and net fixed duration of an operation. If the operational limits of an operation are increased, the workability percentage will increase as operations can proceed for a larger part of the time. This will also increase the length and amount of suitable weather windows. The time to wait for a suitable weather window to occur will therefore decrease. Decreasing the fixed net duration also has a positive effect on downtime. Shortening this duration results in smaller weather windows which occur more often. This is also supported by Sandvik[45]. Taking weather windows into account is thus crucial for the simulation of the complete operation. The operating limits are influenced by the type of tools and vessels used and the installation strategy. The influencing factors for net fixed duration are the same as mentioned in the previous section, with the exception of the amount of WTGs.

[H]

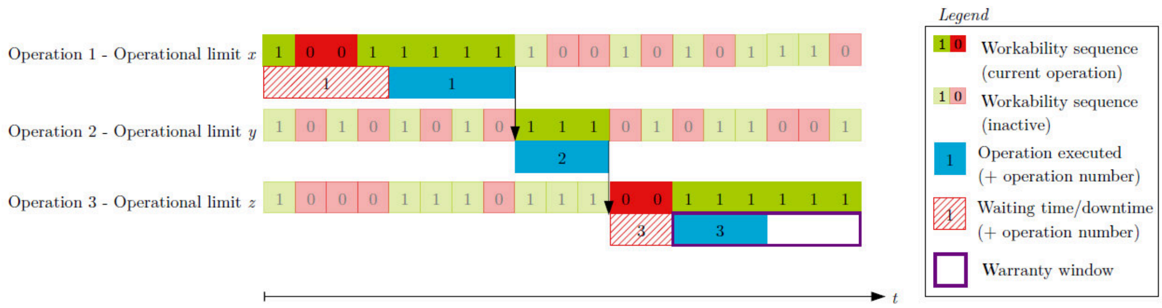

Figure 2.12: Downtime example for a complex operation [44].

2.4.2. Vessel costs

Vessel costs are determined by the type and the number of vessels used to carry out the project. The type of vessel is influenced by WTG characteristics and installation strategy. More complex ships will have a higher dayrate, but can in return probably execute the project faster and with less downtime. The number of ships are determined by the distance to the installation site. For an efficient feeder process, that is: no waiting time for WTIV, at least two feeders are required. With increasing distance, it could be beneficial to use a third feeder to eliminate possible waiting time of the WTIV.

2.4.3. Tool costs

Tool costs depend on the type and amount of tools required. The type of tool has an effect on the dayrate per tool. A more complex tool will require a higher dayrate. The amount of tools has an effect on how many tool dayrates must be paid. The type of tool that must be used will also depend on the WTG characteristics. A simple example follows from the effect of WTG sizes. A larger WTG, will likely need larger tools to execute a successful operation. Larger tools will in turn be more expensive as more resources are required to construct these tools. The types of tools also depends on the installation strategy, a more complex lift is likely to need a more complex tool to safely execute the lift, resulting in higher tool costs.

2.4.4. Mobilisation costs

Costs for mobilization consist of several parts as stated in the previous section. The costs are: Vessel costs, costs for installing and removing seafastening and equipment, transportation and insurance costs. Vessel costs depend on vessel type and the amount of vessels required as is discussed in the previous subsection. Costs for installing and removing seafastening and equipment depend on multiple factors. Costs for seafastening depend on the WTG characteristics and vessel characteristics. The combination of these two parameters determines what type of seafastening is installed and how much reinforcements must be made to bear the calculated loads. Costs for installing equipment will determine the type of tools required and the vessel type. The combination of these two will again determine how much work is required to install the equipment on the vessel and how much reinforcements possibly must be made. Since the cost for installing equipment depends on the equipment that is used, the costs for installing equipment are also related to the WTG characteristic.

2.4.5. Influencing factor overview

Multiple parameters influence the cost drivers identified in section 2.3.3. Some parameters influence multiple cost drivers. This section also identified that certain factors influence each other which is common in complex design problems. To provide an overview table 2.2 shows which factors influence certain cost drivers. For clarity, the duration cost driver is split between downtime and net duration. Overmore, the Design Structure Matrix (DSM) in appendix E shows the influencing factors and their interdependencies. The DSM is read by taking the column as the influencing factor and the row as the factor that is influenced. From the DSM, a distinction can be made between internal and external factors. External factors only influence internal factors and are not influenced by other factors. Internal factors are factors that both influence and are influenced by other factors. External factors thus describe the setting in which the system performs and internal factors are the variables that can actually be changed in order to alter the performance of the system. This thus concludes that vessel type, equipment type and installation strategy are the only factors that can be changed to alter a system's performance.

Table 2.2: Cost driver influencing factors

Influencing Factor	Net duration	Downtime	Vessel costs	Tool/Equipment costs	Mobilisation costs
No of WTGs	x				
Installation strategy	x				
Distance to marshaling port	x				
Mobilisation distance					x
Vessel Type	x	x	x		x
No. of vessels			x		x
Equipment / tool type	x	x		x	x
No. of tools / equipment				x	x
Inner array distance	x				
WTG characteristic			x	x	x
Weather		x			
Insurance					x

2.5. Key Performance Indicators

To objectively assess the performance of the feedering methods, several KPI are defined. KPIs should match the interest of stakeholders. From the stakeholders analysis, stakeholder interest are analysed and transformed to KPIs. Three type of KPIs are defined: costs, duration and risk.

2.5.1. Costs

Costs play an important role. Both for a contractor and a developer. For developers, decreasing the costs of installation results in a lower LCOE which makes investing in an offshore wind farm more attractive. On the contractors side, lowering the costs of installation allows the contractor to fullfill the need of a developer and win contracts. Therefore costs is one of the KPIs used to assess the performance of the feedering method. The costs used to determine this KPI are given by equation 2.5.

2.5.2. Duration

Duration is a key factor for a developer en therefore reflects as an important factor for a contractor. Total project duration is thus seen as a key performance indicator. The definition of total project duration is stated in section 2.4.1

2.5.3. Risk

Developers and contractors both aim to minimize risk. Contractors assist them in this goal by helping with installation methods that minimize risk. Minimizing risk means having a level of certainty regarding costs and duration. This level of certainty depends on the susceptibility of the process to external factors. The desired KPI expresses the degree of which the operation is susceptible to external factors and thus a level of robustness.

Literature states multiple KPIs regarding operational robustness [46] [45] [47]. For identification and benchmarking of mission-oriented vessel capabilities, percentage operability (percOP) and Operational Robustness Index (ORI) can be used. PercOP is a suitable parameter for operational planning and vessel selection if all operational details are available. These details include operational limits, sea area and season. PercOP is defined as the percentage workability, as defined in formula 2.6, given a certain limitation such as maximum roll angle. ORI on the other hand is suitable in early-stage ship design and vessel selection where operational details are not yet specified. The ORI presents seakeeping performance for a specific area independently of the magnitude of the limitation criterion. The ORI is obtained by integrating the percOP curve[46]. This is displayed in figure 2.13.

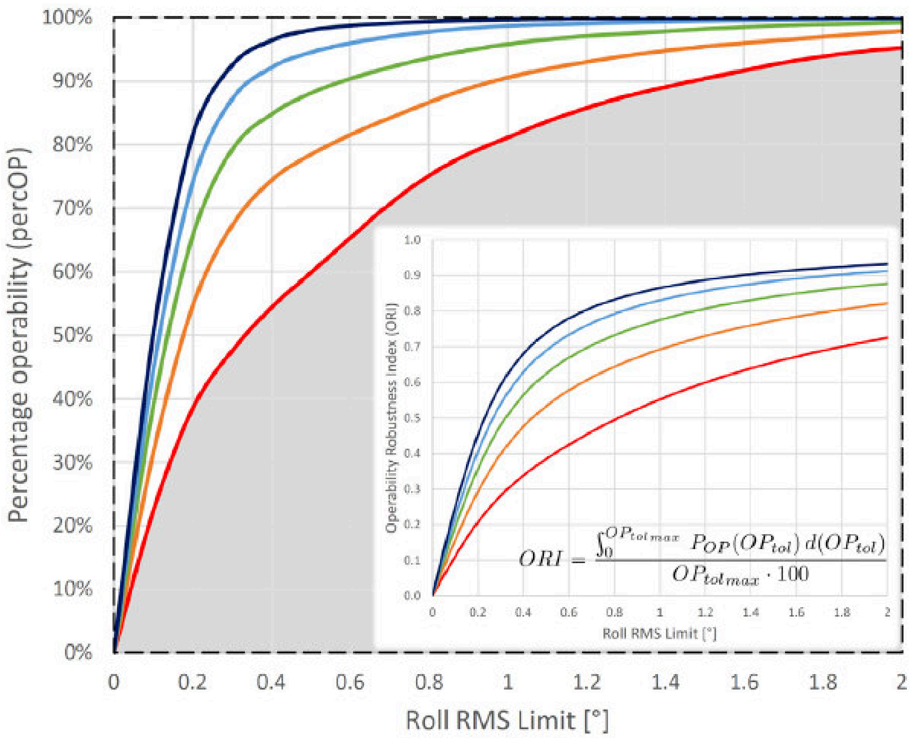

Figure 2.13: ORI and percOP curve [46].

For the design of a vessel including its equipment, both KPIs could be used to compare and show the performance of a certain design. Since for WTG installation, the operational limits with respect to maximum allowable accelerations or forces are known, percOP will also give a good representation of a vessel's performance. The downside of these KPIs is that they don't take into account the duration and sequence of operations and the associated weather windows. This deficit is also pointed out by Sandvik [45]. A third KPI regarding operability is therefore introduced. The Relative Rate of Operation (RRO). RRO quantifies the operation's susceptibility to weather delays as a consequence of limitations in vessel design response characteristics or motion compensation. The RRO is determined by the ratio of operations performed and the operations feasible in the same period of time provided it is not influenced by weather during the operations [45]. This equation is given by formula 2.7. The performed operations can be calculated by means of simulations. Multiple simulations must be run in order to obtain a representative RRO value. Including weather windows in the operational criteria has a significant impact on the susceptibility to weather delays, as is pointed out by Sandvik [45], and must be taken into account for the simulation of installation methods.

$$\text{RRO} = \frac{OP_{\text{performed}}}{OP_{\text{feasible}}} \tag{2.7}$$

For determining both costs, duration and RRO, simulations of the installation need to be run. To obtain convergence for average duration, costs and RRO, a sufficiently large number of simulations need to be run. The average results will then converge to a final value (μ). The variability across simulations (σ), the standard deviation, can then also be used to provide a measure of uncertainty. This measurement for risk is also supported by Muhabie et al. [47]. The variability of time across simulations (σ) will be used as a measure of uncertainty.

2.5.4. KPI tradeoff

It can be expected that none of the optimized methods will trump the other feedering methods on all KPIs and trade-offs must be made. These trade-offs are made according to criteria from developers and contractors. These are mainly criteria driven by their preferences for either minimizing costs, time or risk. These subjective criteria induce difficulties in making trade-offs for external parties. Since the main goal of this research is to provide an understanding of the feedering installation method for future 20 MW WTGs, no trade-off shall be made and only the effects on the individual KPIs will be presented in this research.

2.6. Performance simulation

A simulation is an imitation of the dynamics of real world processes or systems over time. The behaviour of a system can be studied by means of simulation models. These models generally take a set of assumptions about the workings of a system. Once developed, a simulation model can be used to investigate the systems behaviour under a variety of scenarios, predict the effect of system changes before implementing them in the real-world and guide construction of a system during its design. It is important to note that according to George Box, 'all models are wrong, but some of them are useful' [48]. The core of this message is that a model is never 100 % accurate and the focus should be on the useful insight it provides if the model is close enough to reality.

2.6.1. Types of simulation models

Simulation models can be divided into several types, where each type has its characteristics. Figure 2.14 graphically displays this division. The choice for a certain simulation model depends on the characteristics of the system that are to be captured. First, a division can be made between a deterministic and stochastic model. A model is deterministic if its behaviour is entirely predictable. Given a set of inputs, the model will always result in a unique set of outputs. A model is stochastic if it has random variables as inputs, and consequently also random outputs [49].

The second division in modeling types is the division between static and dynamic simulations. Static simulation models represent the system at a particular point in time and are often referred to as Monte-Carlo simulations. A dynamic simulation model represents a system as it evolves over time.

Dynamic simulations can in turn be categorized into discrete or continuous. In Discrete simulation models, the variables of interest only change at a discrete set of points in time. In between these points in time, the state of the system doesn't change. It is thus useless to inspect the system during those times where nothing changes. Time in a dynamic discrete simulation is therefore handled using the *next-event-technique*. The model is only examined at instances where the system state changes, these changes are called events. In continuous models, the variables of interest change over time. In contrast to a discrete simulation, time is handled as continuous. Continuous simulation models are for systems where the variables of interest continuously vary over time. For example, the speed of a car during its journey, or the tension in the crane wire during installation of a WTG.

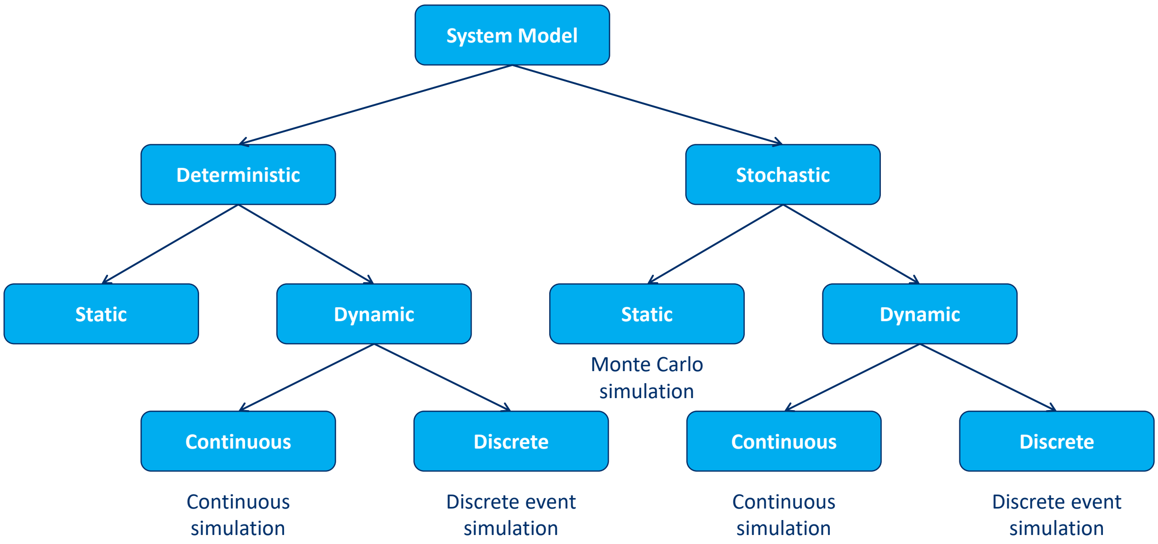

Figure 2.14: Schematic division of simulation models as described by Leonelli [49].

2.6.2. Discrete Event Simulation

The goal is to obtain insight in the performance of the feedering method. It is therefore useful to model the development of the system over time instead of representing a single point in time. Adding to that, the operation phases as mentioned in table 2.1 can be seen as activities during which the systems state doesn't change. Before commencing an activity, operators will check whether it is possible to safely complete the activity. Until the activity is ended, the system's state can be assumed to not change, given that the weather adheres to the forecast and no breakdowns occur. The system's state will then only change when the activity ends. At that instant either a new activity can be commenced or an activity can be delayed due to weather or queuing. Discrete Event Simulation (DES) is therefore a suitable method to model the installation process of WTGs. A discrete event simulation method is also used throughout the literature to simulate both feedering and conventional WTG installation.

The installation process can be modeled in both a deterministic and stochastic manner. In a pure deterministic model, the duration of the activities are set and the operation is modeled with hindcast data. A second option is to combine the stochastic and deterministic model. In this case, the activities are modeled as stochastic with varying duration. The operations can then also be modeled with hindcast data. The third option is to use a pure stochastic model. Here, both the activities and weather are modeled as random variables. For this modeling technique, it is essential to first develop a representable stochastic weather model from hindcast data. The output of the DES model of a single simulation will be the required time to complete the operation and the activities per vessel. For all possible models, it is crucial to run a sufficient amount of simulations in order to obtain a representable and convergent result. From these results, the total vessel costs, equipment costs and VOYEX can be determined. Adding the mobilization costs to the costs obtained through postprocessing of the DES model output, will result in the total costs of the operation. With the variance of the modeled costs, the risk associated with the feedering method can be determined. The DES model is thus able, with some postprocessing, to model all KPIs as presented in section 2.5.

2.7. Conclusion

This research focuses on the transportation and installation of WTG components with a 'practical feeder-ship method' as described in section 2.1.1. The complete feedering operation in this research is considered as all necessary steps to transport and install all WTG components starting with all components stationed at the base port. The analysis of the operation as carried out for Vineyard shows that weather conditions are most stringent for the transfer, offshore approach and offshore departure phases. These phases are therefore critical.

The performance of the feedering method is measured by means of three KPIs. Contractor's costs as given by equation 2.5, total project duration and the variability of the total duration across simulations. The cost drivers are identified as duration, daily vessel costs, daily tool costs, VOYEX and (de)mobilization costs where duration is seen as the main cost driver. Total project duration consists of net duration and downtime. Feedering WTG installation is a complex operation and therefore requires a downtime analysis including weather windows and event sequences to simulate the total project duration. The cost drivers can be deduced to twelve influencing factors. The internal factors are vessel type, number of vessels, equipment type, amount of equipment and the installation strategy. These can be changed by design in order to alter the performance of the feedering method. The remaining factors are external and determine the setting in which the system operates. These factors are the number of WTGs, distance to the marshaling port, inner array distance, WTG characteristics, mobilization distance, insurance costs and weather.

In order to determine the performance of the feedering method, the operation must be simulated including weather windows and event sequences. For this simulation, a DES can be used. The weather and associated downtime are simulated with a deterministic model by using hindcast data and a convergent result is obtained by running multiple simulations starting at various instances in time. The output of a single simulation will be the required time to complete the feedering operation and the activities per vessel. Running sufficient simulations will result in a convergent result and representative variance. The results of the simulations can be used to determine the total costs of the operation. The DES model can thus be used to measure the performance of the feedering method.

3

Future equipment

This chapter provides an outlook on future developments in the offshore wind market. The growth of WTGs is first discussed after which the developments regarding installation vessels and jack-up feeder interfaces are presented and how that influences feedering operations.

3.1. Wind Turbine Generator

Upscaling of wind turbines is a hot topic in the industry. In the past decades, both the number of turbines and the size and power output of installed wind turbines have significantly increased. The drive towards increasing turbine sizes is powered by a more profitable business case. Larger WTGs are able to generate energy with a higher capacity factor and a lower LCOE [50]. The current state-of-the-art capacity that is being installed equals 14 MW and is expected to grow to 15 - 20 MW between 2025 and 2030 according to IRENA [51] in 2019. Figure 3.1 shows the realized and expected growth for offshore wind turbine generators from 2000 to 2027 as presented by the U.S. department of energy [52]. For developing the feedering method, it is essential to have a clear view on the size and dimensions of 20 MW WTG components, as this influences the load-out of the vessel. This section discusses the current state-of-the-art WTGs and the gap towards the characteristics of a commercial 20 MW WTG. This gap is solved by section 5.2 which sets a standard for commercial 20 MW WTG components by means of a scaling analysis.

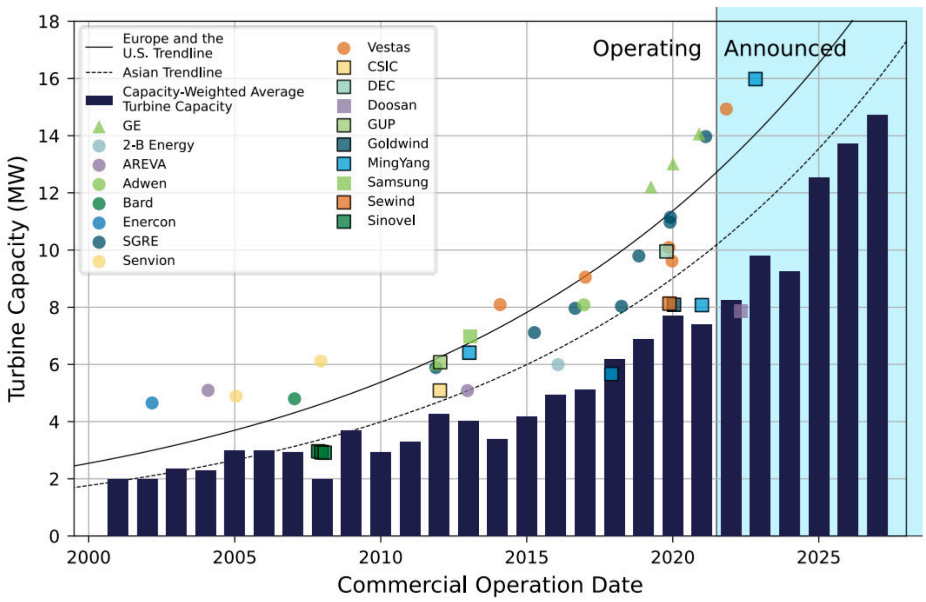

Figure 3.1: Realised and expected wind turbine growth [52].

3.1.1. State-of-the-art Wind Turbines

In order to provide a good base point, the state of the art turbines will be highlighted first. By describing the state of the art, it is easier to take a critical look at future WTG designs. Table 3.1 lists the parameters of the state of the art WTGs. Only publicly available parameters for the turbines are listed. Despite the fact that not all parameters are available, the table provides a good overview of the current state-of-the-art.

Table 3.1: State-of-the-Art WTGs.

Type	Unit	**MHI Vestas V236**[53] [54]	**SG 14-222D** [55]	**Haliade X** [56]
Power	MW	15	14	12 - 14
Hub height	m	148	141	135
Rotor diameter	m	236	222	220
Blade length	m	115,5	108	107
Hub diameter	m	5	6	6
Power density	W/m^2	342,9	361,7	315,5 - 368,3
RNA Mass	t	-	696,8 + hub	825
Blade mass	t	-	65,6	55
Nacelle mass	t	575	500	600
Hub mass	t	-	-	60
Specific RNA Mass	t/MW	-	-	58,9 - 68,8
Specific nacelle mass	t/MW	38,3	35,7	42,8 - 50

3.1.2. Reference Wind Turbines

Two types of turbines can be distinguished, reference and commercial turbines. Reference turbines are defined with publicly available design parameters and are designed to be used as a baseline for studies that explore new technologies or design methodologies. Commercial turbines are turbines that are actually manufactured and installed and are often more optimized and therefore differ from the reference turbines. 20 MW wind turbines are not yet in production, so only data on reference turbines is available. The characteristics of the 20 MW reference turbines as provided by Energy research Centre of the Netherlands (ECN)[57], INNWind [58] and Ashuri et Al. [50] are listed in table 3.2.

Table 3.2: Reference 20 MW WTG characteristics.

Type	Unit	ECN [57]	INNWind [58]	Ashuri et al. [50]
Power	MW	20	20	20
Hub height	m	153	168	160,2
Rotor diameter	m	252	252	276
Blade length	m	123	122	135
Hub diameter	m	6	8	6
Power density	W/m^2	401	401	334,3
RNA Mass	t	2857	1730	1992,8
Blade mass	t	161	118	264,7
Nacelle mass	t	1920	1098	945
Hub mass	t	454	278	252,8
Specific RNA mass	t/MW	142,9	86,5	99,64
Specific nacelle mass	t/MW	96	54,9	47,25
Tower mass	t	1750	1600 - 1780	2350,5
Tower Diameter	m	12	-	12,5

Based on the reference turbines, no conclusion regarding weights and dimensions can directly be made for a future 20 MW offshore WTG. Both in terms of dimensions and weight, the reference turbines differ significantly, especially in terms of the Rotor Nacelle Assembly (RNA) mass. These differences originate from different methodologies and technical improvements over time. The ECN reference turbine dates back to 2011 and uses upscaling with classical similarity rules from the 5MW NREL Upwind wind turbine v.8 from 2007 [59]. Starting with the principle dimensions from the upscaled version, the aerodynamic and structural design of the blades is then executed. The INNWind reference turbine, which dates back to 2016, is also defined by classical upscaling and follows the same methodology as used for the ECN reference turbine. The INNWind turbine however scales up from the more recent 10 MW DTU turbine from 2013 [60]. This clarifies the difference in weights between the ECN and INNwind since the starting point for the scaling assessment is technologically more advanced.

Ashuri et al. recognize the fact that the available reference turbines at the time were not optimized, unlike commercial turbines, and state the need for publicly available large scale wind turbine designs and corresponding data made by manufacturers. To address this need, they developed a 20 MW common research wind turbine model that is publicly available. Unlike the other research turbines, the design of the wind turbine is performed using first upscaling from the 5 MW NREL Upwind wind turbine, followed by Multidisciplinary Design Optimization (MDO) instead of just upscaling. Using just the scaling laws results in a design for which there is no guarantee on its feasibility. Adding to that, the scaled design will not be an optimal design solution. The design by Ashuri et Al. is optimized towards a turbine with minimal LCOE resulting in a feasible and optimum design for a 20 MW turbine. However, it is good to note that the baseline of Ashuri et Al. dates back to 2009 which is a further development of the upwind NREL turbine as used by ECN. This could be a justification for the higher blade weights of the reference turbines by ECN and Ashuri et Al. since a technologically less advanced starting point is used than for the INNWind design. This design features the largest rotor diamter and thus has the lowest power density out ouf the reference turbines. However, The power density falls in the order of magnitude of the commercial scale turbines, indicating that this rotor diameter could be a good reference for a commercial 20 MW WTG.

3.1.3. Future commercial 20 MW WTGs

When comparing the reference turbines to the state-of-the-art commercial turbines it becomes evident that turbines will see a huge increase in mass when scaling up to 20 MW. However, this increase in mass should be analyzed critically since reference turbines are generally estimated too heavy according to industry expert Bart Ummels [61]. According to Ummels, specific RNA mass will remain in the same order of magnitude $[t/MW]$ to remain competitive. This is also backed by the upscaling research of Kikuchi et al. [62].

Comparing the RNA masses of the reference turbines and the state of the art turbines, it is clear that the specific RNA masses of the reference turbines are significantly higher. In geometrical similarity, scale of weight and power follows $m \sim D^3$ and $P \sim D^2$. The relation between rotor diameter and turbine power exactly follows the geometrical similarity [62]. Regarding mass however, scaling with geometrical similarity neglects effects of both scale and technology advancements as is pointed out by Sieros et Al.[63]. Scaling of RNA mass is closer to D^2 which justifies a constant specific RNA mass. The same analysis is carried out just the blades by Loth et al. [64]. where a similar conclusion is drawn. Blade mass scales with $D^{2,1}$ due to technology advancements for longer and newer blades. Comparing only the blade masses, the blade masses are too heavy compared to the state-of-the-art WTGs, even when applying geometrical upscaling. Based on this, it can be concluded that the reference turbines are too heavy to resemble future commercial 20 MW WTGs.

3.2. Future installation fleet

This section covers the current fleet of installation vessels and what its impact is on the feedering method. After setting the current technology state, the future of jack-ups will be discussed and how feedering operations can change due to their changing designs.

3.2.1. Requirements

From section 3.1 a rough estimate can be made regarding the required hook height and crane capacity for the installation of WTGs. Based on the hub height, required hook heights can be determined. Non-disclosed documents by turbine suppliers provide a distance of 15 m between the hook and hub height to leave ample room for the nacelle itself and the lifting tool. Regarding blade installation, the 30°blade installation is most critical with 34 meters above hub height. Using the most conservative hub height estimate, this requires a 202 m hook height above sea level. With respect to the weight, the nacelle-hub lift will be the most critical. Supported by confidential documents and the reference turbines a mass between 1000 and 1500 t can be expected for the nacelle-hub assembly including the lifting tool. Crane capacities above 1500 t will certainly suffice in lifting the nacelle-hub assembly.

According to the bathymetry as provided by the BOEM [13], the installation depth around the Vineyard area ranges between 40 and 60 meters. For the remainder of the planned lease areas on the U.S. east coast, the installation depth varies between 20 and 60 meters. This implies that the minimum required hook height of a jack-up vessel capable of installing 20 MW WTGs in the Vineyard area ranges between 242 and 262 meters with respect to the seabed.

For a jack-up vessel, its hook height above water level is determined by the vessel's hook height and the air gap where the maximum air gap is determined by the leg length and the water depth. Figure 3.2 depicts this. To determine the maximum hook height with respect to the seabed, formula 3.1 is used. It is assumed that the sum of maximum working depth and airgap represents the maximum possible distance from the keel to the seabed. A common airgap for jack-up vessels is 15 meter [65]. An alternative approach is to determine the maximum distance from the keel to the seabed based on leg length. This approach requires extra variables as penetration depth, reserve leg length and amount of leg length in the ship. This method is deemed less robust since it requires more vessel dependent variables.

$$H_{\text{hook-seabed}} = T_{\text{Max}} + H_{\text{airgap}} + D_{\text{vessel}} + H_{\text{crane}} \tag{3.1}$$

Where:
T_{Max} = Maximum working depth
H_{Airgap} = Airgap
D_{vessel} = Vessel depth
H_{crane} = Hook height with respect to vessel deck

3.2.2. Current fleet

To date, all commercial-scale projects have been executed by jack-up vessels [66]. A jack-up vessel is the preferred type of vessel for WTG installation as it can provide sufficient stability for the nacelle and rotor lifts. Due to the offshore transfer associated with feedering, the stability of jack-up vessel is even more desired. For feedering, it is thus highly likely that jack-up vessels will remain the vessel of choice.

In recent years, specialized WTIVs have emerged, starting with the Mayflower Resolution in 2003. This vessel was self-propelled, provided the capacity to carry and install all components of a single WTG and was equipped with a 300 t crane. This design continued as a standard until a change occurred around 2011-2012. Several designs entered the installation fleet with a much higher crane and carrying capacity. These vessels provided the ability to carry and install multiple WTGs per trip while also being able to work in different industries when the offshore wind market was low [67]. During this time, turbine sizes also steadily increased, additionally stressing the need for larger cranes and deck capacity.

With turbines evolving as discussed in section 3.1, changes in jack-up design will follow, requiring even larger cranes and carrying capacity. Table 3.3 shows the current and ordered vessels that are capable of reaching the new installation requirements as mentioned in section 3.2.1. This fleet is pretty

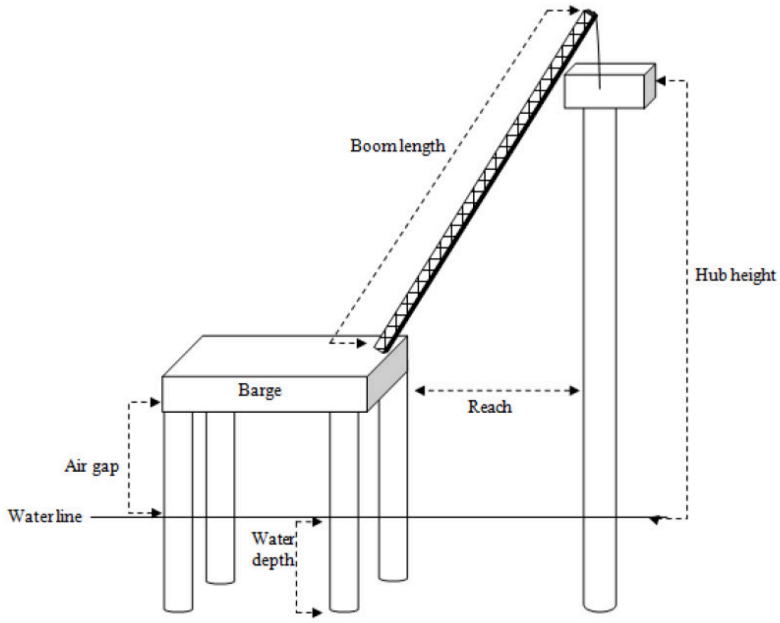

Figure 3.2: Diagram of factors affecting lift height [38].

slim. However, vessels which do not meet the requirements yet can still be upgraded by extending their legs or improving the crane capacity and hook height. Table F.1 in appendix F shows this potential fleet.

Table 3.3: Jack-up vessels capable of installing 20 MW WTGs [54].

Vessel Name	Vessel status	Year Built	Max. water depth (m)	Max Lift (t)	Max. Crane hook height (m)	Max Hook height WRT seabed
Cadeler NG-20000X-G 1	Under construction	2024	80	2000	181	291
Cadeler NG-20000X-G 2	Under construction	2025	70	2000	181	281
Eneti WTIV 2	Ordered	2025	65	2600	185	280
Voltaire	Under construction	2022	80	3000	163	273
Van Oord New Build 1	Ordered	2024	70	3000	163	263
OIM BT-220IU	Ordered		67	2600	165	262
OIM BT-220IU 2	Pre-order		67	2600	165	262
Triumph 1	Pre-order		65	2500	166	261
Eneti WTIV	Ordered	2023	65	2600	162	257
Shimizu Corporation SEP	Under construction	2019	65	2500	161	256
Seaway Ventus	Under construction	2023	65	2500	156	251
VIND 2	Pre-order	2023	65	2500	156	251
Bold Tern	Active in sector	2013	60	1600	158	248
Havfram - VARD	Pre-order	2024	60	1000	150	240
Apollo	Active in sector	2018	70	800	140	240
Charybdis	Under construction	2023	65	2200	144	239
Hai Long Xing Ye Hao	Active in sector	2019	60	1200	145	235
Seajacks Scylla	Active in sector	2015	65	1500	132	227
Wind Osprey	Active in sector	2012	55	1500	132	217

3.2.3. Jack-up feeder interface

During the mooring, transfer and departure phase, the jack-up vessel interacts with the feeder vessel. The feeder vessel moores to the WTIV during the mooring phase and remains in the same orientation until the departure phase. The jack-up vessel is positioned before the feeder vessel arrives and is preferably jacked up in head waves as this leads to the lowest vessel responses. Due to the limited working radius of the crane, the feeder vessel can only moor to the crane side of the vessel, leaving little room for flexibility. However, due to practical reasons such as cables or unfavorable soil conditions, the vessel might not be able to jack itself up in head waves. Since the feeder is moored alongside the WTIV, the mooring, transfer and departure phases will then be executed with an unfavorable wave direction resulting in lower operating limits.

This issue could be mitigated by creating a less 'stiff' interface between the WTIV and the feeder vessel. This could be achieved by using a DP system for the feeder vessel instead of a mooring system. This would allow for a heading misalignment between the WTIV and the feeder vessel. This is called weathervaning [30]. Figure 3.3 provides a top view of the barge approaching and mooring to the WTIV and demonstrates the limited flexibility of positioning the barge alongside especially with the presence of the transition piece.

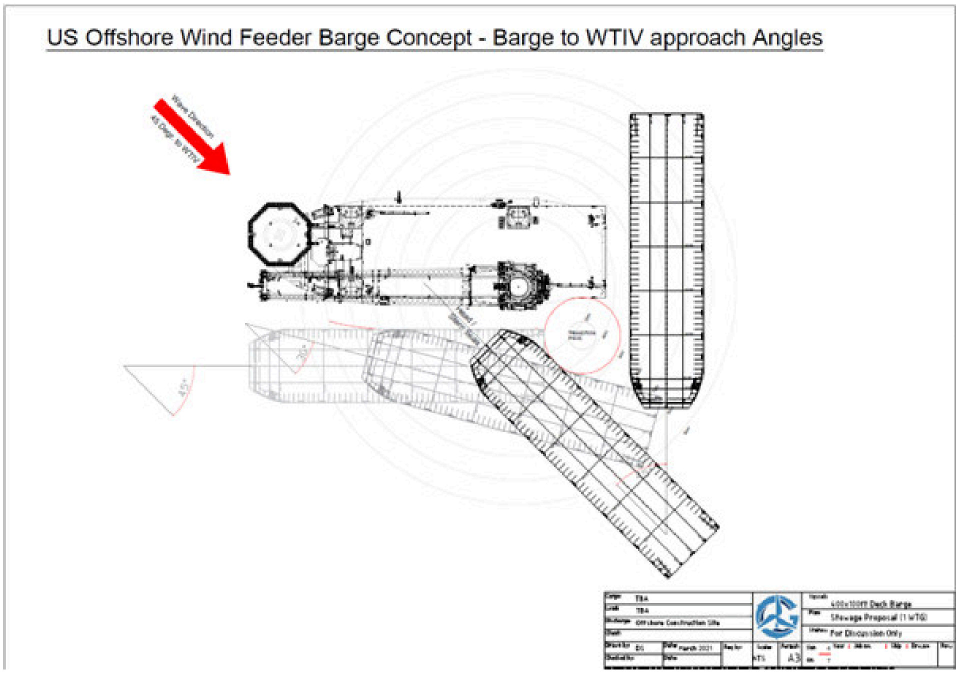

Figure 3.3: Feeder barge with respect to the WTIV [30].

Furthermore, the feeder is moored in such a way that only second order motions are influenced. In reality, first-order motions are influenced as well. The effect on first-order motions by the currently used mooring system is however neglected. To reduce first-order motions or change the Response Amplitude Operator (RAO) of the feeder vessel, alternative mooring systems could be used, which can, in turn, improve the operating limits of the transfer operation. An example of such a mooring system is a system where the barge is pulled down alongside the WTIV, increasing its natural stiffness and altering the vessel's RAO [68]. These types of mooring systems will not be considered for this thesis.

3.2.4. Future jack-ups

As jack-up vessels grow in size and capacity, they face problems regarding vessel strength. A consequence is that more steel must be used in construction, resulting in a higher newbuild price and dayrate. This is caused by the phenomenon of torsion during pre-loading [65].

A jack-up pre-loads in order to ensure its legs stand firmly on the seabed. During pre-loading, a vessel jacks up just above the water level. At this moment, 2 opposing legs are slightly lifted, resulting in the jack-up standing on just 2 legs. This doubles the loads on the legs, putting them firmly in place. This process is then repeated for the 2 other opposing legs[65].

While the jack-up stands on 2 legs. A torsional moment is applied to the hull of the vessel, resulting in critical stresses over the skin of the vessel. In order to cope with these stresses, including the additional stresses present by the variable deck load, thick decks and stiffeners must be used.

A second disadvantage to current jack-ups is the location of the crane on one side of the vessel. To improve the accessibility of the crane, it is usually positioned around one of the stern legs. This puts the crane off-centre, making balancing of the vessel more complex. An additional problem for self-propelled jack-ups is caused by the turbulent flow field of the spudcans. The presence of the spudcans can disturb the inflow of the thrusters resulting in lower propulsive efficiency.

Recent concepts by SeaOwls and Ulstein, [69] and Keppel[67] show vessels shifting towards a diamond shape with the front and aft leg at the centreline and 2 legs at either port side and starboard side. Figure 3.4 shows this configuration. The vessel has a cruciform primary structural arrangement which eliminates torsion during pre-loading. This affects the total steel weight resulting in a 15% decrease which almost directly translates to an equivalent reduction in CAPEX [65]. The configuration of the legs also allows for a centered crane around the stern leg, potentially solving difficulties balancing the vessel. The presented leg configuration also allows for unobstructed thruster placement, allowing for more efficient propulsion and thus reduced VOYEX.

Figure 3.4: Jack-up concept by Ulstein and SeaOwls [70].

An additional possibility is a specialized installation vessel for feedering. This will be a small footprint vessel, with only a small propulsion plant. For feedering, deck space for only one WTG is required allowing for a smaller vessel. evenmore, since the installation vessel will remain at the installation site, a propulsion plant designed for transit conditions might not be necessary. A vessel can be towed towards the installation site, with its propulsion package only designed for inter-array movements. Both changes in jack-up design will decrease the vessels newbuild, and therefore its daily costs.

It can be concluded that changes in jack-up design can reduce the costs for feedering installation methods by reducing daily vessel costs and VOYEX. The possibility exists that operational advantages can be achieved by improved balancing of the vessel or increased crane accessibility. At this stage however, this is hard to quantify, will remain site and situation-specific. The possible operational advantages will therefore excluded for the research part of this thesis.

3.2.5. Feeder concepts

Due to the challenge of the component transfer, alternative concepts for feeder and installation concepts have been developed as well. These are all bespoke solutions focussed on coping with glsus Jones Act limitations and eliminating the motions between the feeder and installation vessel. Development and construction costs for these bespoke vessels are often high, resulting in higher dayrates, which brings in risk when dayrates of concurring vessels come down. However, as long as the installation vessel supply is short, there may be room for these future conceptual vessels.

Appendix G highlights the future concepts to provide an overview of what future concepts could look like. All existing concepts eliminate the floating-to-fixed transfer phase, by fixing the feeder vessel to the installation vessel in a rigid way. The concepts require significant investments compared to the more simple tug-barge combination which will reflect in their dayrate. However, the fixed connection eliminates the need for a critical transfer phase, and therefore saves net project time. This opens up the opportunity for these concepts to be more cost-effective. On the contrary, the ‘approach’ and ‘departure’ phases could take more time and the limits could be more stringent due to the fixed connection potentially creating a bottleneck operation. Adding to that, the flexibility of the concepts is limited.

3.3. Conclusion

This chapter states the need to determine the requirements of a commercial 20 MW WTG as the reference 20 MW WTGs do not represent the characteristics of commercial turbines. Both blade and RNA mass are estimated too heavy. Furthermore, the power density of the 20 MW reference turbines, differs too much to conclude to a rotor for a commercial 20 MW WTG. The characteristics of the WTGcomponents influence the possible installation strategies, loadout, type of feeder vessel and type of equipment used for the feedering operation. Chapter 5 follows up the need from this chapter and presents the characteristics of a commercial 20 MW WTG which are acquired through a scaling analysis.

WTIVs are the preferred vessel of choice for WTG installation due to their inherent stability. WTIV designs will keep evolving together with WTGs to meet the installation requirements of next-generation WTGs. The current and ordered fleet of vessels capable of installing 20 MW WTGs is slim, but vessels could be upgraded to meet the requirements for installing 20 MW WTGs. Future WTIV concepts could operate with lower daily vessel costs and reduced VOYEX decreasing the total costs of installation. Operational advantages could exist for future WTIV designs. However, for the research part of this thesis, future WTIV designs do not influence the feedering operation itself. Industry also developed alternative concepts which eliminate the floating-to-fixed transfer. These concepts could be more effective but have limited flexibility and create potential bottlenecks by creating a fixed connection between the feeder and the WTIV. These concepts will not be evaluated for this thesis.

During the transfer operation, the barge is preferably positioned in head waves, as this provides the highest operating limits. This might not always be possible with the current WTIV - feeder mooring system due to the positioning of the jack-up or a change in wave direction while the feeder is already moored to the WTIV. Dynamically positioned barges with weathervaning capability could provide a solution to this difficulty and increase workability. Operational advantages can also be attained by mooring systems designed to alter the first-order vessel responses. However, these systems will not be considered for this thesis.

4

Problem Analysis and Approach

This chapter analyzes the problem and presents the framework to answer the main question and thus acquire the characteristics of an optimized feedering method for 20 MW WTG installation. First, the problem is presented after which the requirements for the solving method are posed. Section 4.3 consequently presents and explains the solving framework. Finally, section 4.4 discusses the simplifications made for this research.

4.1. Problem analysis

No research has yet been performed on feedering method transportation and installation of the superstructure of 20 MW WTGs. Adding to that, the effects of vessel characteristics, equipment characteristics and installation methods on the performance of the feedering installation method are still unknown. The research focuses on providing the relations between vessel and equipment characteristics and installation methods on the performance of feedering method transportation and installation of the superstructure of 20 MW WTGs.

4.2. Method Requirements

In order to answer the main- and subquestions posed in the introduction and provide a solution to the problem stated above, the solving model must comply with the following requirements:

- the model must capture the requirements for transporting and installing 20 MW WTG components
- the model must capture the influence of varying vessel characteristics on operating limits and daily vessel costs
- the model must capture the influence of varying motion compensation characteristics equipment on operating limits and equipment costs
- the model must capture the influence of the installation method on operating limits, required vessels, required equipment and operational characteristics
- the simulated system models must be feasible
- the performance of the system must be captured by the KPIs mentioned in section 2.5
- the model must capture external influences on the system's performance

4.3. Research Method

The framework fuses the systems engineering framework with Set-Based Design (SBD). Appendix H provides the background to these design methods. The variables in section 2.4 can be divided into external and internal factors. External factors describe the setting in which a system performs and internal factors are variables used to synthesize the different solutions within the design space. Figure 4.1 presents the proposed framework to solve the problem.

4.3.1. Requirements analysis

The factors that are considered external factors only influence other (internal) factors and are not influenced by other factors. From the N2 chart, it can be seen that these factors are: the number of WTGs to be installed, the distance to the marshaling port, inner array distance, WTG characteristics, mobilization distance and the weather. These factors form the input conditions.

The requirements follow from the 20 MW U.S. wind market which is described by combining sections 1.1.2 and 1.1.3 which set out the U.S. wind market, and section 5.2 which describes the characteristics of a 20 MW WTG. The operational needs and constraints are consequently identified and clarified in terms of what the system must do, and what constraints it must fit in section 5.3.

4.3.2. Physical definition

The physical definition step is where the concepts are actually synthesized and where set-based design is used. The solutions follow from variations and combinations of the internal factors. Solutions are synthesized for vessel and equipment type and the installation strategy. These are then combined and assessed for compliance with the system requirements resulting in feasible system models. Chapter 6 covers this definition and relates these three factors to operational characteristics, operability and costs.

4.3.3. Design validation

The last stage validates the model of the system. It is therefore necessary to create a model of the environment with which the system can interact to assess the system's performance. This model will reflect the evaluation criteria to which the system solutions are tested. This is achieved through the use of a DES model. The DES model takes the costs and combined operability of a system and couples this to long-term weather data in order to assess the performance of a system. Chapter 7 describes this DES model.

With this last step, the method distinguishes itself from current design methods and with that introduces a new method to find an optimum within a design space. This method uses a new approach to determine a vessel's performance by simulating and analyzing the actual weather-related downtime. The method distinguishes itself from the work performed by Sandvik [45] by including the costs of every individual configuration. This provides a more complete picture of a vessel's performance. This approach enables the comparison of different operational strategies, similar to the method of Smorenberg [21], while also considering how the operational strategy impacts both a configuration's combined operability and costs. Application of this methodology provides knowledge regarding the weather delay susceptibility and related operational performance of proposed configurations in early design stages.

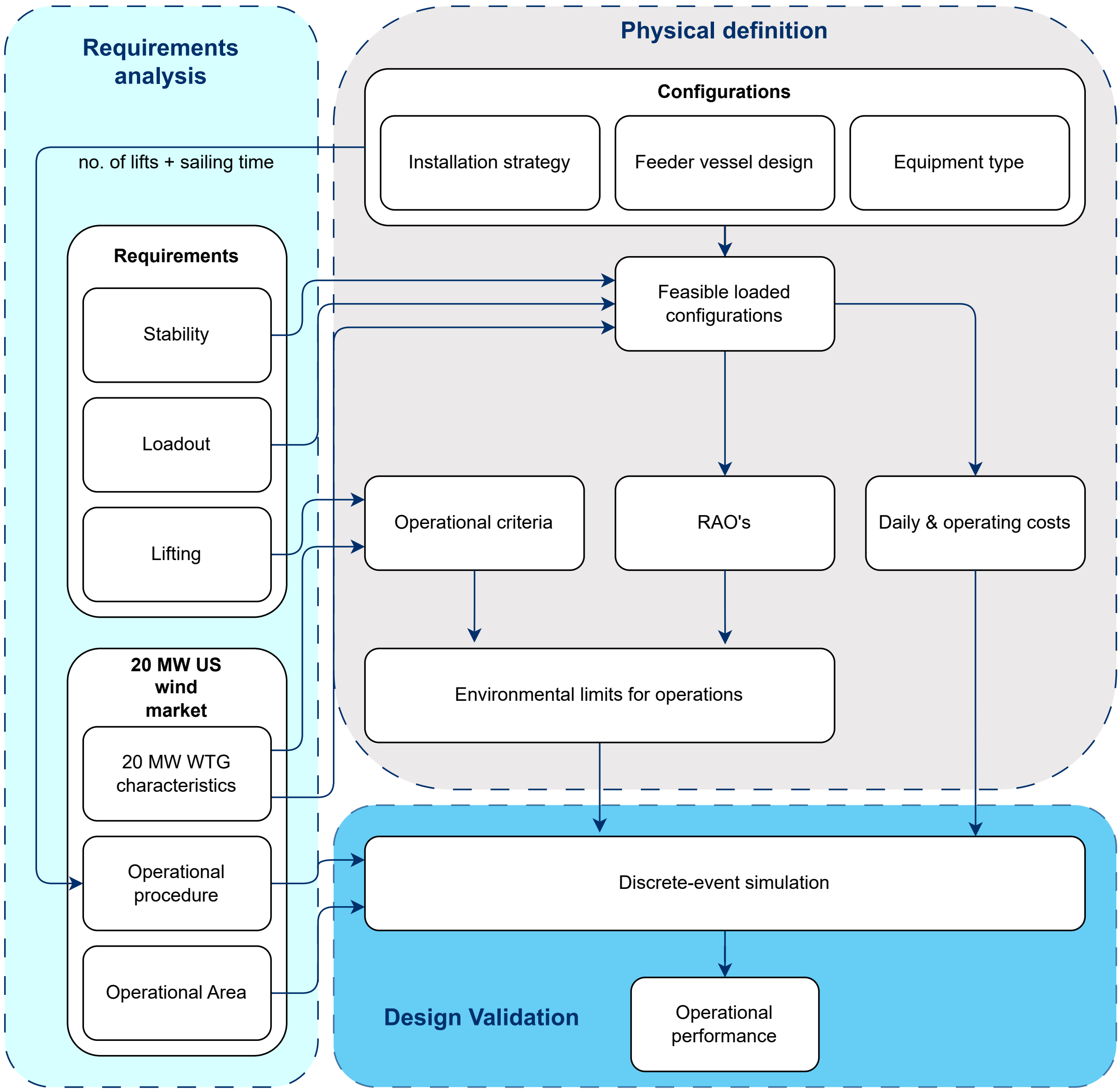

Figure 4.1: Solving Framework.

4.4. Simplification

The analysis of the feedering method for 20 MW WTG installation is a complex problem. In order to address the impact of vessel and equipment characteristics along with various installation strategies while maintaining a high-level perspective, it is essential to simplify the problem. The problem is simplified for determining the operational limits and characteristics used in the simulation in section 4.4.1 as well as for the simulation itself in section 4.4.2.

4.4.1. Operating limits and characteristics

Both the offshore transfer and WTG installation phase as described in sections 2.2.6 and 2.2.11 are modeled by simulating each individual lift. This means that the operating limits for each individual lift must be determined.

The operating limits for the operations where the feeder is included are determined for only two cases: the transit operation and the blade rack lift. This decreases the variables and level of complexity of the problem. For the transfer operation, the feeder is preferably moored in head waves as this leads to the lowest vessel responses. The assumption is thus that the WTIV is positioned in such a way that the feeder will be oriented in head waves, with a 15-degree margin to either side, for all operations where the feeder is moored to the WTIV. In head waves, the H_s at which roll and pitch compensation limits are reached, is higher than the transit H_s limits and will not be reached due to the required weather window used for initiating the transit operation. While the feeder is moored in head waves, it can remain moored up to 3 meters H_s [29]. This means that the vessel can remain continuously moored to the WTIV as these limits will not be governing. For the transfer of the nacelle and the tower components, the limits for transit will therefore be used as the operating limits. According to the Barge Feeder Alliance [30] and the NYSERDA [6], lifting the blade rack is the most critical lift in this orientation due to re-hits. As 20 MW WTG blades are even longer than the ones used in these critical lift assessments, this lift becomes even more critical.

The operating limits for the installation phase where only the WTIV is included are kept equal to the base case as presented in appendix M and thus do not vary for every configuration. The H_s limits used are independent of the peak period. In reality, the peak period influences the operating limits of the operations included in the installation phase, especially for the nacelle and blade installation which are the most critical operations of the installation phase [71]. The wave and wind related operating limits depend on a multitude of factors including the properties of WTG itself, its foundation, the soil conditions and the equipment used for installation. Determining these limits and designing and evaluating innovative lifting equipment is out of the scope this research.

4.4.1.1. Blade rack lift operation

While the barge is in head waves, pitch motions are the most significant. Due to the blade rack's long footprint and absence of pitch compensation, lifting the blade rack and backloading the empty blade rack become critical operations [21] [6] [30]. Lifting of the blade rack becomes critical due to the occurence of re-hits. Although the operation is different, it is assumed that backloading the blade rack has the same limits as lifting the blade rack. In reality,alternative equipment (such as a pitch compensating spreader) could and perhaps should be employed to extend the boundaries of the backloading operation, as opposed to the equipment utilized to enhance the operational limits of lifting the blade rack. Three different loading conditions are introduced in chapter 6 for each barge. For determining the operational limits of the blade rack lifting operation only one loading condition is considered. Only the nacelle is present on the barge after the blade rack is lifted. This means that the difference between the loading conditions can be neglected. This simplification is made to reduce computational intensity.

4.4.1.2. Transit operation

For conventional transit operations, performed by WTIVs, the maximum component accelerations are never reached and do not determine the maximum operating limits. This is due to the large inertia of the WTIV. In this case, a maximum significant wave height, based on the desired workability, is determined to which the seafastening is designed accordingly. However, a feeder is more susceptible to waves and the acceleration limits of the WTG components become governing [72].

During transit, the maximum allowable accelerations of the components shall not be exceeded. These accelerations are provided by the WTG suppliers and determine the operating limits of the feeder. The motion responses and thus the component accelerations vary for every heading orientation. The feeder and its components will experience maximum acceleration when the waves come in at a 90 ° angle, this is the so-called beam seas. Although the feeder could technically orient itself in head waves to minimize accelerations and not surpass component acceleration, the assumption is made that the feeder will not sail out given that it should orient itself in 'survival mode' and not be able to take waves from any given direction. Therefore only the most stringent case of beam seas will be analyzed to determine the maximum significant wave height in which the transit operation can take place. Figure 4.2 shows the considered wave headings when the feeder is moored to the WTIV and during transit.

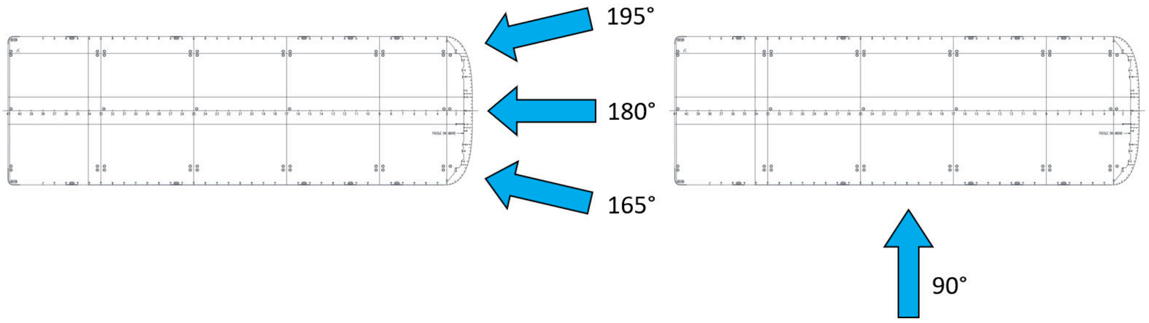

Figure 4.2: Considered wave directions for component transfer (left) and transit (right).

4.4.1.3. Vessel Type

Different vessel types can be used as a feeder vessel for WTG components as described in section 3.2. The GAO stated in their report that besides WTIVs, dedicated DP feeder vessels are also unlikely to be built. This research therefore only incorporates barge-shaped feeder vessels. This simplification could miss the benefit of using a ship-shaped feeder vessel. However, the dayrate for a U.S. built DP vessel is unknown, which makes it hard to qualitatively assess the accompanying dayrates of such vessels. This simplification thus misses out on the potential benefit of a different ship type but improves on the qualitative assessment of costs.

4.4.1.4. Vessel Strength

For all configurations and operations, vessel and seafastening strength are not taken into account. It is assumed that the vessel and the seafastening can withstand the forces acting on it. For a full feasibility assessment, these strengths should be assessed. If the barge and seafastening don't comply with strength criteria, they can be reinforced. This process will add extra weight to the vessel which will, depending on the scale of the reinforcements, change its properties and therefore its dynamic behaviors. Since mass increases due to reinforcements are not taken into account, their effect on vessel behavior is neglected. In addition, for a Jones-Act compliant vessel, it is of the utmost importance that reinforcements are less than 7,5% of the total steel weight in case the reinforcement works are performed outside the U.S. to still comply with the Jones Act [1].

4.4.2. Simulation

The simulation models only weather-related downtime. Downtime due to any other reason such as, but not limited to, equipment failure, maintenance or managerial inefficiencies is not taken into account. The results of the simulation should therefore be assessed on a relative basis and not on their absolute value. Only one cause for downtime is taken into account, which makes it likely that the absolute results of the simulation are off. The simulation thus only models the performance of difference configurations in relation to the weather conditions.

The weather data consists of hourly measurements at the offshore site. No weather data is available for the marshaling port or on the route from the ports to the offshore site, therefore all operations are assessed with the weather at the offshore site. In reality, weather conditions vary between the port and the offshore site, making the simulation for the port and transit operations less accurate. This simplification also avoids the need to use separate datasets for the port and offshore conditions and interpolating between those, or switch to datasets on the route between the port and the offshore site for the simulation of the transit operation. In order to work with the hourly dataset, avoid interpolation and thus allow for computationally less intensive simulations, the duration of all operations and timesteps are discretized to whole hours.

During the installation of the OWF the WTIV remains at the installation site. This means that the WTIV needs to be refueled and resupplied by other vessels, adding extra operations and increasing both total duration and total costs. These processes of refueling and resupplying are not taken into account in the simulations. Next to that, the main and assistance tug will constantly stay with the barge. also when it is moored to the WTIV. The main tug is based on the required bollard pull, while the assistance tug is a 110 ton bollard pull tug for all configurations.

Demobilization is expected to represent a significant part of the total costs according to Kaiser and Snyder [38]. The cost of demobilization depends predominantly on the mobilization time which in turn depends on the mobilization distance and the steel works that have to be carried out. Since the required vessel reinforcements for the vessel are not determined, no conclusion can be made regarding the required steel works. Also for the mobilization distance, no conclusion can be made. The barges are preferably stationed at a location near the marshaling port to minimize the mobilization distance. However, this completely depends on the availability of the barges. Adding to that, the steelworks preferably have to be carried out in a port near the original port of the barge or the marshaling port to reduce mobilization distance and time.

In reality, this does not always happen. The mobilization for Vineyard OWF provides a perfect example. The Jones-Act compliant barges were first transported to the European continent, where the steel works were carried out and sea fastening was installed. They were then towed back across the Atlantic to the New Bedford Marine Commerce Terminal. This example portrays that mobilization can in reality deviate significantly from a theoretical 'efficient' mobilization. The simulation therefore only simulates the operational result where the operation starts with loading the first feeder and ends as the WTIV is jacked down. This simplification makes that the KPI to measure a configuration's financial performance becomes the 'Operational contractor costs'. These are equal to the Total Contractor Costs excluding the mobilization costs. Equation 4.1 presents the formula for these costs and the associated KPI.

$$C_{\text{operational contractor}} = (C_{\text{vessel daily}} + C_{\text{tool daily}}) * t + C_{\text{voyex}} \tag{4.1}$$

4.4.3. Simplification overview

The overview below provides a summary of the simplifications that are made in order to determine the characteristics of an optimized feedering method for the installation of 20 MW offshore Wind Turbine Generators.

- **General**
  - only barge-shaped vessels are analyzed
  - the feeder and its seafastening can withstand the forces acting on it
  - two tugs constantly accompany each barge
- **Simulation**
  - time is passed in whole hourst
  - only offshore weather data is used for the simulation
- **Costs**
  - only contractors costs are included
  - mobilization costs are not taken into account
  - port costs are based on New Bedford Marine Commerce Terminal
  - price levels are for the current market
- **Operational limits**
  - transit limits determined for beam waves
  - blade rack lift limits determined for head waves with 15 ° margin
  - all transfer operations except the blade rack lift and backloading operations have the same wave height limits as the transit operation
  - current is not taken into account
  - there is no wave limit for port operations
  - installation limits remain equal to the base case

5 System requirements

This chapter covers the requirements to which the system shall adhere. First, the environment is specified 5.1. The WTG characteristics are consequently presented 5.2 as these serve as input for the operations that shall be carried out. Finally, the general requirements to which all configurations shall adhere are presented in section 5.3. These requirements cover the requirements regarding stability, vessel loadout and maximum allowable accelerations.

5.1. Environment

The system shall operate in the environment as presented in section 1.1.3.2. The system will install a total of 62 20 MW WTG superstructures. This means that the results from this research are only valid for this specific environment where an equal amount of WTG superstructures are installed. For environments with different conditions or a different number of WTGs, new simulations shall be carried out to determine a system's performance.

5.2. 20MW scaling assessment

The commercial 20 MW WTG is not yet defined. To obtain a clear input for the requirements for the feedering method, the characteristics of 20 MW WTG components must be known. These are obtained through a scaling assessment, the outcomes of which are detailed in this section. The methodology employed in the scaling assessment is outlined in Appendix I.

The physical properties: mass, dimension and inertia of the WTG components influence the loadout and dynamic behavior of the vessel. The general dimensions of the 20 MW WTG and its components used for this thesis are tabulated in table 5.1. The inertia of these components scales with respect to their reference components by a mass and length relation using radii of inertia. The different installation strategies as presented in section 6.1.2 require the WTG tower to be split up into multiple sections. The physical properties of the individual sections are therefore important as well. Figure 5.1 shows the split of the tower in its sections. Table 5.2 presents the physical properties of the individual tower sections and combinations thereof.

Table 5.1: 20 MW WTG characteristics.

Parameter	Value	Unit
Capacity	20	MW
Power density	357,3	W/m^2
Rotor area	55923,9	m^2
Diameter	266,8	m
Hub height	163,4	m
Blade length	130,1	m
Blade mass	90,82	t
Blade COG	34,6	m
Blade rack length	73,5	m
Nacelle mass	1011	t
TP height	20	m
Tower height	136,35	m
Tower mass	1233	t
Tower COG	55,9	m
Tower diameter bottom	10	m

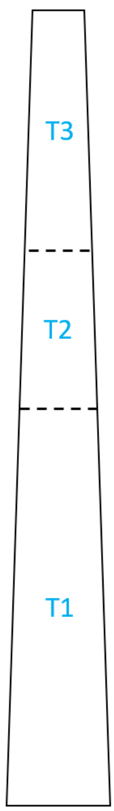

Figure 5.1: Division of the WTG tower into its sections.

Table 5.2: Tower section properties.

	Unit	Full Tower	T1	T2T3	T2	T3
Mass	[t]	1233	750,0	483,1	241,6	241,6
COG height	[m]	55,93	29,33	28,46	9,96	20,81
R1 at COG	[m]	4,180	4,570	3,626	3,898	3,373
Thickness	[m]	0,0441	0,0513	0,0382	0,0508	0,0315
Height	[m]	136,35	65,20	71,16	24,91	46,25
Density	[t/m^3]	7,85	7,85	7,85	7,85	7,85
I_{zz}	[kg · m^2]	21315,67	15486,53	6286,068	3622,704	2723,344
I_{xx}	[kg · m^2]	1921248	273400,3	206990,9	14299,61	44433,45

5.3. Operational requirements

This section discusses the requirements to which each configuration, presented in chapter 6, shall adhere. These requirements follow from rules and standards as presented by DNV-GL and requirements set by WTG manufacturers. The latter can vary for each manufacturer and can change over time due to technological advancements.

5.3.1. Maximum allowable accelerations

According to the confidential documents as provided by WTG manufacturers, the maximum allowable component accelerations differ per turbine manufacturer. The current documents show that GE WTG components can handle the lowest accelerations. In the US onshore market, General Electric (GE) has a market cap of 47% and it is therefore likely that they will also take up a big part in the offshore market [73]. Adding to that GE is a domestic company, making it more likely to supply for its domestic market. Since GE has the most conservative allowable accelerations and is most likely to supply the U.S. market, the acceleration limits of GE are used as governing for the remainder of this thesis.

Table 5.3 presents an overview of the maximum allowable accelerations per component. The accelerations are documented as how the components are loaded on the vessel, with the axis orientation equal to the vessel's axis system. These accelerations shall not be exceeded during any of the performed operations.

Table 5.3: Maximum allowable accelerations for WTG components.

Max accelerations	Unit	Tower	Nacelle	Blade
a_x	m/s^2	5,9	2,943	3,924
a_y	m/s^2	5,9	5,396	7,55
a_z	m/s^2	4,91	4,905	7,55

5.3.2. Stability

All configurations must comply with the general criteria regarding righting lever properties. These criteria are provided by IMO [74] and hold that:

- the initial metacentric height GM_0 shall not be less than 0,15 m
- the maximum righting lever should occur at an angle of heel preferably exceeding 30° but not less than 25°
- the righting lever (GZ) shall be at least 0.20 m at an angle of heel equal to or greater than 30°
- the area under the righting lever curve (GZ curve) shall not be less than 0.055 metre-radians up to θ = 30° angle of heel and not less than 0.09 metre-radians up to θ = 40° or the angle of flooding θ_f if this angle is less than 40°. Additionally, the area under the righting lever curve between the angles of heel of 30° and 40° or between 30° and θ_f, if this angle is less than 40°, shall not be less than 0.03 metre-radians

In addition to the general criteria regarding righting lever properties, IMO poses additional criteria for pontoons and barges. These criteria hold that:

- the area under the righting lever curve up to the angle of maximum righting lever should not be less than 0.08 metre-radians
- the static angle of heel due to a uniformly distributed wind load of 540Pa should not exceed an angle corresponding to half the freeboard for the relevant loading condition, where the lever of wind heeling moment is measured from the centroid of the windage area to half the draught
- the minimum range of stability should be:
  - for L ≤100 m 20 °
  - for L ≥150 m 15 °
  - for intermediate length by interpolation

5.3.3. Loadout & lifting

The vessel loadout requirements follow from disclosed documents provided by several WTG manufacturers. The requirements regarding loadout conclude that;

- the WTG components must have a clearance of at least 1 meter during transit
- the WTG components must have a clearance of at least 3 meters during lifting operations
- all component and seafastening foundations must fit on the deck of the vessel

For this research, no difference will be made between the layout during transit and lifting operations. This means that all components shall have a clearance of at least three meters during any of the operations.

6
Fleet configurations

This chapter describes the configurations within the design space. First, section 6.1 presents an overview where the concepts are defined within the design space and the concepts are introduced on a high level. The following section 6.2 describes the properties of the configurations including the methods and assumptions used to determine their properties. Section 6.3 consequently describes the operational limits and the methodology to determine these limits. Finally, the operational characteristics including day rates and methodology associated with each configuration are determined in section 6.4. A summarized overview of all configurations and their properties can be found in appendix J.

6.1. Configuration overview

The literature study concludes that the effect of varying the feeder vessel, installation methodology and motion compensation have a significant effect on operational performance and must be investigated. This section describes the individual variables and with that sets the design space.

6.1.1. Feeder vessels

The 400 feet barges currently used for the vineyard project are the largest barges available in the U.S. [75] [76] [77]. The report for NYSERDA by Marin USA concludes that larger barges increase the operating limits [6]. These larger barges are currently nonexistent. Therefore, in addition to the currently used barges, Memphis Bridge and Marmac400, three conceptual barges are created. The dimensions of these barges are based on a parametric analysis of various existing launch barges. The lengths of the additional barges are 140, 160 and 180 meters. Breadth and depth are scaled according to trend analysis as a linear function of length. This results in the general dimensions presented in table 6.1. The Marmac400 barge has similar properties as the Memphis Bridge barge and is therefore left out for clarity.

6.1.2. Installation methodology

The current installation methodology is an indirect 6-lift strategy where all the blades and nacelles are installed individually and the towers are split up into two pieces. With the rapid increase of WTG capacity, pre-onshore assembly concepts are difficult to adopt [25]. Strategies including onshore assembly are therefore discarded. Ahn et al. and Smorenberg both conclude that an advantage could be obtained by minimizing the number of lifts [25] [21]. A strategy where the tower is transported, lifted and installed in one piece must therefore be considered in addition to the current two-piece strategy. Finally, splitting the tower into more than two components could result in improved operating limits by lowering the Center of Gravity (COG) of the towers which results in lower roll-induced sway accelerations at the tower's COG. This option will also be considered to analyze a case in which high-capacity motion compensation devices, such as the Heavy Feeder, are insufficiently available or perform below their expectations. The different installation methodologies thus entail an installation strategy in which the tower is split up into either one, two or three pieces.

6.1.3. Motion compensation

Given the simplifications, upgrading the motion compensation devices' roll and pitch compensation capacity will not influence the operating limits of the current transfer operations. Only an increased capacity, in terms of stroke and quick lift velocity, of a quick lift AHC can improve the current transfer limits, where its improvement is limited to the blade rack and backload transfer limits. However, such systems are currently in full development and it is uncertain where future systems will exactly move towards in terms of their capacities. This makes defining an actual future inline AHC more of a guess. This is therefore left out. However, a sensitivity study regarding the parameters of the heave compensator is performed to showcase the potential of future, upgraded inline AHC systems.

Also, the installation strategy where the tower is transported, lifted and installed in one piece requires a roll, pitch compensation platform which almost doubles the tower carrying capacity of the current Heavy Feeder. This type of motion compensation device does not yet exist and its capacity and properties shall be approximated on a high level in section 6.2. Figure 6.1 shows the type of motion compensation systems discussed.

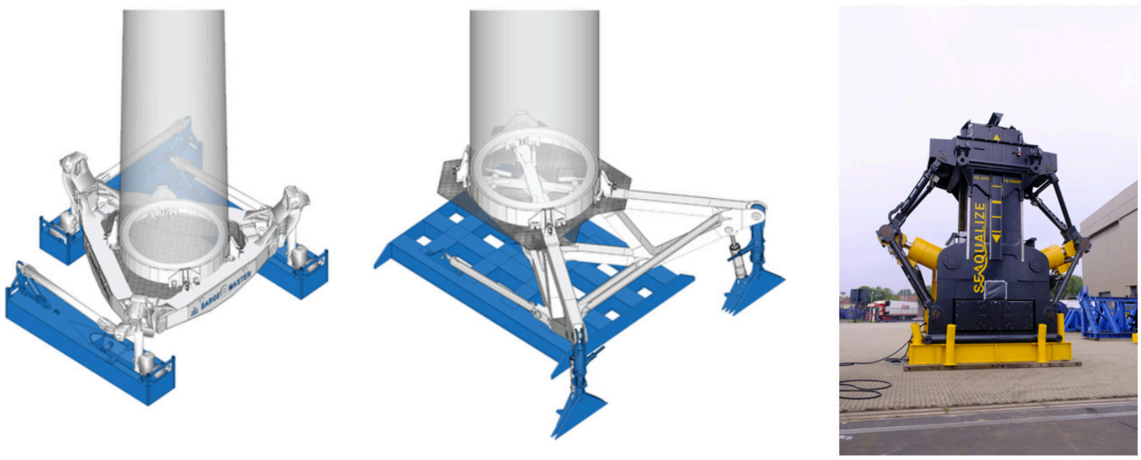

Figure 6.1: From left to right: motion compensation platform T700, motion compensation platform Heavy Feeder [78], inline AHC by Seaqualize [79].

6.1.4. Design space

Combining the individual variables mentioned above provides a two-dimensional design space. Heave compensation is no longer considered as a variable since a sensitivity analysis will be carried out and the variety of roll-pitch motion compensation platforms is a direct effect of the installation strategy, not a variable in itself. This leads to the motion compensation device no longer being a leading variable of the design space for this thesis. However, the importance of motion compensation devices and their influence on operational performance shall not be neglected. Figure 6.2 presents the resulting design space where the cells contain the ID of the configurations.

6.2. Configuration properties

Before the operational limits and characteristics can be determined, several properties of each configuration are required. The operational characteristics hold the operating dayrates and the method by which the installation is taken out. In order to determine these, the mass, inertia and layout of the complete configurations and the 3d model of each barge are required.

6.2.1. Barges

The barge properties are based on the Memphis Bridge barge in terms of weight and inertia. The weight of the vessel is assumed to scale quadratically with length. When a larger barge has to be made, it is assumed that plates of equal thickness will be used, the plates will then only scale in length and width resulting in a quadratic scaling of mass since both length and width scale linearly with λ.

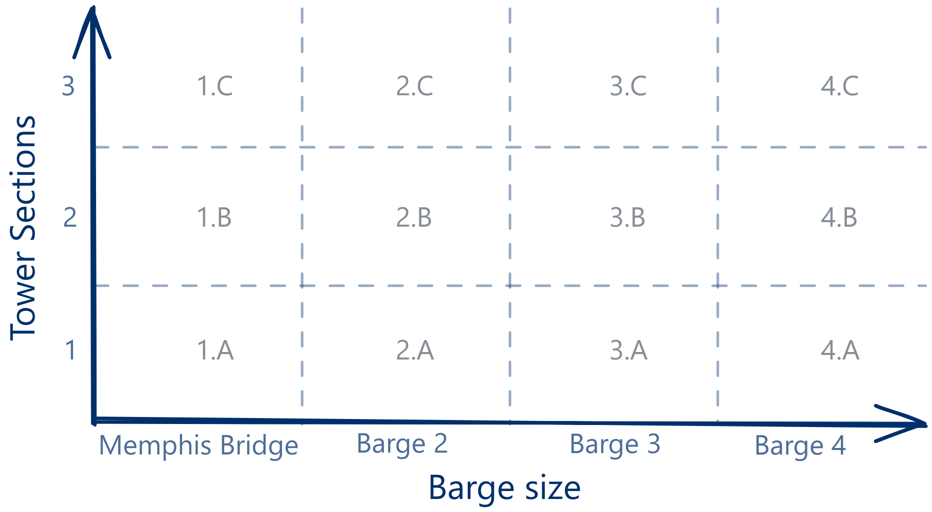

Figure 6.2: Design space of the configurations.

For a vessel with unknown distribution of its solid mass, the radius of inertia can be estimated by formulas 6.1. The barges have the same mass distribution and can thus use the same factor to determine their radius of inertia. The moment of inertia can consequently be determined through equations 6.2. The coupling terms are generally small and can therefore be neglected.

$$\begin{aligned} k_{xx} &= 0,30 \cdot B \text{ to } 0,40 \cdot B \\ k_{yy} &= 0,22 \cdot L \text{ to } 0,28 \cdot L \\ k_{zz} &= 0,22 \cdot L \text{ to } 0,40 \cdot L \end{aligned} \tag{6.1}$$

$$\begin{aligned} I_{xx} &= LSW_{barge} \cdot k_{xx}^2 \\ I_{yy} &= LSW_{barge} \cdot k_{yy}^2 \\ I_{zz} &= LSW_{barge} \cdot k_{zz}^2 \end{aligned} \tag{6.2}$$

These equations show that the radii and moment of inertia can also be directly obtained through scaling laws. The scaling laws for mass, radii of inertia and moment of inertia used for this research are displayed in equation 6.3 [43]. The coupling terms are generally small and therefore neglected. Table 6.1 provides the non company confidential properties of each barge.

$$\begin{aligned} \lambda &= \frac{L_{\text{New barge}}}{L_{\text{Memphis Bridge}}} \\ LSW_{\text{New barge}} &= LSW_{\text{Memphis Bridge}} \cdot \lambda^2 \\ k_{\text{New barge}} &= k_{\text{Memphis Bridge}} \cdot \lambda \\ I_{\text{New barge}} &= I_{\text{Memphis Bridge}} \cdot \lambda^4 \end{aligned} \tag{6.3}$$

Where:
λ = Length based scaling factor

For the diffraction analysis, a generic barge is used which is scaled to the right dimensions for each conceptual barge. The generic model is based on a Crowley 455 Barge. Figure 6.3 presents a 3D model of the barge.

Table 6.1: Barge properties.

Barge	L [m]	B [m]	D [m]
Memphis Bridge [80]	122,76	30,4	6,55
Barge 2	140	35,7	8,47
Barge 3	160	40,8	10,22
Barge 4	180	45,9	11,97

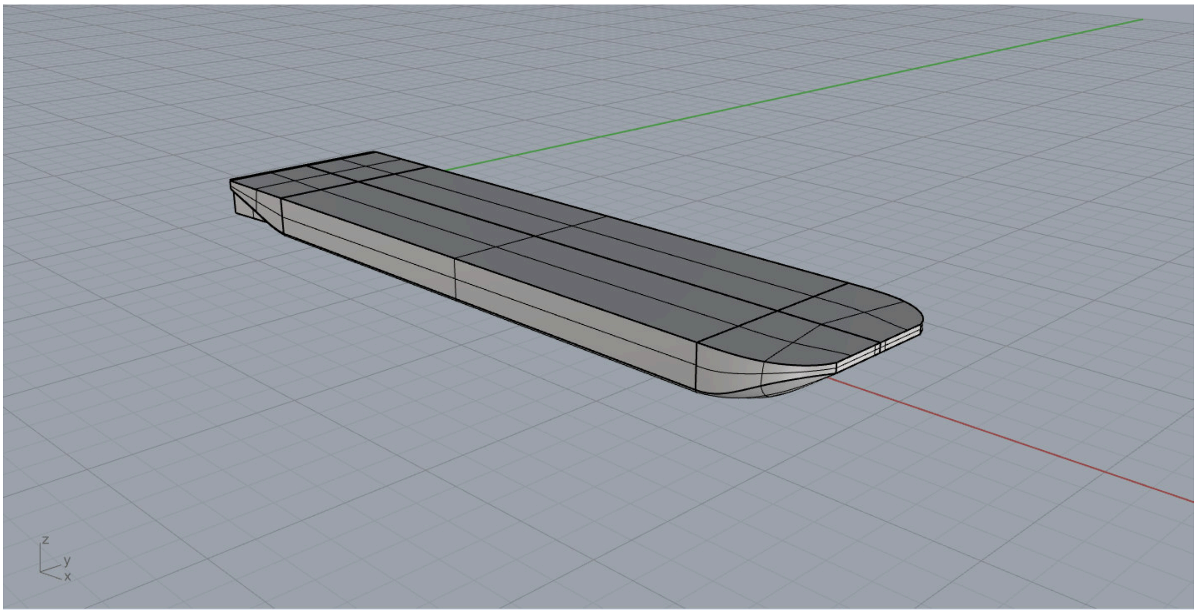

Figure 6.3: 3D model of the barge.

6.2.2. Motion compensation

The three motion compensation platforms considered are the Bargemaster T700, Barge Master Heavy Feeder and a conceptual motion compensation platform, further referred to as the Mega Feeder, which is a scaled-up version of the Barge Master Heavy Feeder. The properties of the T700 and Heavy feeder are known and provided by TWD under disclosure. Based on the properties of the heavy feeder and the loading conditions for the Heavy Feeder and the Mega Feeder, the properties of the conceptual Mega Feeder can be estimated. The Heavy Feeder is able to carry Tower 1+2 and Tower 2+3 of the Haliade X tower while the the T700 can only carry Tower 1, 2 or 3 and not a combination of any of those [78]. The mass, COG height and section height of these tower sections are company confidential.

The capacity of a motion compensation platform can be expressed in the overturning moment it can compensate. An overturning moment is created as a roll or pitch motion is introduced since the COG of the tower will no longer be above the center of the motion compensation platform. This is schematically visualized in figure 6.4. For small angles, the overturning moment is expressed by equation 6.4. It can be seen that the overturning moment scales linearly with both tower mass and height of the tower's COG.

$$M_{\text{overturning}} = \theta \cdot h_{cog} \cdot m_{\text{section}} \cdot g \tag{6.4}$$

To withstand a larger overturning moment, the dimensions and therefore the mass of the conceptual motion compensation platform shall increase with respect to the Heavy Feeder. The Heavy, and Mega Feeder are complex structures and a structural analysis to determine the exact properties of such systems, is out of the scope of this research. However, it is known that the mass and dimensions will increase which will also impact the vessel's behaviour. Therefore a simplified scaling analysis is performed to obtain the order of magnitude of the properties of the conceptual motion compensation

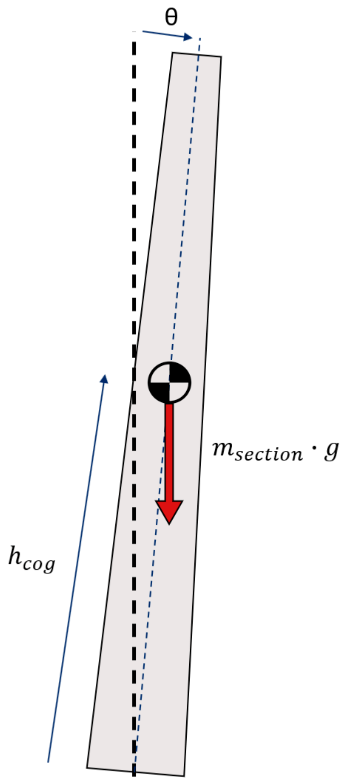

Figure 6.4: Visualization of overturning moment.

platform. This method should not replace an actual structural analysis, and it is therefore recommended to execute such an analysis in future work to assess the viability of such a system.

The heavy feeder's structure is simplified as a simple beam and it is assumed the complete structure is scaled to withstand the larger moment. Just as for the barges, mass scales with λ^2 since the heavy feeder is assumed to be a plate-based structure. The scaling is based on the formula for maximum bending stress in a structure where the maximum ending remains the same. This gives the relations provided by equation 6.5. The resulting parameters of the scaling analysis are company confidential.

$$\begin{aligned} \sigma &= \frac{M \cdot c}{I} \rightarrow M = \frac{\sigma \cdot I}{c} \\ I &\sim \lambda^4 \wedge c \sim \lambda \rightarrow M \sim \lambda^3 \\ m &\sim \lambda^2 \rightarrow M \sim m^{1,5} \end{aligned} \tag{6.5}$$

Where:

σ	= Bending stress
M	= Bending moment
c	= Distance of outer fiber to the neutral axis
I	= Second moment of inertia
λ	= Length based scaling factor
m	= Mass of the platform

6.2.3. Layout

The layout of the vessel determines its COG and inertia. Layout optimization can be an intensive iterative process. For this research, no iteration is performed on the actual layout. Every installation methodology with, one, two or three tower sections, has its own layout which is applied across all barges. During all operations, motions are desired to be as low as possible. This is attained by keeping all components as close to the overall COG as possible while still respecting the required clearance of three meters for lifting components. The layout for Vineyard OWF is used for the two-tower sections strategy and used as a base for the one- and three-tower section strategies. The simplified layouts are displayed in figure 6.5, where the blue cube represents the nacelle. It can be seen that the blades protrude from the vessel. This will be the case for all loading conditions on the Memphis bridge barge and on Barge 2.

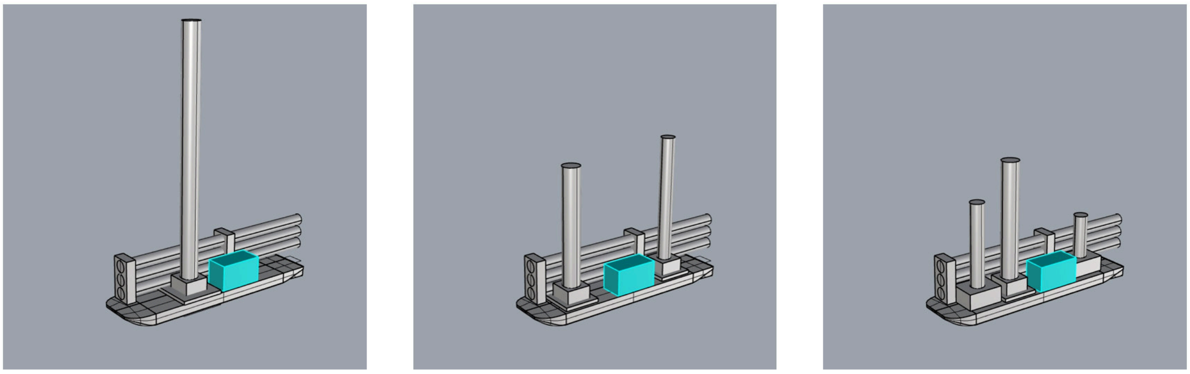

Figure 6.5: From left to right, loading condition one to three.

The layouts including all miscellaneous items present on the barge create a unique weight distribution for each configuration. To prevent heel, the barges are ballasted until the COG is above the keel line. Regarding the total inertia of the vessel, components with a weight below 1% of the total weight are assumed to have a negligible moment of inertia with respect to the total inertia. These components are thus treated as point masses. For all other objects, the inertia around the vessels COG is calculated by means of Steiner's theorem which is displayed in equation 6.6. The stability check performs a feasibility check on each configuration. Formula 6.7 calculates metacentric height (GM) for each concept. This value shall be higher than 0,15 meters to comply with initial stability criteria. All configurations comply with the initial stability requirements. All concepts also comply with the remaining criteria set in section 5.3. These criteria are assessed by comparing the Vertical Center of Gravity (VCG) for the most critical case regarding stability, configuration 1, to the VCG tables from the stability booklet of a similar barge.

$$I_{COG} = I_{cm} + m \cdot d^2 \tag{6.6}$$

Where:

I_{COG}	= Moment of inertia with respect to the global COG
I_{cm}	= Local moment of inertia
m	= Mass of the object
d	= Distance between COG of the object and global COG

$$GM = KB + BM - KG \tag{6.7}$$

6.3. Operating limits

Each operation has its operational limits to which it can proceed. These limits are determined by maximum allowable accelerations, velocities or displacements. These motions are predominantly caused by waves that excite the vessel. Section 6.3.1 provides an introduction to vessel motions, responses in irregular seas and assumptions used for the motion analysis. Sections 6.3.2 and 6.3.3 describe the associated operating limits for the transit and blade rack and backload operations respectively which are all driven by the responses of each configuration.

6.3.1. Vessel motions

The response characteristic of a vessel due to waves can be described by a RAO. Displacement RAOs describe the motion response of the vessel per meter wave amplitude at a specified frequency. A RAO consists of an amplitude and a phase part. The amplitude part relates the amplitude of the vessel motion to the amplitude of a wave. The phase part defines the timing of the vessel motion relative to the wave. The RAOs are determined with ANSYS AQWA, a diffraction analysis software.

As a vessel rolls, it dissipates energy. The amount of energy that dissipates is a crucial parameter for the proper estimation of the vessel's behaviour in seaway [81]. The diffraction analysis excludes viscous roll damping. To compensate for this absence, the additional roll damping value is set to 6% of the critical roll damping to make the vessel motion analysis comparable to the motions analysis as performed for Vineyard OWF.

When a vessel is excited by regular waves, the RAO can directly be used to determine the response of the vessel. However, the sea has irregular waves. These can be described as a summation of regular waves. A wave spectrum describes this summation of waves. This research uses a JONSWAP spectrum with peak periods (Tp) ranging from 4 to 20 seconds. The spectrum is further described by a peak enhancement factor (γ) of 3,3 and a wave spreading with 10 wave directions and a spreading coefficient of 11. These values are recommended by Det Norske Veritas (DNV) [82] and TWD respectively. A comparison between the motion analysis performed by DEME for Vineyard OWF and the motion analysis performed for this research as described in section 6.3.2 proves that the described parameters of the JONSWAP spectrum are representable for the Vineyard site.

6.3.2. Transit limits

During the transit operation, the maximum allowable component accelerations shall not be exceeded. These accelerations are provided by the WTG suppliers and determine the maximum seastates in which the feeder can operate. The feeder and its components experience maximum acceleration when the waves come in at a 90 ° angle [83]. Although the feeder could technically orient itself in head waves to minimize accelerations and not surpass maximum allowable component accelerations, the assumption is made that the feeder will not sail out given that it should orient itself in 'such an orientation' and is not able to take waves from any given direction. Therefore only the most stringent case of beam seas will be analyzed to determine the maximum significant wave height in which the transit operation can take place.

The accelerations at the COG of the tower are the most critical according to the documents provided by TWD. This is due to the high COG of the tower components which result in high sway accelerations due to a roll motion. The COGs of the tower components are thus seen as the points of interest. Through the use of OrcaFlex, the spectral response can be calculated at these points of interest for a three-hour simulation. The spectral report response holds the Most Probable Maximum (MPM) for all 6 accelerations (translational and rotational) at each point of interest for a specified H_s.

To calculate the effective translational loads on the components, the resulting accelerations are combined with the components of the gravitational acceleration due to the roll and pitch angles and gravity itself. This results in an effective acceleration presented in equation 6.8

$$\ddot{y}_{eff} = \ddot{y} + g\sin(\varphi_{max}) \tag{6.8}$$

Where:

$\ddot{y}_{\text{eff}}$	= Effective sway acceleration
$\ddot{y}$	= Sway acceleration
φ_{max}	= Maximum roll angle

The assumption that beam seas result in the most significant accelerations is verified with the motion analysis performed by DEME for Vineyard OWF [83]. This motion analysis is compared to the simplified motion analysis on the Memphis Bridge Barge, with a loading condition equal to the one in DEME's motion analysis, where only beam waves are taken into account. The same case proved that accelerations in the zero-speed case are more severe than the forward-speed case. To reduce the computational intensity, only RAOs and spectral responses of the zero-speed case are considered to determine the operating limits during the transit operation.

For all peak periods from 4 to 20 seconds, the spectral response is determined. With the spectral responses, the maximum H_s for which the critical accelerations are reached can be determined. These are the design significant wave heights. When an operation takes longer than 30 minutes to complete with no chance of returning to a safe state, an extra safety margin should be built in [43]. This is called the alpha factor [27]. This is a factor between 0 and 1 and dependent on the operational time, the design H_s, the weather monitoring and the type of operation. The design H_s is multiplied with this factor to obtain the operational H_s as is displayed by formula 6.9. The operational H_s is the maximum H_s for which an operation is allowed to proceed. The maximum operational H_s are tabulated in figure 6.6

$$H_{s,operational} = \alpha \cdot H_{s,design} \tag{6.9}$$

Figure 6.6: Operational transit H_s [m] limits for all configurations.

Tp [s]	1.A	1.B	1.C	2.A	2.B	2.C	3.A	3.B	3.C	4.A	4.B	4.C
4	12,24	9,56	10,12	8,64	6,85	6,91	6,73	5,79	5,72	5,62	5,36	5,28
5	11,20	8,38	8,32	7,58	5,60	5,39	5,76	4,55	4,34	4,71	4,27	4,12
6	10,31	7,22	6,69	6,44	4,12	3,79	4,47	3,26	3,05	3,45	3,21	3,07
7	9,70	6,08	5,19	5,46	2,98	2,71	3,32	2,51	2,36	2,56	2,71	2,62
8	9,30	4,89	3,90	4,48	2,28	2,12	2,49	2,31	2,26	2,05	2,79	2,75
9	8,99	3,88	2,99	3,55	2,09	2,10	1,96	2,66	2,66	1,91	3,26	3,24
10	8,66	3,11	2,41	2,83	2,46	2,54	1,78	3,21	3,19	2,15	3,84	3,81
11	8,17	2,68	2,43	2,30	2,99	3,05	2,02	3,73	3,70	2,56	4,43	4,39
12	7,46	2,85	2,94	2,08	3,46	3,50	2,44	4,26	4,23	2,97	5,04	5,00
13	6,64	3,43	3,51	2,29	3,91	3,96	2,83	4,81	4,79	3,38	5,65	5,61
14	5,85	4,00	3,96	2,73	4,38	4,44	3,19	5,37	5,36	3,80	6,28	6,25
15	5,12	4,47	4,39	3,17	4,89	4,96	3,56	5,96	5,94	4,25	6,94	6,91
16	4,45	4,91	4,82	3,55	5,40	5,48	3,94	6,56	6,56	4,73	7,62	7,60
17	3,98	5,36	5,29	3,90	5,92	6,03	4,36	7,19	7,19	5,22	8,32	8,30
18	3,89	5,82	5,77	4,26	6,47	6,59	4,81	7,83	7,85	5,72	9,03	9,02
19	4,15	6,30	6,27	4,64	7,04	7,17	5,25	8,49	8,51	6,24	9,75	9,75
20	4,58	6,81	6,79	5,03	7,62	7,77	5,71	9,15	9,18	6,78	10,46	10,47

6.3.3. Blade rack lift and backload limits

The blade rack transfer limit is determined by the occurrence of re-hits. A re-hit occurs when the barge hits a component after it has been lifted. This is a non-linear phenomenon which means that RAOs can not be used directly to determine the limit. A time-domain simulation must therefore be carried out to determine the operational limit regarding re-hits. Re-hits occur at the corner points of the WTG components. The barge motions at the corner points are therefore the points of interest for the re-hit study. There are three methods to determine the occurrence of re-hits. These are presented and compared, in order to make a founded choice for the method that will be used in this research. The three proposed methods are using actual measurements, the high-fidelity MARIN USA method and the simplified method.

6.3.3.1. Actual measurements

The most realistic way to determine the limits for which a blade rack transfer can take place would be to use real data from performed operations in real-life or simulation centers. Using this data or executing actual tests takes into account the skill and experience of the vessel's crew and would therefore represent the actual operation in a very accurate way. However, both executing actual tests or lifting simulations in simulation centers are time-, cost- and asset-intensive. As this type of operation is not yet carried out at the time of writing, no information regarding actual lifts is available. It is likely that lifting simulations have been executed for the blade rack transfer operations of Vineyard OWF. However, this data is not available and the data would be only valid for loading scenarios similar to that of Vineyard. These data would thus not be suitable to determine the operating lifts for lifting a 20MW blade rack, let alone using different barges. The method of actual measurements or performing operations in simulation centers is therefore not suited to determine the operation limits.

6.3.3.2. High fidelity MARIN USA method

The method proposed by Marin USA in the NOWRDC report [6] and further supported by the internal reports[84] [85], takes a high-fidelity model to simulate the occurrence of re-hits. Marin USA defined this method to propose an industry standard for analysis. A high-fidelity model must be created where all components of the actual vessels, lifting equipment and WTG components are modeled. This approach then uses a time-domain analysis for different environments (wave height, period and direction) and 10 seeds (instances in time where the lift is executed). This variety of simulations results in a certain amount of re-hits that occur, which can be correlated to acceptable vessel motions. Marin USA correlates the probability of a re-hit to the RMS value of the heave motion at the corner points of the WTG components on the barge. These acceptable RMS values are determined in the time domain for every lifting configuration. The RMS values can also be determined in the frequency domain for a certain vessel and thus used to determine the operating limits of different vessels once the allowable RMS values of the corner points for a given lifting configuration are known. The crux of this method is that operating limits can be determined in an efficient manner for a large variety of vessels since the RMS value of a point at a vessel can be determined in the frequency domain [84] [86].
The question is, how translatable the RMS values to determine the occurrence of re-hits are when a different vessel is used. The RMS values contain information regarding the heave amplitude of the vessel, but don't capture the influence of heave velocity. A larger vessel could have a similar heave RMS for its cornerpoints, but a slower heave velocity. This gives the crane and quick-lift more time to create clearance between the barge and the WTG component, lowering the chance for a re-hit. Adding to that, analyzing only 10 seeds for each environment might not be enough to capture the variability within a given sea state.

6.3.3.3. Simplified method

The simplified method is created in consultation with engineers from TWD and analyses the vessel motions of each vessel in the time domain [87]. This approach takes only the corner point that is situated furthest away from the vessel COG and analyses its motion throughout time. The simplified approach is based on the lifting and position trajectories of the blade rack corner and its related position of the barge. These trajectories are compared, and if the barge trajectory crosses the lifting trajectory, a re-hit occurs. Figure 6.7 visualizes the point of interest for the re-hit study and the graphical re-hit analysis where the red cross resembles a re-hit. This method allows to model the quicklift and crane in a mathematical way using only their kinematic properties namely: hoisting acceleration, hoisting velocity and quick-lift stroke. This simplified method is a lower fidelity model as it does not model all details of the lifting arrangement and WTG components but represents their behavior in a simplified way.

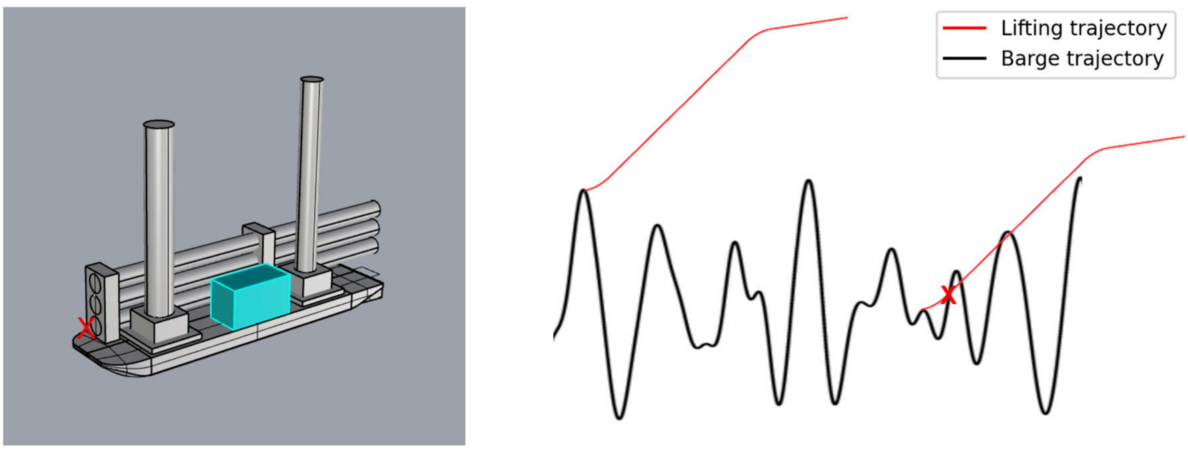

Figure 6.7: Visualization of point of interest and the simplified re-hit analysis.

6.3.3.4. Preferred method

The simplified method is preferred due to time constraints and the lack of direct availability of usable high-fidelity models regarding the heave compensator and crane. This method is only conceptually validated and not founded with existing models or measurement data. The results of this method should therefore only be compared on a relative basis. The re-hit probability is first determined for the case of Vineyard OWF, this value is then used as the benchmark probability value for which the chance of a re-hit is deemed acceptable. The simplified method is first discussed in depth to provide a better understanding of the process and to explain the assumptions.

6.3.3.5. Modelling the blade rack lift

The simplified method is based on comparing the lifting and position trajectories of the blade rack corner points and the corresponding locations on the barge. The position trajectory of the corner points on the barge follow from a three-hour time-domain analysis for global heave motion. To model the lifting trajectory, it is critical to understand the way the quick lift AHC works.

Before a component is lifted, the quick lift builds up tension till 90% of the load and keeps this tension. At this instance, the quick lift AHC is ready to lift and guarantees that no premature lift-off occurs. The next step is to release the seafastening after which the operator gives the 'green light' and the component is ready to be lifted. The quick lift AHC automatically quick lifts at the next wave peak and starts when the bottom of its stroke, while compensating heave at 90% tension, is reached. This means that a lift is only initiated as soon as the lifting point moves downward (negative Z velocity). The simplified model simulates the barge motions using the loading condition where only the nacelle is still situated on the barge. Only 10% of the weight of the blade rack is still supported by the barge before liftoff. Its influence is therefore neglected in the motion analysis.

The simplified method simulates a lift for every instance where the lifting point of the blade rack moves downward. The time-domain analysis is carried out for 3 hours with timesteps of 0,25 seconds and with hoisting properties as displayed in table 6.2. Figure 6.8 shows the related lifting trajectory of the quick lift AHC. The re-hit analysis is performed for head waves and a situation where waves come in at a 165 ° angle. The 165 ° case is found to be governing. Performing this simulation for the Vineyard loadout results in a re-hit probability of 4,27 % when including all time instances and 8,54 % when including only the time instances where the lifting point moves downward and the component is actually lifted. The latter is taken as the reference value to determine if the re-hit probability is deemed acceptable. Figure 6.9 presents the operating limits for every barge. The alpha factor is found to be irrelevant for this operation since the actual lift takes less than 30 minutes to complete.

Table 6.2: Quick lift and lifting characteristics.

Stroke [m]	Stroke speed [ms^{-1}]	Stroke acceleration [ms^{-2}]	Crane hoist speed [ms^{-1}]
3,0	0,5	0,3	0,09

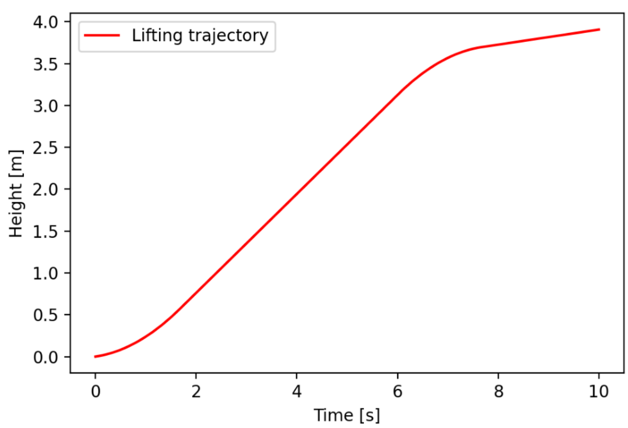

Figure 6.8: Default lifting trajectory of quick lift AHC.

Figure 6.9: Operating limits H_s [m] for blade rack transfer.

Tp [s]	Memphis Bridge	Barge 2	Barge 3	Barge 4
4	2,50	2,50	2,50	2,50
5	2,50	2,50	2,50	2,50
6	2,50	2,00	2,50	2,50
7	2,10	2,10	2,50	2,50
8	1,90	2,30	2,50	2,50
9	1,70	2,10	2,50	2,50
10	1,50	1,90	2,50	2,50
11	1,50	1,70	2,30	2,50
12	1,50	1,70	2,10	2,50
13	1,50	1,70	2,10	2,50
14	1,50	1,70	2,10	2,50
15	1,70	1,90	2,30	2,50
16	1,70	2,00	2,30	2,50
17	1,90	2,10	2,50	2,50
18	2,10	2,30	2,50	2,50
19	2,30	2,30	2,50	2,50
20	2,50	2,50	2,50	2,50

6.3.4. Heave compensator sensitivity analysis

MARIN USA demonstrated that the characteristics of the heave compensator influences the operating limits [6]. Therefore a feasibility study regarding the motion compensator's characteristics is carried out. The lifting trajectory of the blade rack is described by the kinematic properties of the heave compensator and the crane as tabulated in 6.2. Increasing the stroke results in exactly the same amount of re-hits, indicating that the stroke is not limiting for the current heave compensator. Increasing the stroke velocity from 0,5 to 0,8 ms^{-1} results in slightly less, 50, re-hits. This decreases the chance for a re-hit by 0,23 %. This is an insignificant difference as the number of re-hits at higher significant wave heights remains above the threshold. The operating limits thus remain the same and heave velocity is not seen as a limiting factor. Further increasing stroke velocity from 0,8 to 1 ms^{-1}, did not result in any improvements. Increasing the stroke acceleration from 0,3 to 0,5 ms^{-2} does result in a significant increase in the operating limits. This increase is shown in figure 6.10. Increasing the stroke acceleration results in a larger improvement than the increase in barge dimensions from the Memphis bridge to Barge 2 and slightly less than increasing barge dimensions to that of Barge 3. This shows that improving the quick lift AHC is an effective way to improve operating limits. Adding to that, contractors are more willing to invest in technical assets such as lifting equipment than larger feeder barges [37].

6.4. Operational Characteristics

The previous sections discussed the approach to determining the operating limits for the different characteristics. However, not only the operating limits change but also the way certain operations are carried out, where different vessels are required and the associated dayrates for barges and equipment vary for each concept. Section 6.4.1 discusses the operational differences and changes in the required vessels for each configuration. Section 6.4.2 consequently discusses the financial aspects that vary for each concept.

6.4.1. Operational differences

The Memphis Bridge barge is currently on the limit in terms of the allowed width to enter the port of New Bedford. Other barges have to resort to ports elsewhere. Table 1.1 shows that the New London State Pier is the only viable port the other barges can enter with towers loaded on deck. This results in the fact that the Memphis Bridge barge has to sail 53 nm and the other barges 77,8 nm from port to

Tp [s]	Default	Improved
4	2,50	2,50
5	2,50	2,50
6	2,50	2,50
7	2,10	2,50
8	1,90	2,30
9	1,70	1,90
10	1,50	1,70
11	1,50	1,70
12	1,50	1,70
13	1,50	1,70
14	1,50	1,90
15	1,70	1,90
16	1,70	2,10
17	1,90	2,10
18	2,10	2,30
19	2,30	2,50
20	2,50	2,50

Figure 6.10: Operational limits H_s [m] for Memphis Bridge Barge with default and improved quick lift AHC.

the WTIV, which relates to a 10 and 14-hour transit time. The same duration holds for the empty transit which the feeders have to make from the WTIV back to port. Using different marshaling ports can also change the port costs. However, tariffs for the New London State Pier were not available. Therefore the same costs as for New Bedford, as provided by the port itself [88], were used.

The difference between the installation strategies lies in the number in which the tower is split up. Having fewer tower pieces means that fewer lifts from the barge to the WTIV, and fewer installations from the WTIV have to take place in order to transfer and install a full tower. Each lift and each installation takes 2 hours to complete. This means that the one-piece strategy holds a 4-hour net advantage, and the three-piece a net 4-hour deficit in comparison to the current 2-piece installation methodology.

By altering the type of barge and the loading condition, the towing resistance of the barge changes. This in turn changes the required tug and its associated dayrate. Changing the dimensions of the barge influences mostly hydrodynamic resistance. Changing the loading conditions influences the air resistance of the barge. For the one-piece tower strategy the air resistance is significant. Next to that, the draft of the vessel varies with every loading condition thus also slightly influencing its hydrodynamic resistance. The loading condition thus influences the resistance of the barge. Finally, the desired seastate in which the barge is to be towed influences the wave drift resistance [82]. Thus the design wave height, determined by the operating limits, determines part of the barge resistance. The required effective and static bollard pull for every configuration is determined by the internal Bollard Pull tool by TWD. For the air resistance calculation, only the highest tower and the blade rack are used to determine the total frontal area. This tool calculates the required bollard pull according to the standards as provided by DNV in DNV-RP-205, DNV-ST-N001 and DNV-RP-N103 [82] [27] [89]. The bollard pull calculation for configuration 1.A can be found in appendix K, the remaining bollard pull calculations follow the same methodology. Table 6.4 provides an overview of the operational characteristics of every configuration.

6.4.2. Financial differences

Varying the types of barge and equipment influences the associated dayrates. Dayrates can be approximated in a multitude of ways according to Kaiser and Snyder [38]. A dayrate should at least cover the OPEX and CAPEX of a vessel, the remaining part of the dayrate is return on investment. According to Kaiser and Snyder, 40 to 65 % of a vessel's dayrate consists of the part that covers the OPEX. For the Memphis Bridge barge of which the dayrate is known, it is assumed that the OPEX part is 40% of the total dayrate. Furthermore, the OPEX is assumed to be constant for all barges. The remaining part of dayrate is assumed to represent the CAPEX part, which scales with building costs. The costs for constructing a vessel in turn scale with Light Ship Weight (LSW) which is presented in section 6.2.1 [90] [75]. The operational properties for each barge can be found in table 6.3. The dayrates of these barges are company confidential

Table 6.3: Operational properties of each barge.

Barge	Transit time [h]
Memphis Bridge	10
Barge 2	14
Barge 3	14
Barge 4	14

The dayrates for a Barge Master T700 and Barge Master Heavy Feeder are provided under disclosure by TWD. The dayrate of the Mega Feeder can be determined by means of a scaling analysis of the Heavy Feeder. For both the Heavy - and the Mega Feeder, the dayrate consists of a 'steel' part and a 'hydraulics' part. The steel part is determined with the assumptions that dayrate = $CAPEX/1000$ and that the CAPEX equals 10 $ per kg steel [75]. The remainder of the dayrate is the hydraulic part, which scales linearly with the overturning moment. When the overturning moment doubles, twice the hydraulic power is required, which translates to double the amount of components. The dayrates of these systems are company confidential.

Table 6.4: Characteristics of each configuration.

Configuration	GM [m]	Motion compensators	Tn [s]	Hs design transit [m]	Hs operational transit[m]	Hs min lift [m]	Static BP [t]
1.A	13.52	MF	18	4.46	3.89	1.5	192
1.B	16.38	2x HF	11.2	3.13	2.62	1.5	114
1.C	16.13	HF + 2 T700	10.5	2.83	2.41	1.5	116
2.A	31.84	MF	12.1	2.67	2.27	1.7	105
2.B	33.53	2x HF	8.8	2.68	2.09	1.7	93
2.C	32.93	HF + 2 T700	8.6	2.69	2.1	1.7	119
3.A	53.44	MF	9.9	2.3	1.94	2.1	132
3.B	54.48	2x HF	8	2.95	2.52	2.1	137
3.C	53.36	HF + 2 T700	7.8	2.89	2.47	2.1	135
4.A	80.41	MF	8.9	2.45	2.07	2.5	144
4.B	80.51	2x HF	7.6	3.43	2.95	2.5	170
4.C	78.48	HF + 2 T700	7.5	3.32	2.85	2.5	167

6.5. Conclusion

This chapter answers the research questions regarding the effects of vessel characteristics, equipment characteristics and the installation strategy on operating limits, costs and operational characteristics. It shows that increasing the barge size does not necessarily lead to increased operating limits. Although the critical limits for blade rack transfer increase with increasing barge size as the barge becomes less susceptible to waves, the limits for the transit first decrease, then slightly increase. This is attributed to the increased GM for larger barges. Although the vessel becomes more stable, the natural period of the vessel decreases resulting in higher accelerations and thus lower allowable wave heights. The transit limits then slightly increase as the barge grows in size and becomes less susceptible to waves. The natural roll period decreases as the barge increases in size. This is an important phenomenon since this can result in the fact that the natural roll periods can fall in the range of peak periods frequently occurring at the Vineyard site which will have a significant impact on workability.

As a result of the simplifications of the problem, improving the motion compensation capabilities of the motion compensation platforms will not increase the operating limits. The motion compensation platforms then become dependent on the overturning moment of the WTG tower sections that is determined by the installation strategy. The costs for these platforms are determined by scaling the steel weight and required hydraulic power. The quick lift AHC has a significant influence on the operating limits of the blade rack lift. With the quick lift AHC operating limits can be increased with just an 'add-on' single piece of equipment. However, it is uncertain what future characteristics future quick lift systems will have and what costs would be associated with such systems. It is therefore recommended that this technology should be further researched and developed in terms of increasing hoisting acceleration and velocity and their influences on financial properties.

The effect of the installation strategy becomes clear on both the operational side, since each tower section takes 2 hours to install, and on operating limits as shown in figure 6.6. For the operating transit limits, the effect is not straightforward. Splitting up the tower into more sections lowers the VCG. This leads to a higher GM and decreased inertia. Both decrease the natural roll period of the vessel leading to increased accelerations. On the other hand, transporting the tower in a single piece causes the tower COG to be located far away from the center of gyration. This leads to higher roll-induced sway accelerations. In addition to that, the effect of the installation strategy on the operational transit limits also depends on the barge on which the WTG components are loaded.

Due to both its low GM and high inertia, configuration 1.A is the least susceptible to beam waves making this a 'robust' configuration for transit. Paired with the fact that this configuration boasts the fewest lifts, the shortest transit time, and ranks as the third lowest in daily costs, this concept holds promise as a high-performing option.

7

Discrete-Event Simulation

This chapter describes the DES model that is used to assess the operational performance of the fleet. Section 7.1 introduces the software used to build and run the DES. Section 7.2 describes the goal and accompanying framework, working principles and assumptions of the simulation where section 7.3 covers the output following from the simulation. Section 7.4 concludes by assessing the model behaviour and thereby validating the model.

7.1. Toolbox

DES is an established method to support decision-making for planning tasks in production and logistics [91]. Multiple simulation software for DES exists ranging from purpose-built to open-source. This research uses Simpy for Discrete-Event Simulation. SimPy is a process-based DES based on Python which allows for processes to interact with each other and for processes to use shared resources [91]. SimPy is therefore suitable for modeling the feedering method.

Salabim provides an alternative to SimPy. Salabim is also an open-source Python-based discrete-event simulation package. Salabim holds an edge over SimPy as it supports additional modeling concepts and allows for animations and video production [91] [92]. Since SimPy is better known, providing more support in addition to the manual, and fit for the purpose of modeling the feedering method, the SimPy package is preferred over Salabim.

7.2. Setup

The goal of the simulation is to gain insight into the effects of operational fleet characteristics on the performance of the feedering method for constructing an OWF. For the simulation, only the operational characteristics of the fleet are taken into account. Therefore, the simulation is not set up to deal with equipment failures or logistical, managerial or engineering inefficiencies. This prioritization is supported by Lerche as unfavorable weather is the most important reason for delay in constructing an offshore wind farm which can be mitigated by the right choices for a fleet design [93].

7.2.1. Simulation

The construction of an OWF can be seen as a repeatable sequence of dependent events. This process is visualized on a high level by figures 2.5 and 2.6. In order to improve the simulation, the process must be split up into a more detailed level allowing for more insight into the actual process and bottlenecks. The DES describes each step during the installation as an event. Each step is seen as an activity that requires a certain time to complete and cannot be paused anywhere during the activity. Each activity that requires a go/no go decision is thus seen as an individual event. This holds that the WTG installation and component transfer phases are split up into multiple events. Appendix L presents the detailed PFD for the construction of an OWF.

Each event has its own duration, environmental limits and weather window. The environmental limits are significant wave height and wind speed. Significant wave height represents the total sea state and consists of a wind-sea part and a swell part. The wind speed represents the wind speed measured 10 meters above mean sea level [94]. The limiting H_s for an operation differs for every peak period and is thus assessed per peak period. The interval size used to determine the maximum significant wave height for a given peak period is one. The event characteristics used for the base case simulation can be found in appendix M and are based on the values presented in section 2.2 and the estimations by TWD. The H_s limit is the same for every peak period for the base case events.

Limits regarding mooring are based on estimates provided by TWD experts [95] and the NYSERDA report [28]. The limit used for the base case is 1.5 m H_S. The transit limits, and thus the tower- and nacelle transfer limits are based on the vineyard transit limits. The limit for blade rack transfer and backload is 1.5 m H_S for the base case according to the study performed by Seaqualize [96]. The actual limits of these lifts are determined per concept in section 6.3.3.

For an ideal representation, multiple years of hindcast data should be collected from all WTG locations, the waypoints along the possible routes and the potential marshaling ports. However, processing all this data would be computationally intensive and only weather data on the Vineyard site is available. The weather input used is therefore not fully representable for the conditions in port and along the routes. Environmental conditions along the route and in port are less severe than offshore. The weather data used will thus lead to a conservative representation of the inshore events. The hindcast dataset holds hourly measurement data from 01-01-1979 till 01-01-2018 for a single point located at the Vineyard OWF location. With the hindcast data being available for every hour, the duration of events, and therefore the order of magnitude of simulation time, is rounded to whole hours. The dataset allows to repeat simulations with the same starting date for different years. The results of these simulations provide an average and a spread regarding the operational results which allows us to qualitatively analyze the simulation results and draw conclusions accordingly. The hindcast data also contain data regarding current velocity and direction. However, current limits are not taken into account for this research.

Before the start of every event, it is assessed whether the environmental conditions stay within the operating limits for the duration of the corresponding weather window of the event. If the environmental conditions stay within operating limits, the event is executed and the duration of the event is passed. In case the operating limits are exceeded, the simulation delays the operation until a suitable weather window occurs. Figure 7.1 visualizes this cycle. An event is initialized at T1. The weather data is then used to find the first available weather window for the specific activity and its corresponding weather window and environmental limits. The start of this suitable weather window is at instance T2 which equals the actual starting time of the event. The instance of T2 can be equal to T1 in case a suitable weather window starts at T1. The time between T1 and T2 is waiting time for a suitable weather window and thus downtime. Finally, the event is executed and time is passed with the event duration to T3 at which instance the following events are triggered directly or with a certain delay.

For all operations, the required weather window is equal to the duration of the operation except for the transit operation. The feeder is only released from the port if it can safely transport and carry the WTG components for as long as there are components on the feeder. This holds that the operational limits for transit are not exceeded from the start of the transit operation up until the point where the feeder disconnects from the WTIV following the safe-to-safe principle.

The simulation starts with loading the WTG components on the feeder vessels. Although loading the vessel consists of multiple steps, this process is not split up into its individual activities and modeled as a whole. The environmental limits for (un)loading the feeder are high since the operation takes place in a sheltered area. Since the operation is sheltered, only the windlimits are taken into account. These high limits make it likely that operators opt to start or delay the full operation instead of assessing and waiting on weather for every individual lift. This makes it unnecessary to simulate downtimes within the (un)loading phase of the feeder. At the first instance of loading the feeder vessel, the WTIV is already at the installation site. The trip from the port to the installation site by the WTIV is not modeled. This is

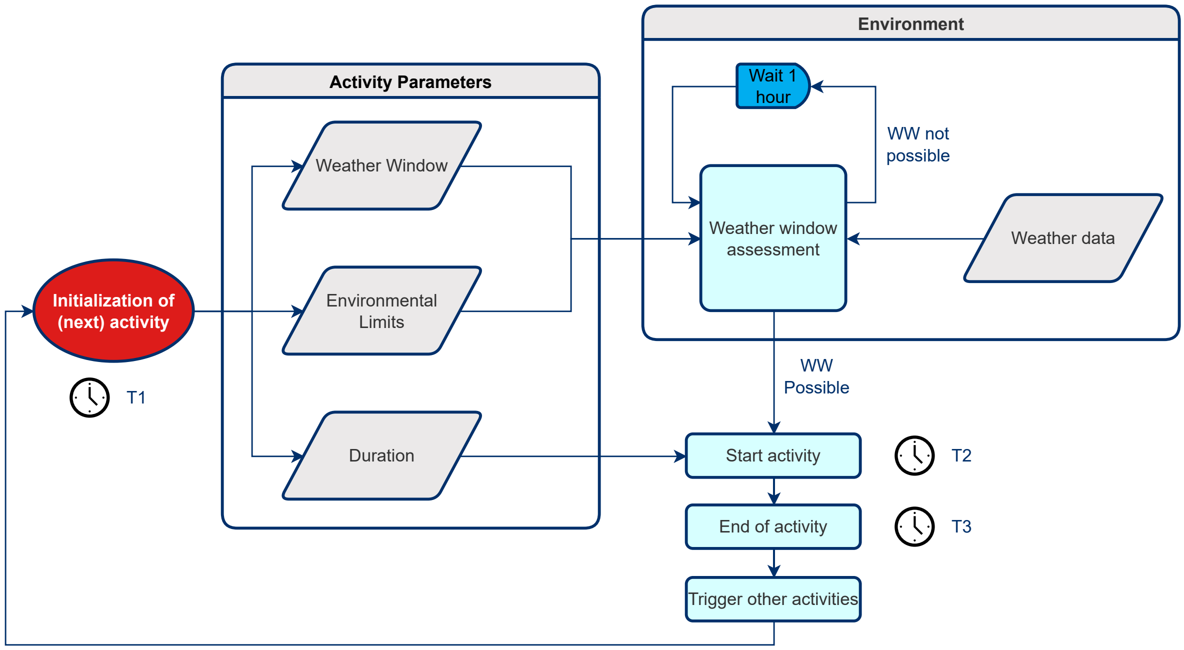

Figure 7.1: Schematic visualization of event processing.

because the WTIV can come from any location in the world except a U.S. port. This makes it a variable that is too random for a representative model. Also, it will be the same for every configuration and therefore not provide any information regarding the operational performance of the feedering method for different feeder vessel configurations.

When loading is finished, the feeder vessel waits in port in case it cannot sail out due to weather, or the fact that the WTIV will not yet be ready to receive the feeder vessel after the feeder vessel's transit is finished. To determine this waiting time for the second cause, the feeder must know when to leave the port in order to arrive exactly at the same time that the WTIV is finished with relocation, jacked up and ready to receive the feeder. This synchronization is achieved by releasing the feeder at the instance where the required time to finish relocation and jacking-up, exactly matches the transit time of the feeder in a situation without weather delay. This means that in case a delay is encountered during the installation of the WTG, the feeder has to wait offshore for the WTIV to be ready to receive the feeder.

The remainder of the process follows the PFD as displayed in appendix L. The simulation stops when all WTG components are installed and the WTIV is jacked-down and the feeders are back in port.

7.2.2. Costs

The costs are calculated following equation 2.5. The costs for chartering vessels and equipment are based on their daily costs and the time for which these are chartered. For each vessel and every piece of equipment, the total duration is used for the charter time. In reality, the charter time of especially the feeders and tugs can be different as these arrive back in port and are ready for demobilization before the WTIV has installed all WTGs. This possibly leads to a slight overestimation of the total chartering costs.

The VOYEX are calculated by means of total fuel consumption and port costs. The fuel consumption rates for sailing, idle, positioning and operating (WTIV only) are used in combination with logged vessel activity to determine the total fuel costs. The assumption is made that a vessel is at idle when it encounters downtime. The operating mode per operation is included in appendix M. Table 7.1 provides an overview of the dayrates and fuel consumptions per operating mode of the vessels.

Port costs are determined by means of the time the vessel is in the port, rounded upwards to the nearest day, and the port fees. The port fees used are based on the fees for the New Bedford marine commerce terminal.

Table 7.1: Dayrates & fuel consumption.

Activity	**WTIV**	**Tug 90 BP** [97]	**Tug 120 BP**[98]	**Tug 150 BP** [99]	**Tug 180 BP** [100]	Value
Dayrate	225000 [12]	Confidential	Confidential	Confidential	Confidential	$/day
Idle consumption	6,00 [101]	1,34	1,16	1,25	1,34	t/day
Sailing consumption	44,0 [102]	9,79	20,65	25,90	25,10	t/day
Positioning consumption	22,5 [101]	16,91	28,93	33,10	34,00	t/day
Operating consumption	14,0 [102]	-	-	-	-	t/day

7.3. Output

The main outputs of the DES are the total duration and the total contractor costs. Figure 7.2 shows the installation progress over time for different years. Each line represents a different year where the simulation is started at the same date, in this case the 1st of March. The y-axis indicates the amount of completed installation cycles. The x-axis represents the time and therefore the project duration. The individual results represent a situation where a simulation is started on March 1st 2024 and the exact same weather conditions as in 'year x' would be encountered. The straight line represents the P_0 duration. This is the duration of the project without delays or downtime.

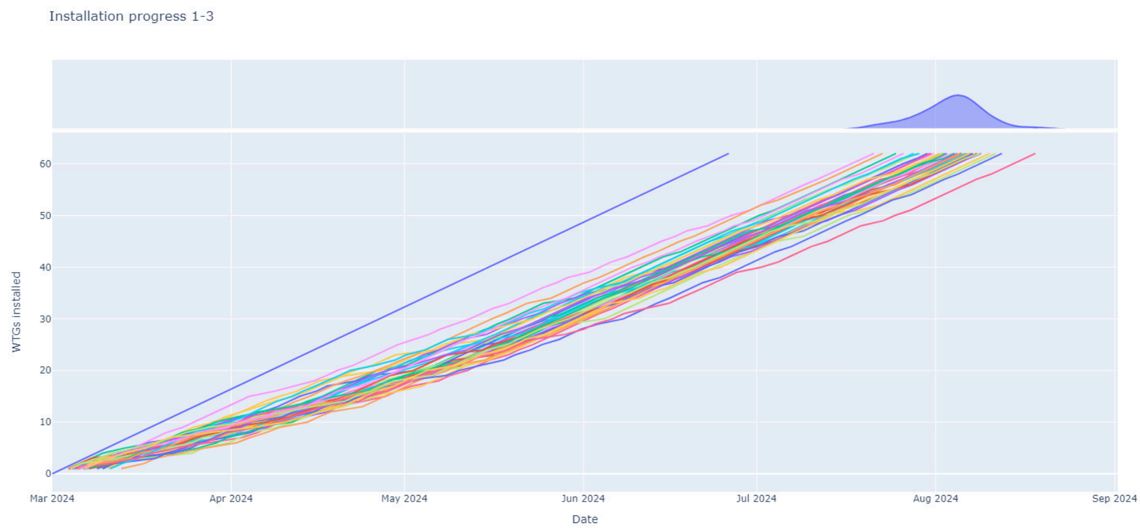

Figure 7.2: Installation progress.

The progress lines of figure 7.2 deviate from the P_0 duration. The figure shows that the slopes of the progress lines are less steep than P_0 in March and gradually become steeper as the installation progresses. This means that later during the installation progress, less downtime is encountered and the activities are executed more closely to a P_0 situation. This behavior is to be expected. Weather conditions are less favorable in early spring than in summer which translates to the fact that there is less downtime in summer and thus delay in summer than in early spring. Figure 7.2 also shows a clear spread between the simulations. This spread is used to determine the variance of the results and therefore provide a quantification of the weather sensitivity and the associated risk of the operation.

Next to the duration, the simulation calculates the operating expenses. These, including their division, are shown in figure 7.3. The graph represents the costs a contractor would encounter given that the weather is the same as in the year, depicted on the x-axis, belonging to that specific bar. The charter costs are directly related to the total duration. Only port and fuel costs are activity-dependent. However, these costs only represent a marginal portion of the total costs. Fuel costs represent 4,5% of the total costs and fall in the same order of magnitude as the analysis from Smorenberg [21].

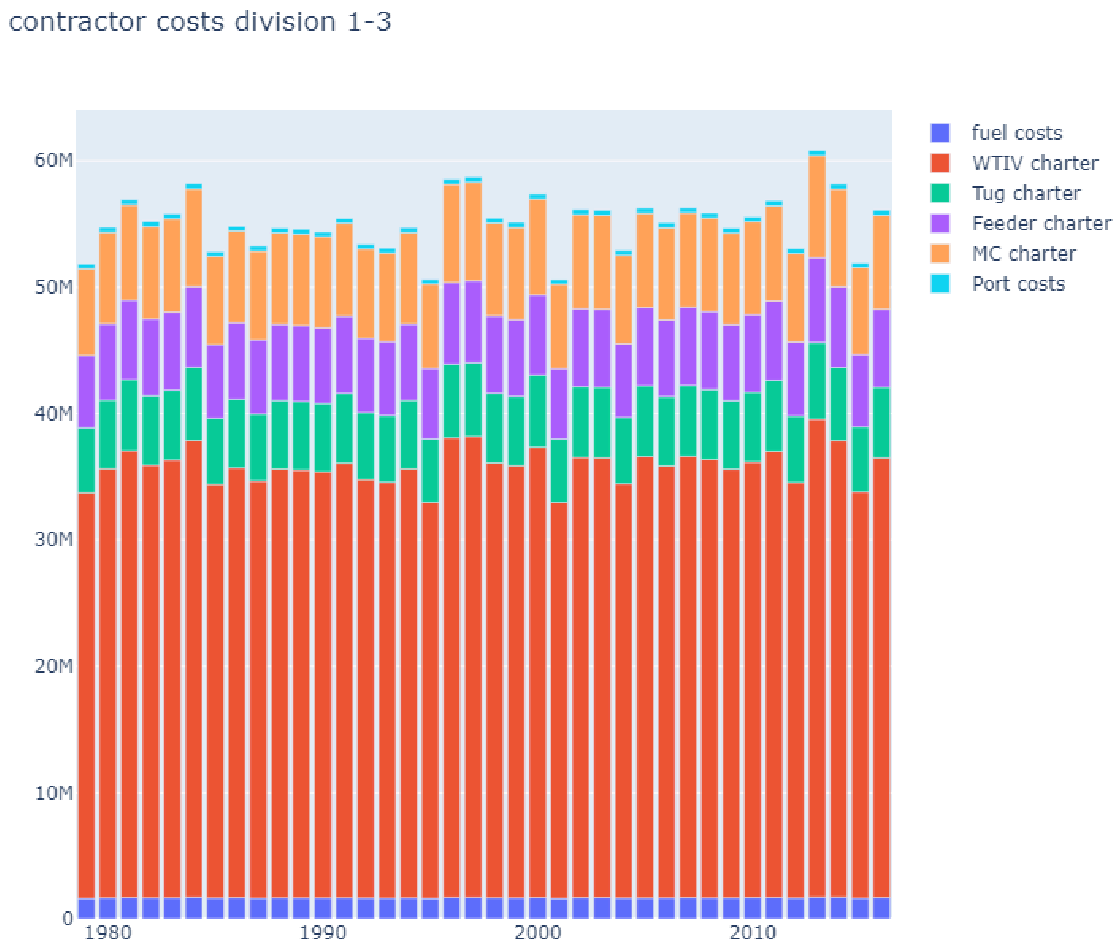

Figure 7.3: Cost build-up per year.

7.4. Verification and Validation

The model is validated using the guidelines presented by Sargent in Verification and validation of simulation models [103]. The variables of interest are both discrete and random variables. The system's properties are discrete variables. The weather, although discrete historical data, is seen as a random variable. The mean, median and variance of the output results are therefore of primary interest and used to determine model validity.

7.4.1. Conceptual validation

The simulation set-up is created in collaboration with experts from TWD. During the creation, daily guidance was provided by S. van den Munckhof and guidance on request was regularly available. After completion of the model and its input, a review session took place at 17-10-2023 which was visited by several experienced engineers. The goal of this session was to pinpoint inaccuracies and faulty assumptions in the conceptual model. The minutes and attendance of this session can be found in appendix O. The review session led to the following remarks. The peak period is important and should definitely be taken into account. When planning an offshore operation, we want to know with which environment we deal with so we can optimize for this environment. Being precise regarding the discretization of peak period therefore only helps to improve and unlock the potential of an operation. Peak periods should therefore be taken into account as how it is currently implemented, each second, and not with a lower definition. The second remark is that the results of the simulation should not be interpreted as absolute results. Real operations encounter more than weather-related downtime which is also stressed by Lerche [93]. The results should therefore be compared relative to each other to assess the potential of each conceptual configuration.

7.4.2. Data validity

Although technically a deterministic variable as the data is historical and remains constant in every simulation, the weather data is seen as a stochastic variable as it differs per simulation year. The internal validity of the model should therefore be checked to determine the amount of 'stochastic' variability related to the weather data. The results should converge after a certain amount of simulations in order to be of value. Figure 7.4 shows the convergence of the simulation results for simulations starting on the 1st of January. Appendix N contains all convergence tests of the simulation model. The figures show that the mean result is sufficiently converged after 38 simulation years. This indicates that the obtained weather data can be used to execute simulations and obtain results with a representable spread.

Figure 7.4: Convergence test.

7.4.3. Computerized verification

The simulation is constructed using Python, a high level programming language. Computerized verification therefore concerns that the simulation functions and the computerized models are programmed and implemented correctly. This is achieved by dynamic testing of the model, where the simulation is executed under different conditions. The values obtained, including the ones generated during execution, are used to determine if the computer program and its implementations are correct.

During the construction of the simulation, traces were added in the form of print statements to keep track of the simulation. This allowed to assess the modeling behaviour and determine if simulation functions were programmed correctly. Constructing the model step by step and running simulations as functionalities were added allowed to identify errors as they were made, and correcting them before developing the model further.

Figure 7.5 shows the Gantt chart generated by the model. This Gantt chart plots the executed activities on a time scale and allows to see when activities take place and which take place in parallel. The annotations in the Gantt chart highlight processes and events that can be observed. By analyzing the Gantt chart, it can be concluded that the computerized model, in terms of processing sequence, downtime and parallel activities, is programmed correctly. The figure also shows that the feeders wait in port for a significant time. In a P_0 situation, the time increase by using one instead of two feeders is only three hours. This makes the choice for 2 feeders questionable as the time decrease is minimal while the daily costs increase. However, opting for 2 feeders increases redundancy, allowing installation to continue if systems on one of the feeders fail, and leaves more room for errors regarding planning and scheduling with port operations. The number of feeders is therefore fixed to two feeders.

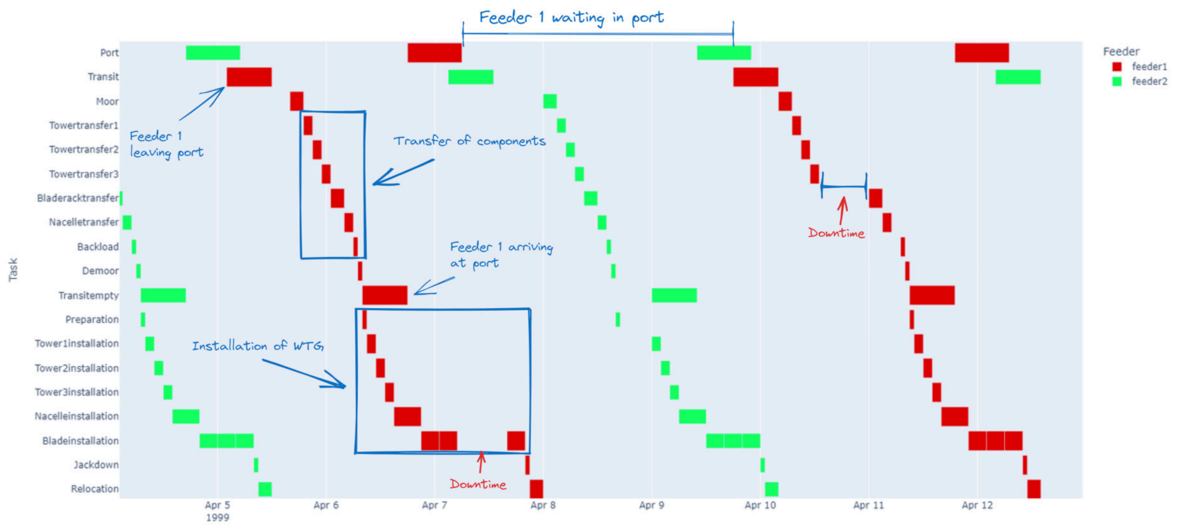

Figure 7.5: Gantt chart.

7.4.4. Operational validity

The operational validity of a model holds that the model has the required accuracy for the model's intended applicability. The simulation model is used in operational validation and deficiencies found can be caused by the steps involved in developing the simulation model. These thus include: developing system theories, computerizing the model or using invalid data.

The analyzed system is not observable. This slims down the available options for assessing operational validity to three options: exploring model behavior, comparing to other models and comparing to other models using statistical tests. With no models including qualitative results available for comparison, exploring model behavior is the only method to assess operational validity. The simulation's output behavior should therefore be explored as thoroughly as possible and comparisons or checks should be made whenever possible.

In addition to analyzing the Gantt chart, a P_0 simulation is executed to verify that the simulation works according to the PFD as presented in appendix L. A P_0 simulation is recreated by setting the environmental limits of the operation to an unrealistically high value, which causes the operational limits to never be exceeded during the simulation. With the durations of the events as presented in table M.1 in appendix M, the feeder maintains a continuous supply. The total project duration, excluding delays, can therefore be analytically calculated using the cycle time of one WTG (all phases from mooring to relocation excluding 'empty transit'), the amount of WTGs and the time it takes to load and transport the first WTG. The results of the analytical, deterministic approach and the P_0 simulation match exactly. In addition to ensuring that the simulation works according to the PFD, this extreme test also increases the confidence in the function that assesses the available weather windows. All moments in time are seen as a possible weather window for the unrealistically high limits.

The results of the simulation are affected by the encountered downtime and thus by the weather. It can be expected that during summer less downtime is encountered than during winter. It is thus expected that simulations starting in the summer months will have a shorter duration than the ones starting in winter. Figure 7.6 shows the results in terms of total duration for simulations starting on the first day of the month for different starting months. The figure clearly shows that a significant advantage can be obtained by starting in the right months. For the reference case used, May is the best month to commence construction. From May onwards, the total duration and especially the spread increases. This is due to encountered storms in September. Further down the year, it is more certain that weather conditions are unfavorable which causes the average duration to keep increasing while the spread decreases.

A critical note to these observations is that the benefit from starting in months in which the simulation encounters little downtime becomes less as the number of WTGs increase. As the number of WTGs increase, the operation will come close to a 'year round' operation in which there are no more seasonal advantages. This holds for all amounts of WTGs where the total duration equals or is close to one or more full years. Depending on the signed contract, it might then be a good idea to halt the installation during winter and continue in spring as environmental conditions improve.

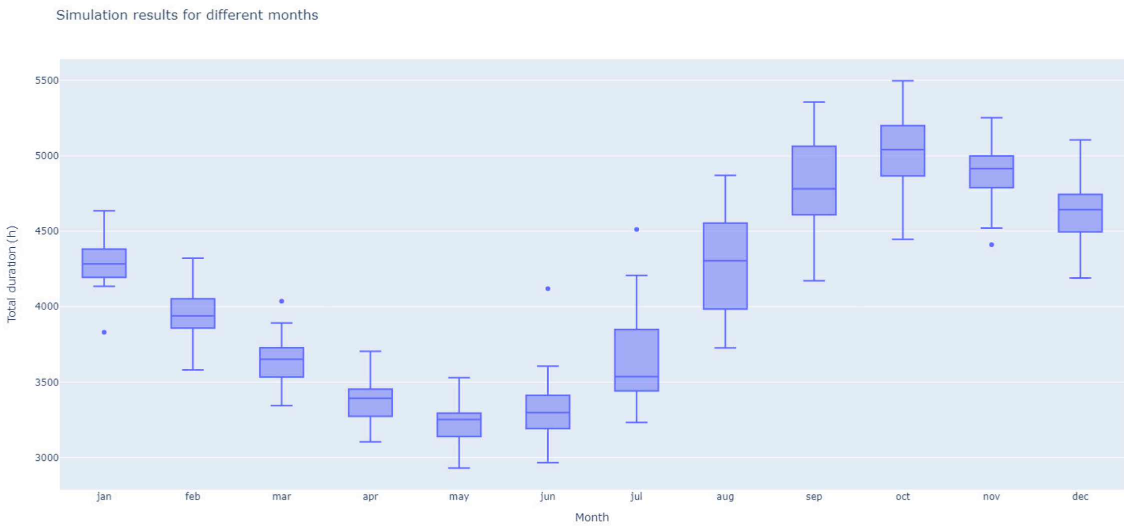

Figure 7.6: Simulation results for different starting months.

Downtime is logged for every event. This allows to identify the bottlenecks in the complete operation. Figure 7.7 shows the downtime for every individual event for simulations starting in March. This shows that the following operations can be identified as bottlenecks: transit, mooring, blade rack transfer, backload, nacelle installation and blade installation. The figure shows that practically no downtime is encountered during the transfer of tower components. This is because these operations are preceded by the mooring operation for which the environmental conditions are assumed to be the most stringent. The mooring operation therefore acts as a 'filter' since the seastate changes gradually and will not increase from 1.5 to 2.5 m H_s in an instance. This means that the tower transfer operations are executed with little to no downtime given that the mooring operation, a more constrained operation, can be executed. The same relation holds for the blade rack transfer and the nacelle transfer operations.

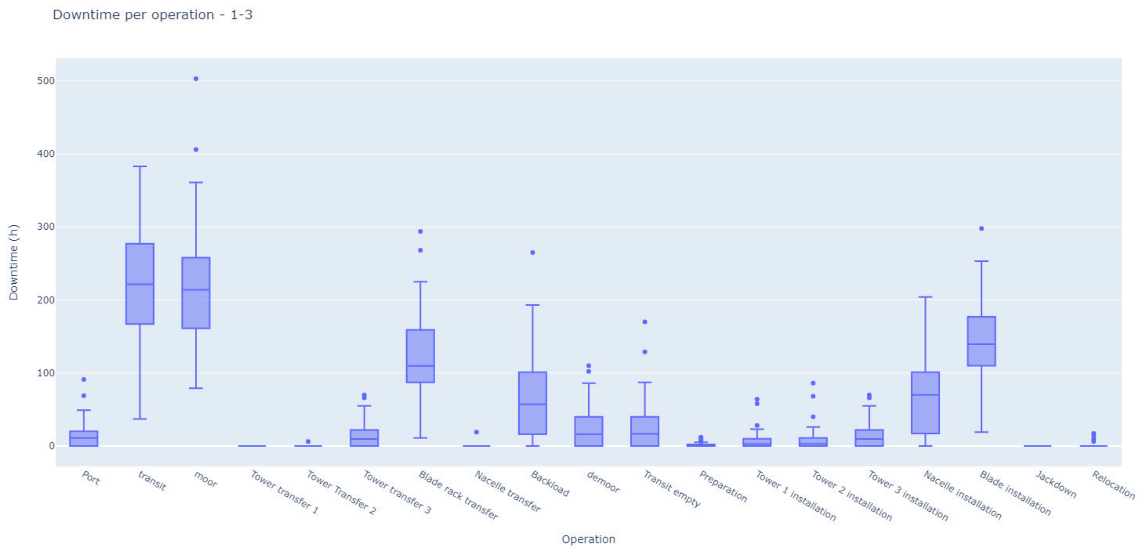

Figure 7.7: Downtime distribution for operations starting in March.

Although the environmental limits for transit are relatively high, this operation encounters the most downtime. This is caused by the required weather window that covers all operations until the feeder is decoupled from the WTIV ensuring a safe-to-safe principle before the feeder is released from the port. Shortening this weather window to just the duration of the transit operation has little effect (20 hr) on the total duration. In this case the downtime shifts from the transit operation to other operations, predominantly to the mooring and blade rack transfer operations. The same holds for increasing the environmental limits of the transit condition. Increasing these (to 3.0 m H_s), results in the downtime shifting to other operations and only has a small effect (14 hours) on the total duration. So although transit is the operation with the most downtime, the transit operation is not classified as a bottleneck.

The nacelle and blade installation operations are known bottleneck operations to occur at conventional WTG installation. This also shows in the bottleneck identification as these operations feature the most significant downtime for the operations that are not related to the feeder vessel. The nacelle and blade installation operations can be improved by innovative lifting or installation equipment. The design and use of such equipment is out of the scope of this thesis. Improvement of these operations is thus not included and their limits are kept equal to the base case for all performance simulations.

The blade rack transfer, backload and (de)mooring are seen as feeder-specific bottleneck operations. These operations have the most constraining environmental limits and a slight improvement in operational limits results in noticeable improvements regarding total duration. However, improving the limits for, for example, blade rack transfer and backload is not sufficient as these operations are followed by the demooring operation. If the limits for (de)mooring cannot be improved, downtime mostly shifts from the blade rack transfer and backload operations towards the (de)mooring operation instead of decreasing total downtime. Figure 7.8 shows this phenomenon.

In order to decrease total downtime and duration of the construction, it is thus important to improve the limits of all critical operations. These are the operations with the lowest operating limits. This is stressed by table 7.2. This table shows the mean total durations in the hypothetical situation where the wave limits of all critical operations, blade rack transfer, backload and (de)mooring, are increased with steps of 0.2 m H_s for the starting months March and August and compares this to a situation where the limits for (de)mooring remain fixed at 1.5 m H_s. This table also concludes that it is useless to improve operating limits for a non-critical operation as the benefit will be negligible.

More tests were executed to inspect and analyze the model behaviour. These tests and conclusions

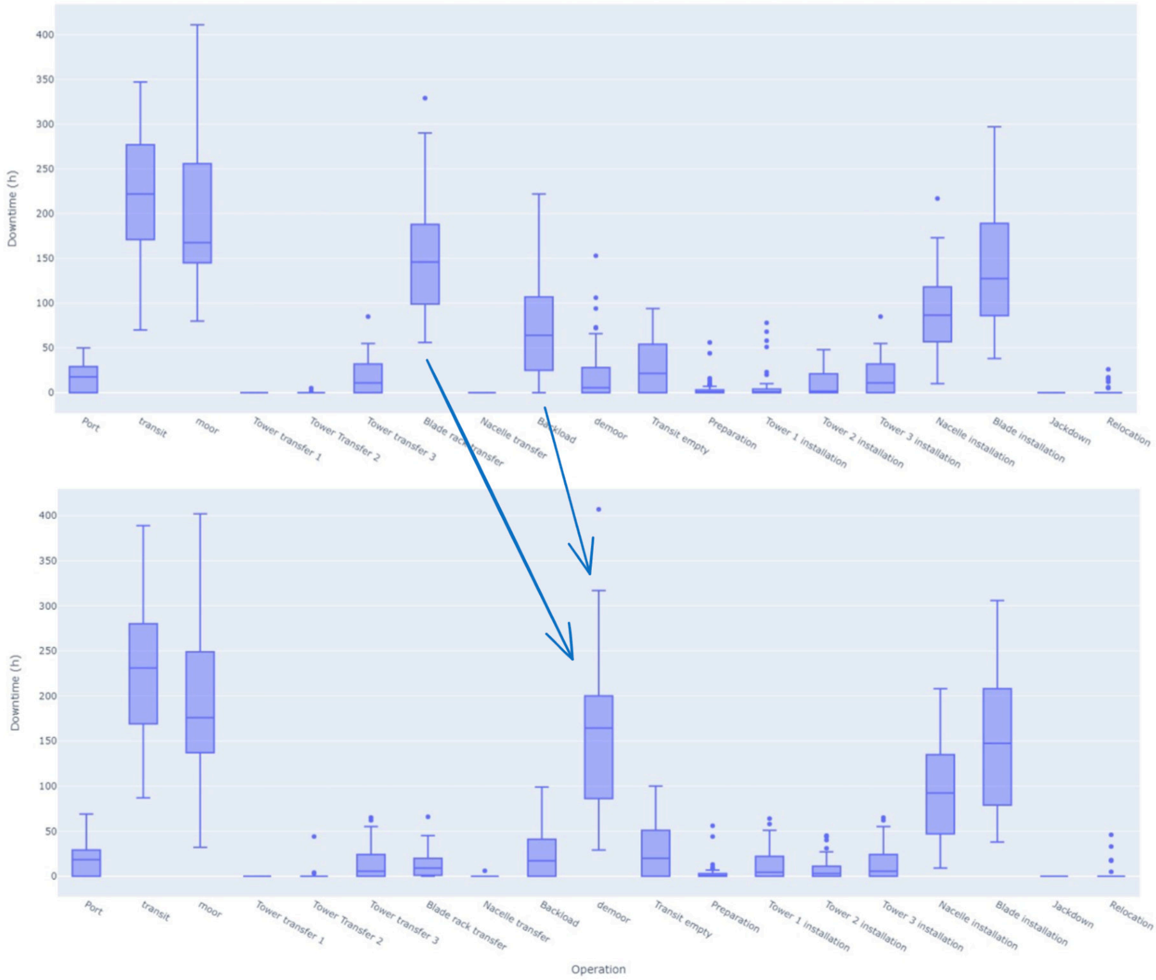

Figure 7.8: Downtime shifting to other operations when a bottleneck operation is improved.

can be found in table 7.3. The model behaves as expected and also works outside the 'base' conditions concerning the number of WTGs and feeders. The test results show that operations influence each other. The effect of improving the limits of a certain operation is therefore less straightforward. In general the following applies: when increasing the operational limits of an operation, the total downtime and the downtime encountered at that specific operation decreases. The downtime encountered at that specific operation will decrease significantly. However, this decrease will not fully contribute to the overall downtime decrease as the follow-up operations will encounter slightly more downtime. Therefore, it is critical to run simulations to determine the operational effectiveness of certain specific improvements.

7.4.5. Simulation scenarios

The limits for (de)mooring are determined by experience by engineers from TWD and in congruence with the mooring study performed by Crowley [28] for NYSERDA. Due to its stringent operating conditions (de)mooring is a critical operation. The estimated limit of 1.5 m H_s provided by TWD engineers is based on limits for anchor handling, as this seems a representable operation since this also required human actions on the deck of the vessel [95]. In addition, Crowley performed navigation simulations for the mooring operations which were executed by captains for various environmental conditions. These simulations show that mooring with 1.5 m H_s is definitely possible and can even be executed in the range between 1.5 and 2.1 m H_s at captains discretion. So a range exists from 1.5 to 2.1 m H_s in which (de)mooring might be possible. This range makes that the exact operating limit for (de)mooring is uncertain. The limit of this operation can have a significant impact on the operation, as is stressed

Table 7.2: Improvement potential for various blade rack and backload transfer limits and fixed and varying (de)mooring limits.

Case	Blade rack lift H_s limit [m]			
	1.5	1.7	1.9	2.1
March - mooring limits fixed	3652	3621	3615	3615
March - mooring limits variable	3652	3500	3422	3375
August - mooring limits fixed	4305	4206	4186	4183
August - mooring limits variable	4305	3928	3747	3669

by table 7.2, so the uncertainty range must also be taken into account.

To deal with the uncertainty, different scenarios for every configuration are created, where each scenario has a different operational limit regarding the (de)mooring operation. The simulations will then show the potential of certain configurations given that an operating limit for (de)mooring can be attained. The simulation results then provide insight into how the operational capacities and performance of different concepts relate to each other. The scenarios are enumerated from scenario 1 to scenario 4 where the operational limits for (de)mooring increase from 1,5 to 2,1 meters H_s with a stepsize of 0,2 meters.

7.5. Conclusion

This chapter answers the research question of how the operating limits and required weather windows translate to operational performance. This is achieved by means of a DES model where the operating limits and weather windows are combined with the operation sequence, the duration of individual operations and the environmental conditions. The DES model only accounts for weather-related downtime. The simulation results converge over time providing a mean result and a spread which is used to asses the variability of the results. The financial performance is determined by means of the vessel activity, which determines the VOYEX and the total duration, which determines the total costs for chartering vessels and equipment. The simulation identifies (de)mooring, lifting the blade rack and backloading as bottleneck operations and shows that it is key to improve all bottleneck operations in order to decrease the total downtime and improve operational performance. To account for the uncertainty regarding the operational limits of the (de)mooring operation, which would be a bottleneck, multiple scenarios will be simulated to obtain the results for the configurations mentioned in chapter 6. For these scenarios, the operational limits for (de)mooring are increased from 1,5 to 2,1 meters H_s with steps of 0,2 meters. This chapter shows that simulating the sequential operations is necessary to capture the influence of operations on each other. This is critical in order to determine the performance of the total system and assess the effectiveness of an improvement to an operational step within the process. A DES is therefore crucial to gain insight into the performance of the total system.

Table 7.3: Model tests.

Test	Subject of what is tested	Hypothesis	Result
Increase duration of a single operation	Weather window check	Increase will be more than no WTG times extra duration per WTG.	1h mooring increase lead to 73,5 hour increase on average. Hypothesis confirmed
Increase/decrease number of WTGs	Creation of entities, time continuity, model consistency	Total duration will increase. As the amount of WTGs increase, difference between starting months will become less as the total duration reaches year-round. For less WTGs relative difference will be larger.	Hypothesis confimed
Increase blade rack transfer limit	Weather window, dependencies	Less downtime	Less downtime, but effect is minimal as other operations remain on a critical path as well
Increase transit limit	Weather window, dependencies	Less downtime at transit but more downtime during the offshore operation	Hypothesis confirmed
Increase blade installation limit	dependencies	Less downtime, more significant increase as less 'critical' operations are close to it.	Less downtime encoutered, for blade installation. Downtimes for following operations increase slightly.
Decrease the amount of feeders	Queing and requesting of feeders	Duration will be larger. However, advantages can be obtained in costs as a dual feeder ony has a 3 hour net advantage per WTG.	Longer duration, lower costs.

8 Results

This chapter covers the results of the simulations for the configurations as presented in chapter 6 and discusses their performance.

8.1. Duration

The results show that the installation method is the dominant factor regarding the total duration of the installation of all 20 mw WTGs. Figure 8.1 shows the results for simulation scenarios 1 and 4 and that there is almost no difference regarding the operating time with different barges. In scenario 1, the assumption is that the limits for (de)mooring are 1.5 m H_s. This means that all configurations essentially feature the same bottleneck operation. All configurations are limited by the same operation, in which case it is profitable to shorten the total net. duration by changing the installation strategy. What also becomes apparent is that the transit operation is not on the critical path. This was already found by analyzing the base case in section 7.4.3 and is again confirmed by the results. This becomes evident since the difference in total duration between the Memphis Bridge barge, sailing between New Bedford and the offshore site, and barges 2, 3 and 4, the barges sailing between the New London State Pier and the offshore site, are almost equal, while the sailing duration is 4 hours longer. If this operation were to be critical, the total duration would have increased by at least 248 hours.

The differences between the configurations should become more apparent when the bottleneck operation is lifted. This is most apparent in the case of scenario 4, where the (de)mooring limits are 2.1 H_s. Figure 8.1 shows the comparison between the different scenarios. Comparing the results from scenarios 1 and 4 shows at first that lifting the bottleneck operation has a significant effect on the total duration as this decreases with roughly 350 hours for each configuration. The decrease in duration is most evident for the step from scenario 1 to 2 and becomes less and less pronounced for the steps from scenario 2 to 3 and scenario 3 to 4 respectively. However, the way the configurations perform with respect to each other stays roughly the same. This can be seen in appendix P. Concluding, also for scenario 4 there is almost no difference regarding operational time when using different barges. This result was unexpected initially but is explained by analyzing the simulation input.

Section 7.4.4 shows that simulation results differ per month. Figure 8.2 shows the mean duration for all configurations and all starting months. This figure displays the results for scenario 4, as these simulations are the least restricted by the (de)mooring operations and with that better able to show the differences between the different configurations. The results are conditionally formatted per month which shows that each configuration has similar performance with respect to the other configurations for all possible starting months. There are thus no preferred configurations depending on the season in which it needs to operate. Configuration 2.A is in this case the preferred concept, as this configuration requires the least time to install all the WTGs. Configuration 1.A would be the second preferred configuration. This configuration requires 15 hours more to complete the installation of all WTGs. The difference between these concepts is less than a day, or 0,5 % with respect to their total installation

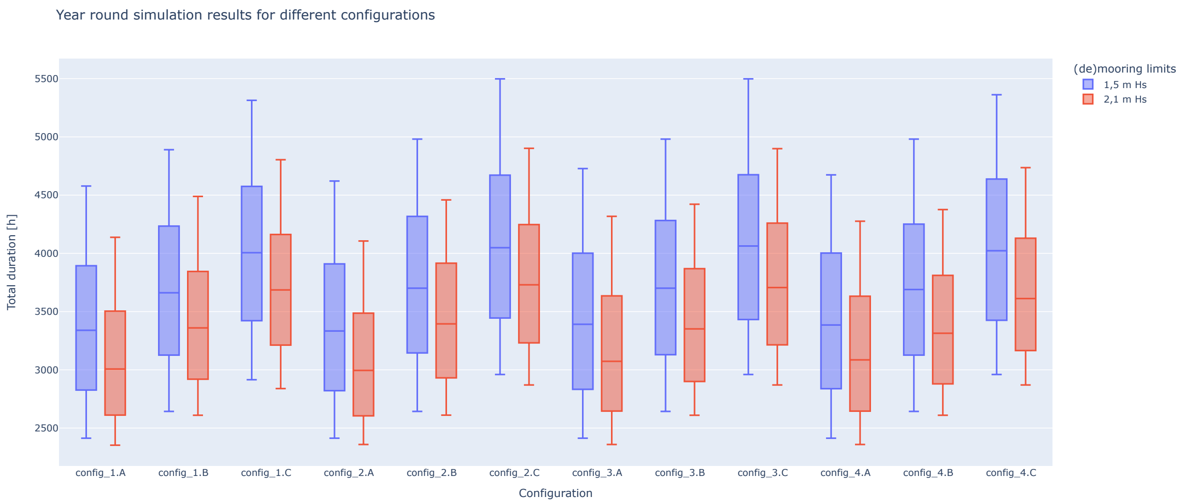

Figure 8.1: Total duration for scenario 1 and scenario 4.

time and can thus be considered insignificant.

	January	February	March	April	May	June	July	August	September	October	November	December	Year round
config_1.A	3431,71	3132,11	2883,84	2649,00	2491,74	2485,18	2586,50	2883,50	3337,29	3660,89	3803,84	3675,89	3085,12
config_1.B	3682,05	3383,76	3140,16	2896,89	2760,08	2769,34	2920,37	3290,95	3759,34	4050,26	4115,66	3958,58	3393,95
config_1.C	3952,63	3647,74	3396,24	3151,18	3025,84	3064,74	3260,42	3716,08	4177,32	4421,11	4416,39	4237,89	3705,63
config_2.A	3409,21	3114,05	2865,76	2632,18	2483,79	2476,47	2563,11	2856,82	3322,45	3657,39	3800,18	3661,18	3070,22
config_2.B	3732,05	3423,08	3166,00	2925,82	2775,61	2773,55	2923,37	3319,63	3839,16	4132,05	4182,61	4023,66	3434,72
config_2.C	4010,55	3692,95	3433,03	3180,63	3049,11	3090,18	3282,13	3763,08	4264,63	4519,63	4495,34	4308,53	3757,48
config_3.A	3511,45	3198,32	2936,71	2692,84	2517,47	2494,95	2591,79	2909,79	3441,97	3797,79	3939,50	3796,74	3152,44
config_3.B	3674,13	3377,24	3128,84	2894,26	2754,05	2752,13	2890,58	3278,39	3778,58	4071,39	4124,29	3965,18	3390,76
config_3.C	3990,34	3676,45	3418,05	3165,39	3046,79	3079,71	3278,76	3763,68	4273,84	4517,74	4491,89	4302,11	3750,40
config_4.A	3511,97	3194,68	2933,47	2682,76	2522,13	2494,32	2600,42	2922,32	3459,21	3800,63	3947,18	3792,53	3155,14
config_4.B	3638,63	3344,79	3103,26	2872,87	2744,42	2737,00	2869,24	3239,32	3719,29	3997,97	4060,95	3910,29	3353,17
config_4.C	3905,13	3606,53	3366,87	3129,37	3017,87	3038,03	3224,47	3645,76	4118,68	4371,45	4369,42	4198,05	3665,97

Figure 8.2: Mean total duration per month for scenario 4.

The lack of difference between the simulation results can be explained by analyzing the simulation input. Looking at the wave period occurrence, it becomes evident that 80 % of the peak periods occur in the range between 4 and 9 seconds. Looking at the operating limits, it can be concluded that between a peak period of 4 and 9 seconds, the operating limits of the configurations are fairly similar regarding the critical blade transfer lift. For barges 2, 3 and 4, their natural roll periods are closer to or even in the 4 to 9-second range. Combined with their larger metacentric height, their operating limits regarding the transit operations between the peak periods of 4 and 9 seconds are lower than for the configurations with the Memphis Bridge Barge. This also means that the slight operational advantage that the larger barges had regarding the blade rack lift is canceled out by their lower operating limits regarding the transit operation.

8.2. Costs

Taking the costs into consideration has both a leveling and a diverging effect on the results. Since the daily costs for transporting the WTG towers in one section are higher than transporting them in two sections, the difference between the one-, and two-piece installation strategy becomes relatively smaller then when only total installation time is taken into account. On the other hand, the three-piece installation strategy is the most cost-intensive installation strategy, due to the high dayrate of the T700 platform. This causes the difference between the results for two- and three-piece installation strategies to increase with respect to their relative time-based difference.

The daily costs for the barge increase as the barges increase in size. In combination with the conclusion above that there is no significant time advantage when using bigger barges, this means that the total costs only increase when opting for bigger barges. Unfortunately, no costs could be acquired for the different tugs. The costs used to model the tugs are based on the dayrate for the current tugs which are 110 BP tugs with a dayrate of 9000 $. It could be that, depending on the market, a 180 BP tug could cost up to but not limited to more than double the dayrates of the current tugs. This will have the most significant impact on the financial performance of configurations that require tugs with a high bollard pull. Intuitively this will have the most effect on the configurations with higher barges, making them financially even less attractive. However, the required tugs are determined by taking the desired transit operating limits (minimal H_s) into account as well, which has a significant impact on the required bollard pull of a tug. Due to its high operating limits, configuration therefore requires a tug with high bollard pull as well. Its financial performance will therefore be slightly less than depicted in figure 8.3. Based on costs, configuration 1.A holds the advantage over all other concepts. This is due to its short time to install all WTGs and a low dayrate for the barge.

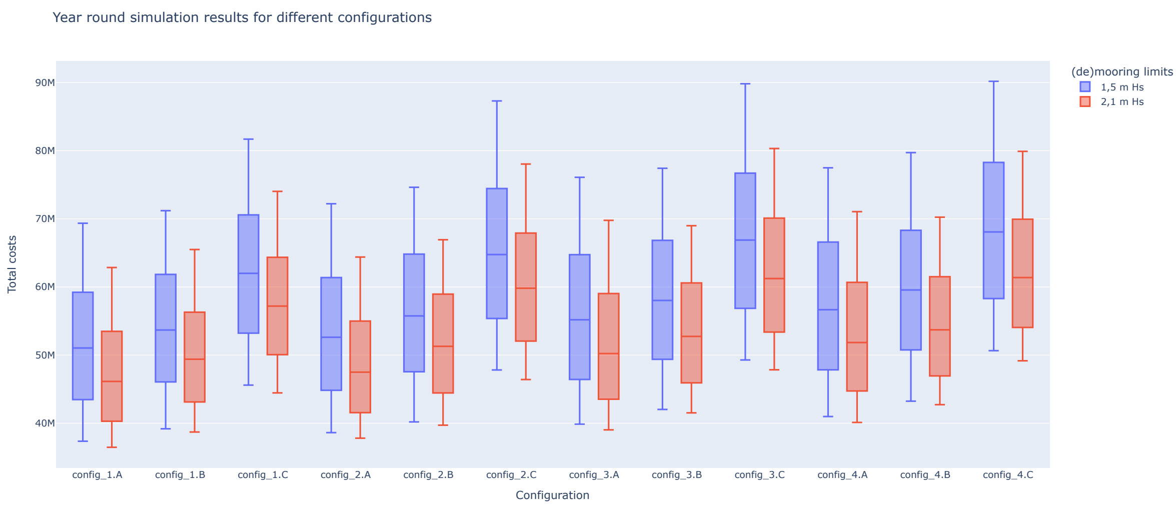

Figure 8.3: Total costs for scenario 1 and scenario 4.

8.3. Risk

Section 2.5 identifies risk as the third performance indicator. Risk is seen as the variability across simulations and quantified by the standard deviation (σ). The variability across the total duration is used to assess the associated risk. Variability over the total costs is not seen as a good indicator due to the assumptions made for the cost components and the market-driven variability regarding dayrates. The violin plots in figure 8.4 visualize the distribution of the total duration for year-round simulations in scenario 4. Only scenario 4 is observed as this provides the most significant differences between the results of the different configurations. The results do not show unexpected behavior given the discussed results. It is observed that longer duration is paired with larger variability across simulations. In the results, this is most apparent for the different installation strategies. These require more installation steps, providing more moments in which downtime can be encountered, resulting in a larger spread. This results in the fact that the configurations that perform well in terms of total installation time, also perform well with regards to their associated risk. The simulation results for scenario 4 show an interesting result when comparing configurations 3.A and 3.B, and configurations 4.A and 4.B. Both configurations 3.A and 4.A outperform configurations 3.B and 4.B respectively in terms of installation time. However, the variability for configurations 8 and 11 is slightly less, providing more certainty that the complete operation can be executed in the estimated time. This tradeoff shall be made according to a contractor's preferences. However, as the increased certainty is so small, it is safe to say that in this case, a contractor would opt for the faster configuration.

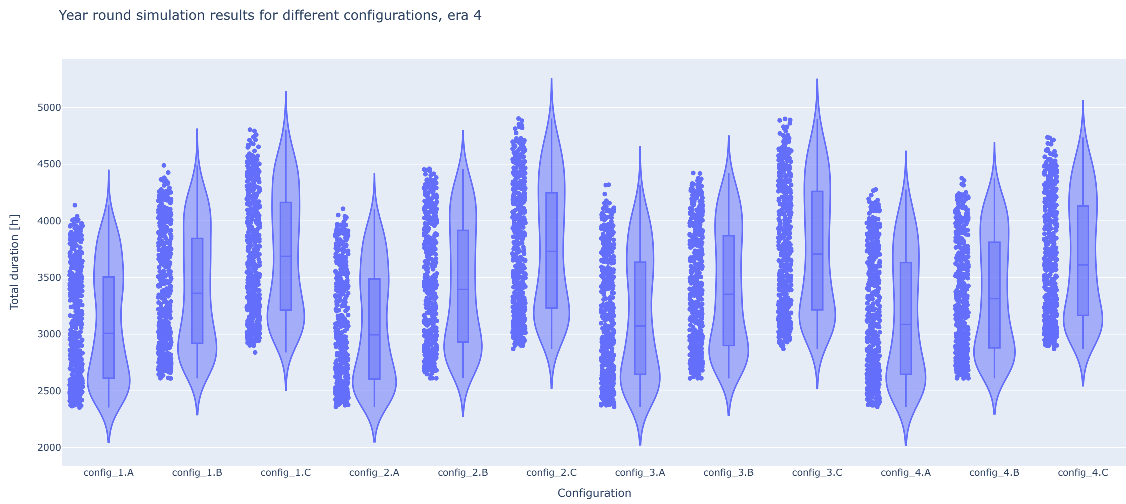

Figure 8.4: Violin plots for scenario 4.

8.4. Excluding period dependency

The simulation considers the peak periods to determine the performance of the configurations. This differs from the earlier research concerning Discrete Event Simulation for the construction of OWFs. To stress the importance of incorporating the peak period, simulations are also performed where the lowest allowable H_s is used as the limit for all peak periods. These results differ significantly from the original results. scenario 4 is the least restricted by the (de)mooring operations, therefore the differences between configurations are more pronounced. Only the results regarding the total duration of scenario 4 will therefore be discussed.

Figure 8.5 shows the year-round simulation results without period dependency for scenario 4. The total duration is longer for all simulations, which is to be expected as the lowest operating limit is now used as the operating limit for all peak periods, effectively decreasing the workability of each configuration. An interesting phenomenon can be observed for configuration 11. This configuration has high limits for both the blade rack transfer and the transit operation. This makes that it encounters less downtime than configuration 1.A, resulting in a lower variability over the total duration and an extra mean installation time of only 60 hours while this configuration requires a net 240 extra hours for lifting the extra tower section. This configuration is thus less susceptible to weather delays.

Analyzing the results per month stresses the fact that configuration 4.B is less susceptible to weather delays. Figure 8.6 shows the mean total duration per month where the results are conditionally formatted per month. These results show that configuration 4.B performs specifically well in months where weather conditions are generally worse, due to its high operating limits. This case thus has preferred configurations depending on the season in which a configuration needs to operate. In such cases, it could also be attractive for a contractor to opt for a configuration that is generally slower but allows to operate in more conditions and with that decreases the chance of weather-related delays.

The results of the simulations for excluding period dependency show that the peak periods have a significant influence on the results of the simulation and can even influence the choice for an optimal concept. When planning and preparing operations, it is important to take into account the environment as accurately as possible, such that you can design and optimize your operation for your specific environment. Taking the peak period into account is thus key for optimizing your operation. The case stated above for excluding peak periods shows the effect of neglecting peak periods on prospected performance and optimization trade-offs. Adding to that, this case shows the possible trade-off that can be made between duration and risk and that a DES is able to show this in the results of the simu-

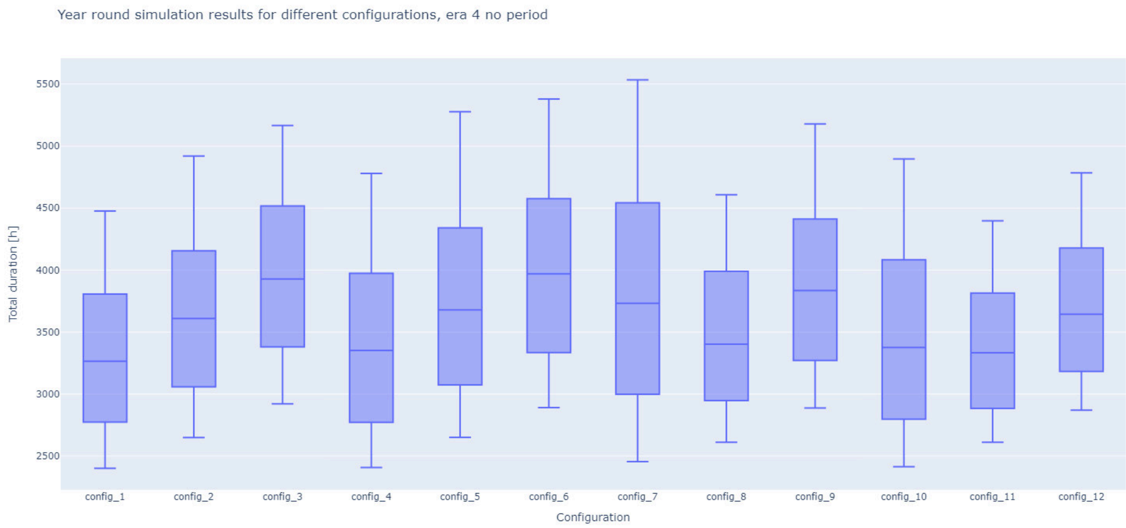

Figure 8.5: Total duration for scenario 4 simulations excluding period dependency.

	January	February	March	April	May	June	July	August	September	October	November	December	Year round
config_1.A	3647,03	3335,27	3057,49	2799,89	2614,41	2589,51	2742,65	3146,03	3697,51	4010,65	4109,05	3946,78	3308,02
config_1.B	3920,57	3588,70	3315,84	3037,22	2874,62	2883,97	3082,65	3579,38	4155,22	4443,84	4445,43	4232,16	3629,97
config_1.C	4186,97	3856,30	3566,46	3292,84	3159,68	3223,84	3517,35	4100,51	4603,84	4807,76	4750,16	4508,22	3964,49
config_2.A	3737,22	3373,03	3078,24	2792,24	2605,43	2594,78	2752,43	3215,27	3904,16	4264,00	4285,81	4082,54	3390,43
config_2.B	4040,41	3665,27	3350,03	3053,22	2887,14	2901,43	3110,68	3714,51	4382,65	4689,46	4640,70	4395,11	3735,88
config_2.C	4217,35	3867,49	3567,84	3282,35	3149,08	3197,32	3484,14	4164,00	4679,03	4898,86	4828,68	4577,65	3992,82
config_3.A	4118,62	3693,51	3327,65	2994,95	2766,68	2760,05	3016,11	3823,68	4690,73	4969,78	4856,49	4536,49	3796,23
config_3.B	3760,19	3434,14	3177,08	2926,57	2777,57	2777,14	2938,68	3379,84	3927,59	4229,73	4245,51	4072,05	3470,51
config_3.C	4106,49	3768,84	3481,70	3205,89	3079,95	3125,08	3358,19	3911,57	4459,65	4721,89	4666,65	4442,08	3860,67
config_4.A	3801,70	3419,43	3106,81	2816,35	2616,27	2600,70	2779,51	3305,32	4059,32	4402,11	4402,38	4163,92	3456,15
config_4.B	3647,51	3351,43	3109,43	2877,41	2745,11	2743,38	2871,54	3247,16	3736,11	4016,38	4080,51	3920,65	3362,22
config_4.C	3934,14	3628,86	3382,76	3142,54	3026,05	3042,49	3235,65	3670,92	4150,95	4422,51	4414,24	4230,51	3690,14

Figure 8.6: Mean total durations per month for scenario 4 excluding period dependency.

lation. The results of the simulation are different for each environment and simulations and trade-offs should be made for each environment that is to be considered.

8.5. Conclusion

The results show that configuration 1 is the optimum within the design space. Although configuration 2.A performs slightly better in terms of total duration and risk, the difference between the performance of configuration 1.A and 2.A for these KPIs is negligible. Configuration 1 trumps all other concepts based on costs, and can therefore be appointed as the optimal configuration. This is due to the fact that this configuration sports the installation strategy where the tower is transported, transferred and installed in a single piece, saving net. operation time. In addition to that, this configuration has high operating limits for the transit operation. Configuration 1.A has the lowest operating limits for the blade rack lift, but for the peak periods occurring most frequently at the Vineyard site, the blade rack lifting operation is less critical than expected. The benefit of scaling up to a larger barge in order to remove the initially identified 'bottleneck' created by the blade rack lift is therefore minimal. In addition to this, configuration 1.A has the lowest daily costs regarding the barge and can be realized with U.S. barges that are currently available. Combined with the fact that it is not attractive to invest in barges, makes that configuration 1.A is more ready for implementation than all configurations sporting barges 2, 3, and 4. The optimal configuration is therefore likely to be a barge equal or similar to the Memphis Bridge barge, where the tower is transported, transferred and installed in a single piece. This configuration will be equipped with one large motion compensation platform and lifts will be executed with an inline AHC. The inlineAHC is likely to be improved if the operational benefits outweigh the increased dayrate.

By identifying an optimal configuration, the results also prove that the presented framework can be used to design and optimize a feedering method. This research adds DES as a tool for ship designers to assess and optimize the performance of their designs. The use of DES is not limited to the complete configuration and can also be used to assess methodologies or improvement of equipment.

8.6. Jones Act compliant WTIV scenario

To showcase the potential of the optimal feeder configuration in the Vineyard area, a comparison is made to a conventional strategy with a Jones Act compliant WTIV for the construction of an OWF. For this comparison, the scenario with (de)mooring limits of 1,5 meters H_s is used. The conventional strategy uses the nearest U.S. port that can be entered by a WTIV according to NREL, the New Jersey Wind Port, as the marshaling port [14]. This port is situated 290 nm from the Vineyard site, resulting in a 29-hour loaded and 24-hour unloaded transit time. The WTIV loads and installs 4 sets of WTG components per trip [104].Table M.2 in appendix M presents the full characteristics of the simulation for the conventional strategy. The dayrate for the Jones Act Compliant WTIV is estimated by Hans Simons at $ 450000, which is twice the dayrate of the foreign WTIV [12]. Due to the cost overruns of the Jones-Act compliant WTIV that is currently under construction, it is likely that the actual dayrate will be even higher [7].

Figures 8.7 and 8.8 show the performance of the conventional and optimal feedering strategy in terms of duration and costs. The conventional strategy outperforms the feedering strategy from September to December in terms of duration. In addition, the conventional strategy has a significantly smaller spread in terms of duration which shows that the conventional strategy is less susceptible to weather conditions. However, when taking into account the costs, the feedering strategy has a clear advantage over the conventional strategy. This is due to the high dayrate of the Jones act compliant WTIV. Despite the 29-hour journey to the installation site and the subsequent 24-hour return to the marshaling port for the WTIV, the conventional strategy is not heavily outperformed by the feedering strategy and even outperforms the feedering strategy for certain months.his is because the conventional strategy eliminates the need to unload a feeder vessel, a process that takes net 12 hours to complete, and that the WTIV is able to load 4 sets of WTG components. For regions closer to a port that is accessible by a WTIV or WTIVs with a larger carrying capacity, the conventional method is expected to improve in terms of duration with respect to the feedering method.

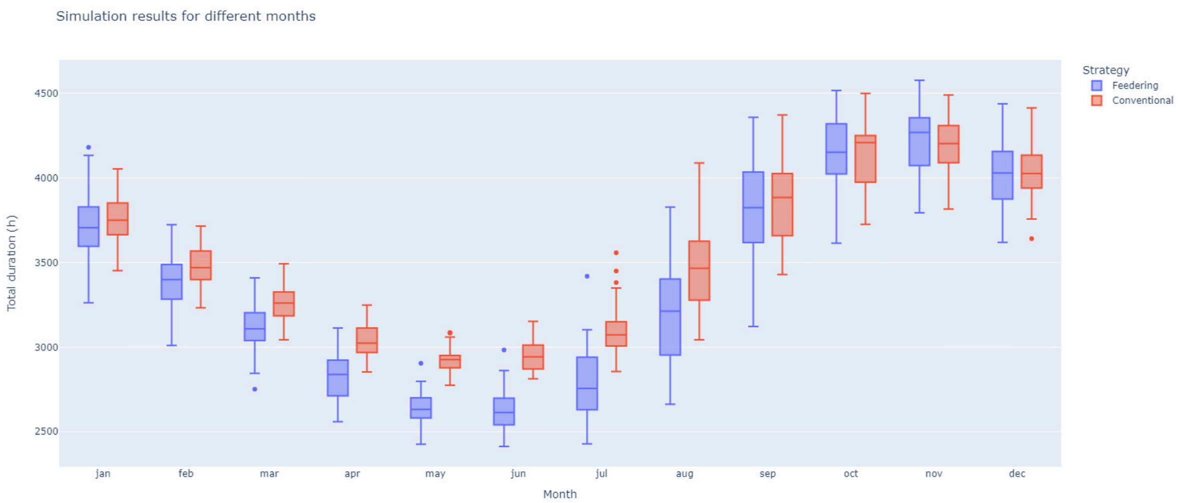

Figure 8.7: Duration comparison between the feedering and conventional installation method.

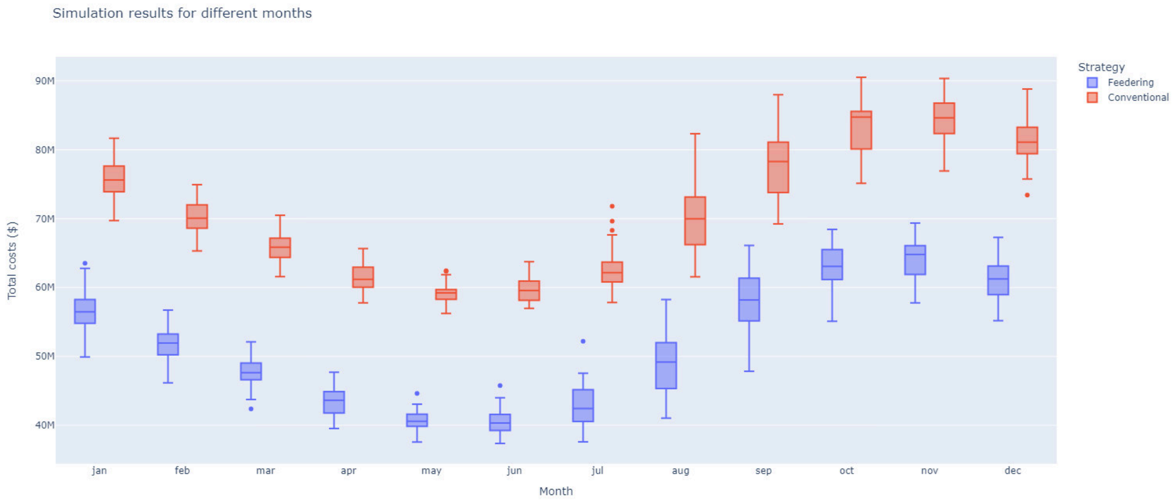

Figure 8.8: Cost comparison between the feedering and conventional installation method.

9 Conclusion

This chapter first discusses the results of this thesis after which it answers the main- and sub-questions. Section 9.3 provides a high-level overview of the contributions of this thesis. Finally, section 9.4 recommends how the potential of the methodology presented in this thesis can be exploited even further and which research can add value to this or related topics.

9.1. Discussion

The goal of this thesis is to obtain an understanding of the Jones Act compliant feedering installation method for future 20 MW WTGs and to optimize the feedering method for this future operation. The results show that a future optimized feedering method for the installation of 20 MW WTGs in the Vineyard environment will be characterized by a 400 ft barge, similar to the Memphis Bridge barge, and an installation strategy where the tower is transported, transferred and installed in a single piece. The method will include the use of a single large motion compensation platform and a quick lift AHC to increase the operating limits for the component transfers.

The single-piece installation strategy is in line with the conclusion of Smorenberg [21]. This research also includes the varying operating limits when changing the installation strategy. With this addition, this research proves that the operational advantage of a single-piece installation strategy can actually be attained and that this strategy is not being limited more by weather conditions than two or three-piece installation strategies. NYSERDA stated that larger barges will have an operational advantage in terms of their operating limits for the transfer lifts. This research agrees with their findings and shows that the operational limits for lifting the blade rack indeed increase for larger barges. However, no research was executed regarding the effect of increasing the barge size on operational transit limits. This research addresses this effect and concludes that the natural roll period decreases for increasing barge size and that the operational limits first decrease due to increased accelerations associated with the lower natural roll period. The operational limits then slightly increase as the barge becomes less susceptible to waves as it further increases in size. The barge size at which this phenomenon occurs depends on the loading condition of the barge. Both studies neglected the costs associated with different installation strategies or feeder vessels. This research tries to address these associated costs, so the performance of a potential configuration can also be financially assessed. Finally, this paper sheds light on the importance of improving the (de)mooring operation. If this operation stays limited to 1,5 m H_s there is no enormous need to improve the other operations as the (de)mooring operation remains the bottleneck operation. The results show that improving these limits has a significant effect on the operational performance of all configurations. It is therefore advised to conduct future work on improving the operating limits of the (de)mooring operation.

The decrease in the operational transit limits for increasing barge dimensions was not expected. For some peak periods, the limits even decrease to such an extent that the transit operation becomes a bottleneck operation in simulation eras 3 and 4. The DES therefore resulted in unexpected results as well. It was expected that increasing the barge sizes would result in significantly decreased total time due to the increased operational limits for the blade rack transfer and the backloading operations, improving the identified bottlenecks. However, it turns out that this effect differs per loading condition and its magnitude is limited. The magnitude is limited due to the fact that the operational limits for the blade rack transfer of the different barges are fairly similar for the common peak periods at the Vineyard site. Combined with the decreased transit limits for increasing barge size, this results in the fact that the total time does not decrease as expected for larger barges.

This research assumes that the barge and seafastening can withstand the loads acting on it. This assumption is reasonable for the loading conditions where the tower is transported in two or three sections as this will not differ too much from the loads that act on the barge for the Vineyard project. However, the single-piece installation strategy will result in significantly higher loads. It is unknown if the barge and seafastening can actually withstand these loads. It is therefore recommended to conduct research regarding vessel strength and seafastening design for the single-piece installation strategy in order to further assess the feasibility of the single-piece installation strategy.

This research uses the maximum allowable accelerations of the WTG components to determine the operational transit limits. These accelerations are provided by the WTG manufacturer as governing for all tower sections or combinations thereof. It is expected that the allowable accelerations decrease as the tower sections are pre-assembled due to a higher internal bending moment. In addition to that, the allowable accelerations differ significantly per WTG manufacture as some allowable accelerations are twice the allowable accelerations as presented in section 5.2. According to NYSERDA, WTG manufacturers express concerns that component accelerations will be reduced for larger turbines [105]. It can thus be concluded that there is no consensus for the allowable accelerations of 20 MW WTG components. Since the transit operation is already critical for some configurations, the allowable component accelerations can significantly impact the operational performance of the configurations. Additional research should therefore be executed regarding the maximum allowable accelerations of WTG components including the effect on allowable accelerations for pre-assembled towers.

The simulation provides the optimal configuration for operational areas similar to the Vineyard site. Different sites can have different weather conditions which can change the performance of a configuration and also the optimal configuration. For sites with longer wave periods, it is expected that there will be more differences between the performance of different barges. This is expected as the difference in the blade rack lifting limits for longer wave periods is more pronounced. Other operational areas should be researched as well to assess the performance of the configurations in different areas and determine if certain configurations are 'robust' enough so they can excel in multiple areas or to determine a configuration that has the best overall performance for a selection of sites. The performance for different sites can easily be determined by changing the weather data and the duration of the transit operations. Unfortunately, no weather data for different sites was available. It is therefore recommended to assess the influence of the operation site on the performance of the configurations in order to determine the robustness of the current optimal configuration and an overall best-performing concept.

The study addresses the need for different tugs associated with each configuration. However, no dayrates were available regarding the tugs, except for the ones used at the Vineyard project. These dayrates can have a significant impact on the financial performance of a configuration. This makes the financial assessment performed for the configurations incomplete. Additional work should therefore be devoted to model the dayrates of tugs in order to improve the financial assessment.

The assumption is made that the barge is oriented in head waves with a 15-degree margin to either side during the transfer operations. It is not assessed to what extent this is actually possible and if the wave directions actually remain within the 15-degree margin. If this assumption is not valid, the workability of each transfer operation decreases, negatively influencing a configuration's performance. It should therefore be checked to what extent this assumption is valid. In case it is not possible to remain in head waves, the relevance of a DP system to keep the geographical position of the barge is stressed. A DP system allows the barge to slightly weathervane, and remain more oriented in head waves. A

DP system also removes the mooring operation, potentially removing a bottleneck, dependent on what the operating limits of the DP system are. It is therefore also recommended to assess the viability of using a DP system to keep the barge next to the WTIV.

This research further presents a simplified method for assessing the probability of re-hits during the blade-rack lift. This method is not verified, and therefore only compares the results on a relative basis. Also, the relative results of this method could be well off. This simplified method should therefore be verified with high-fidelity models in order to determine its validity. In case the method is found to be valid, this method could save intensive computational time.

The business case for the feedering strategy in the Vineyard area is proved by the comparison between the optimized feedering method and the conventional installation strategy. Due to the lack of available ports near the Vineyard area, the feedering strategy provides a faster, but more susceptible to weather delays, alternative for OWF construction. Feedering requires a larger vessel spread and more specialized equipment than the conventional strategy, driving the daily costs. However, due to the high estimated dayrate for a Jones Act compliant WTIV, the feedering method well outperforms the conventional strategy in terms of costs. It must be stated that the cost based performance of the conventional strategy highly depends on the dayrate of Jones Act compliant WTIV. The used dayrate is estimated according to the newbuild costs of the WTIV. Due to the cost overruns of the project, it is likely that this dayrate will be even higher. On the other side, dayrates are market dependent and the market could force the dayrate to drop, making the conventional strategy more competitive to the feedering strategy.

This research provides an understanding of the feedering installation method for future 20 MW WTGs and optimizes this future operation for operational areas similar to the Vineyard site. Thereby it provides a novel framework to optimize a feedering operation and demonstrates its applicability in optimizing such operations. This knowledge and understanding contribute to the development and realization of future U.S. OWFs. This in turn helps the U.S. in attaining their renewable energy goals and contributes to the energy transition. The framework and the model are ready to be used in industry and can support decision-making regarding operational methods, vessel design, equipment design, or a combination thereof. TWD values the framework and the included simulation and sees great value for both method and equipment design. For method design, it can add great value in the heavy, near-shore civils market. The contractors executing these projects are less familiar with workability and DES studies but take on huge projects that are often influenced by wind and sea conditions. The proposed framework can assist in designing their installation methods or in making a proper time, cost and risk assessment. Regarding equipment design, the framework can assist in setting the right requirements for equipment. This helps in designing fit-for-purpose equipment. TWD can use the framework to show clients what the potential benefit is of improving certain types of equipment. This helps TWD to meet their clients' need and avoids the costs of overdesigned equipment.

9.2. Conclusion

This section answers the main and aiding sub-questions posed in this research. The objective of this research is to answer the following main question:

'What are the characteristics of an optimized Jones Act compliant feedering method for the installation of future 20MW offshore wind turbine generators?'

To answer this main question an approach is used that fuses the systems engineering framework with set-based design and discrete-event simulation. This methodology is capable of generating insight into the characteristics of an optimized feedering method for 20 MW WTG installation. This research shows that Discrete Event Simulation can be used as a tool for ship design to determine and optimize the performance of a design. Given that the environment in which the system operates is comparable to the Vineyard environment for which the feedering method is optimized, the optimized feedering will feature a 400ft barge similar to the Memphis Bridge barge where the tower is transported, transferred and installed in a single piece. This configuration is the best-performing configuration for the given environment within the design space. The main question is resolved with the aid of the sub-questions posed in section 1.3 and which are summarily answered below. The conclusions of chapters 2, 3, 4, 6 and 7 provide the full answers, including the background, to these sub-questions.

What are the steps in the U.S. WTG installation process from load-out to installed WTG and related duration, workability and costs, as performed for Vineyard Offshore Wind Farm with a traditional Jack-up vessel and barge?

This question is answered in chapter 2. This chapter presents the method used for Vineyard and possible alternatives. The duration and workability of each step are presented for the Vineyard specific project and how they are described throughout the literature. This provides the basis of the simulated operations in this thesis. The costs are described in a general way and traced back to their cost drivers and influencing factors. (De)mooring the vessel to the WTIV still has uncertainty regarding its operational limits and requires, simulating different scenarios to account for the uncertainty.

Which method can be used to measure the performance of a feedering method

This question is answered by sections 2.5, 2.6 and 4.4.2. Sections 2.5 and 4.4.2 state how the performance of the feedering method can be measured with KPIs regarding time, costs and risk. The KPIs are 'Total duration', 'Operational contractor costs' and 'Variability (σ)'. Section 2.6 consequently explains how these KPIs can be modeled with the use of Discrete-Event Simulation.

What are the characteristics of future WTGs and installation vessels

Chapter 3 answers this question in depth. Throughout the literature, no congruent answer is found on the characteristics of a future 20 MW commercial WTG. Therefore, the characteristics of such a WTG are determined in section 5.2. The future installation vessel will not influence the operation itself. Looking at developments in the WTIV market, designs might shift towards a diamond-shaped design or a dedicated feedering WTIV. These concepts will have a lower CAPEX than current jack-up designs, which will translate to a lower dayrate. The operation itself will not be influenced. Several custom-built jack-up vessel and barge combination concepts are proposed by the industry. However, the performance of these concepts is not evaluated.

Which method can be used to design an optimized feedering method?

Chapter 4 presents the full method to design an optimized feedering method. This proposed methodology fuses the systems engineering framework with set-based design and Discrete-Event Simulation. The methodology creates multiple feasible system concepts and simulates their performance by means of a DES model to identify the optimal system concept within the design space and the given environment.

What is the effect of vessel characteristics on operability and vessel costs?

Chapter 6 answers this sub-question. The vessel characteristics that are assessed are the global dimensions of a feeder barge. The daily vessel costs increase as the barges increase in size. Larger barges also require stronger tugs due to their increased resistance. This increases both the costs for tugs and their fuel consumption. In addition to that, barges larger than the Memphis Bridge barge are required to sail a longer distance due to the port restrictions of the New Bedford Marine Commerce Terminal. This increases both the VOYEX and the required weather window. Increasing the barge size has a positive effect on the operational limits for lifting the blade rack, increasing the operability and workability for that specific operation. However, increasing the barge dimensions also increases the metacentric height of the configurations. This results in a lower natural roll period and with that increased accelerations. For the largest barge, the operational limits start to increase again, as larger vessel becomes less susceptible to waves.

What is the effect of equipment characteristics on operability and equipment costs?

Chapter 6 answers this sub-question. The equipment is not used as a variable itself by varying the motion compensation capabilities. The motion compensation platforms are varied as a result of the installation strategy. A motion compensation platform that can compensate for a larger overturning moment results in increased daily costs for motion compensation. The quick lift AHC is an important piece of equipment that can improve operating limits for the blade rack lift significantly which is shown by a sensitivity study. However, it is unknown what characteristics are desired for future quick lift AHC systems and what costs are associated with these systems. The effect of varying the quick lift AHC system is therefore not taken into account for the operability costs and total performance of the configurations.

What is the effect of the installation method on operability, required vessels required equipment?

Chapter 6 answers this sub-question. The installation method has the most significant effect, also when analyzing the total performance, on the net. operation time. Reducing the amount of lifts significantly reduces the net. and with that the total operation time. The effect of the installation strategy on operability is not straightforward. Transporting the tower in more pieces lowers the inertia and increases the metacentric height of a loaded vessel. This causes the natural roll period of the vessel to decrease resulting in higher roll accelerations. On the other hand, transporting the tower in a single piece causes the tower COG to be located far from the center of gyration. Which leads to higher roll-induced sway accelerations. Adding to that, the effect of the installation strategy on the operating limits also depends on the vessel on which the WTG components are loaded. In terms of daily costs, it is beneficial to transport, transfer and install the tower in two sections as this leads to the lowest cost regarding the required motion compensation platforms.

How do the operating limits and required weather windows translate to operational performance?

Chapter 7 provides the background to and answers this sub-question. The combined operability and required weather windows are combined in a Discrete-Event Simulation together with the installation sequence, the duration of individual operations and the environmental conditions to determine the operational performance of a given configuration. The simulation results in a series of simulated operations for different operational years and thus different weather conditions. The mean and variance are the variables of interest for these result sets. During the simulation, the activity of each vessel is tracked which allows to determine the VOYEX for each configuration. Adding the VOYEX to the vessel and equipment costs provides the financial performance of a configuration. The DES allows to model the susceptibility to weather-induced delays of an operation. The simulation identifies bottleneck operations and shows that it is key to improve these operations in order to decrease downtime and improve operational performance.

9.3. Contributions

This research contributes to academia and industry with the following aspects:

- identification of the optimal configuration for feedering method installation of 20 MW WTGs in the Vineyard area
- a new framework including set-based design and DES that can be used for, but is not limited to, the design of a feedering method. With this, it brings DES to the ship design field
- introduction of a simplified method to assess the chance of a re-hit for lifting operations
- identifies the effect of general barge dimensions and installation strategies on transit limits
- introduces a method to justify and assess the effects of different installation strategies for marine operations and improving the operating limits for vessels or equipment

9.4. Future Work

Section 9.1 states the possibilities for future work. This section highlights and elaborates on the most relevant topics for future work.

The design of the seafastening and the vessel strength assessment are crucial steps for determining the technical feasibility of the proposed feedering solution. Future work is thus required to realize the proposed solutions. It is expected that more seafastening and structural reinforcements are necessary compared to the Vineyard project. These factors drive the mobilization costs. A financial assessment should be made as well to ensure that the operational benefits of the optimized solution outweigh the increased mobilization costs. This future work aids in proving the feasibility of the installation strategy where the tower is transported, transferred and installed in a single piece.

The limits for (de)mooring the vessel to the WTIV have a significant impact on the performance of the operation. The current range for these limits is uncertain, but all captains agree that executing these operations are definitely possible up to 1,5 m H_s. To unlock the potential of the feedering method, systems should be designed that increase the operating limits of this operation. This could be systems that provide a physical interface between the feeder and the WTIV or a dynamic positioning system that enables a barge to move to and remain in its position while not being physically attached to the WTIV. In the latter case, it should be examined whether the DP system is able to keep the barge position within a desired margin and it is recommended to design a system that prevents a critical collision between the barge and the WTIV in case the DP system fails.

This research determines the optimal configuration for a single operational area. The weather conditions influence the performance of each configuration and thus influence the optimal solution. Additional research should be carried out into the performance of the solutions for other areas assigned for the development and construction of OWFs in the U.S. This work should identify which solution is preferred for each area and identify an optimum overall solution. This aids the industry in decision-making regarding new investments and academia by identifying the area in which future research should be conducted. The overall optimum solution can set industry standards and help shape the developing U.S. offshore wind market as standardizing a method helps decrease overall costs and risk.

Bibliography

[1] House of Representatives, "46 U.S.C. 55102 - Transportation of merchandise." https://www.govinfo.gov/app/details/USCODE-2011-title46/USCODE-2011-title46-subtitleV-partD-chap551-sec55102/summary, 2011. Accessed: 2023-2-26.

[2] MaritimeFedWatch, "Custom Issues Comprehensive Offshore Wind Jones Act Ruling." https://www.winston.com/en/maritime-fedwatch/customs-issues-comprehensive-offshore-wind-jones-act-ruling.html, 2022. Accessed: 2023-2-20.

[3] Nadja, Skopljak, "ABS to class first US wind turbine iinstallation vessel." https://www.offshorewind.biz/2021/02/24/abs-to-class-first-us-wind-turbine-installation-vessel/, 2021. Accessed: 2023-2-20.

[4] GOA, "Offshore wind energy: Planned project may lead to construction of new vessels in the u.s., but industry has made few decisions amid uncertainties," Tech. Rep. GAO-21-153, United States Government Accountability Office, Washington, DC, December 2020.

[5] T. W. House, "FACT SHEET: Biden Administration Jumpstarts Offshore Wind Energy Projects to Create Jobs." https://www.whitehouse.gov/briefing-room/statements-releases/2021/03/29/fact-sheet-biden-administration-jumpstarts-offshore-wind-energy/-projects-to-create-jobs/, 2021. Accessed: 2023-3-13.

[6] A. Voogt, A. Sreenivasan, S. Wang, and M. Saint James, "Project 107: Final report comparative operability of floating feeder solutions," Tech. Rep. 107, NYSERDA, Albany, NY, June 2022.

[7] Adrijana Buljan, "Dominion Confirms First US Wind Turbine Installation Vessel Will Be Completed Later than Planned." https://www.offshorewind.biz/2023/11/09/dominion-confirms-first-us-wind-turbine-installation-vessel-will-be-completed-later- November 2023. Accessed: 2023-11-13.

[8] Z. Jiang, "Installation of offshore wind turbines: A technical review," *Renewable and Sustainable Energy Reviews*, vol. 139, p. 110576, 4 2021.

[9] R. Varghese, V. Pakrashi, and S. Bhattacharya, "A Compendium of Formulae for Natural Frequencies of Offshore Wind Turbine Structures," *Energies*, vol. 15, no. 8, 2022.

[10] T. Powers, A. Sajadi, and B. M. Hodge, "The current opportunities and challenges for offshore wind in the United States," *Electricity Journal*, vol. 35, no. 7, 2022.

[11] T. Stehly and P. Duffy, "2021 Cost of Wind Energy Review," tech. rep., December 2022.

[12] H. Simons, "Feeding the Beast, Optimising the Supply Chain for Offshore Wind Installation," tech. rep., HoTai Energy Consult, 2022.

[13] BOEM, "Outer continental shelf renewable energy leases," Tech. Rep. OREP-2022-2001, Bureau of Ocean Energy Management, Washington, DC, January 2023.

[14] M. Shields, R. Marsh, J. Stefek, F. Oteri, R. Gould, N. Rouxel, K. Diaz, J. Molinero, A. Moser, C. Malvik, and S. Tirone, "The Demand for a Domestic Offshore Wind Energy Supply Chain," Tech. Rep. NREL/TP-5000-81602, National Renewable Energy Laboratory, Golden, CO, 2022.

[15] “New Bedford Marine Commerce Terminal.” https://www.masscec.com/our-focus/offshore-wind/new-bedford-marine-commerce-terminal-nbmct. Accessed: 2023-5-15.

[16] “MARMAC 400 - ABS class Load Line deck barge.” https://www.mcdonoughmarine.com/assets/mcd-spec-sheets_v8-marmac_400.pdf. Accessed: 2023-5-15.

[17] M. Solutions, “MetOceanView Hindcast squared.” https://app.metoceanview.com/hindcast-squared/#/. Accessed: 2023-5-9.

[18] A. Ait Alla, S. Oelker, M. Lewandowski, M. Freitag, and K.-D. Thoben, “A study of new installation concepts of offshore wind farms by means of simulation model,” 06 2017.

[19] S. Oelker, A. Ait-Alla, M. Lütjen, M. Lewandowski, M. Freitag, and K.-D. Thoben, “A Simulation Study of Feeder-Based Installation Concepts for Offshore Wind Farms,” vol. All Days of *International Ocean and Polar Engineering Conference*, 06 2018. ISOPE-I-18-332.

[20] K. Maloney, K. Humphreys, D. Bourg, and C. Townsend, “An analysis of alternatives for the development of jones act compliant windfarm construction vessel fleets,” 2018.

[21] Marius Smorenberg, “An investigation of installation strategies to install next-generation offshore wind turbine generator components,” Master’s thesis, Delft University of Technology, Delft, September 2021.

[22] A. F. Haselsteiner, J.-H. Ohlendorf, S. Oelker, L. Ströer, K.-D. Thoben, K. Wiedemann, E. D. Ridder, and S. Lehmann, “Lifting wind turbine components from a floating vessel: A review on current solutions and open problems,” *Journal of Offshore Mechanics and Arctic Engineering*, vol. 141, 2 2019.

[23] Valkyrie3, “BARGE – 455-8 WITH SHAVER TUGS.” https://www.flickr.com/photos/valkyrie3/4839005738/in/photostream/. Accessed: 15-04-2023.

[24] C-JOB, “Offshore Wind Feeder.” https://webapp.c-job.com/wind-feeder/. Accessed: 15-04-2023.

[25] D. Ahn, S. C. Shin, S. Y. Kim, H. Kharoufi, and H. C. Kim, “Comparative evaluation of different offshore wind turbine installation vessels for Korean west–south wind farm,” *International Journal of Naval Architecture and Ocean Engineering*, vol. 9, pp. 45–54, 1 2017.

[26] D. Rippel, N. Jathe, M. Lütjen, and M. Freitag, “Evaluation of loading bay restrictions for the installation of offshore wind farms using a combination of mixed-integer linear programming and model predictive control,” *Applied Sciences*, vol. 9, no. 23, 2019.

[27] Det Norske Veritas, “DNV-ST-001 Marine operations and marine warranty,” 2021.

[28] M. Hertel, C. Hooper, and A. Mohtat, “Nowrdc agreement 103, technical validation of existing u.s. flagged barges as a feeder solution for the u.s. offshore wind industry: Maneuvering simulation to indicate operational limits technical report,” Tech. Rep. 103-213025-NOCM3.4, NYSERDA, Seattle, WA, May 2022.

[29] M. Hertel, C. Hooper, and A. Mohtat, “Nowrdc agreement 103, technical validation of existing u.s. flagged barges as a feeder solution for the u.s. offshore wind industry: Dynamic barge motions and mooring study technical report,” Tech. Rep. 103-213025-NOCM2.4, NYSERDA, Seattle, WA, November 2022.

[30] Barge Feeder Alliance, “Barge feeder alliance brings combined innovative, cost-effective, and practical solutions for the offshore wind industry,” tech. rep., Barge Feeder Alliance, 2021.

[31] D. Rippel, S. Peng, M. Lütjen, H. Szczerbicka, and M. Freitag, “Model transformation framework for scheduling offshore logistics,” 09 2020.

[32] S. Jalili, A. Maheri, and A. Ivanovic, “Decommissioning cost modelling for offshore wind farms: A bottom-up approach,” *Sustainable Energy Technologies and Assessments*, vol. 48, 101628, sep 2021.

[33] TWD, “Feeder model - 2022,” 2022. Not publicly accessible.

[34] S. Oelker, A. Sander, M. Kreutz, A. Ait-Alla, and M. Freitag, “Evaluation of the impact of weather-related limitations on the installation of offshore wind turbine towers,” *Energies*, vol. 14, no. 13, 2021.

[35] Y. T. Muhabie, C. Petcu, P. Rigo, and J. D. Caprace, “Weather Down Time Analysis for Offshore Wind Farm Installations,” *PIANC Yearbook*, 2016.

[36] M. Stopford, *Maritime Economics*. Abingdon: Taylor & Francis, 3 ed., 2009.

[37] Peter Kortekaas, 2023. personal conversation.

[38] M. Kaiser and B. Snyder, *Offshore wind energy cost modeling: Installation and decommissioning*, vol. 85. 2012.

[39] Will Kenton, “Operating Expense Definition and How It Compares to Capital Expenses.” `https://www.investopedia.com/terms/o/operating_expense.asp`, 2023. Accessed: 2023-3-27.

[40] M. Kaiser and B. Snyder, “Offshore wind energy installation and decommissioning cost estimation in the u.s. outer continental shelf,” Tech. Rep. 648, U.S. Dept. of the Interior, Bureau of Ocean Energy Management, Regulation and Enforcement, Herndon, VA, November 2011.

[41] Law insider, “Operating day rate definition.” `https://www.lawinsider.com/dictionary/operating-day-rate`. Accessed: 2023-3-28.

[42] M. J. Kaiser, *Offshore service industry and logistics modeling in the gulf of Mexico*. Springer cham, 2015.

[43] Temporary Works Design, “Heavy Feeder Dynamic Analysis,” 2023. Document provided under disclosure.

[44] Jolien Rip, “Probabilistic downtime analysis for complex marine projects,” Master’s thesis, Delft University of Technology, Delft, December 2015.

[45] E. Sandvik, M. Gutsch, and B. E. Asbjørnslett, “A simulation-based ship design methodology for evaluating susceptibility to weather-induced delays during marine operations,” *Ship Technology Research*, vol. 65, no. 3, 2018.

[46] M. Gutsch, S. Steen, and F. Sprenger, “Operability robustness index as seakeeping performance criterion for offshore vessels,” *Ocean Engineering*, vol. 217, 2020.

[47] Y. Tekle Muhabie, P. Rigo, M. Cepeda, M. de Almeida D’Agosto, and J.-D. Caprace, “A discrete-event simulation approach to evaluate the effect of stochastic parameters on offshore wind farms assembly strategies,” *Ocean Engineering*, vol. 149, pp. 279–290, 2018.

[48] G. E. P. Box and N. R. Draper, *Empirical model-building and response surfaces.* Wiley series in probability and mathematical statistics., Oxford, England: John Wiley & Sons, 1987.

[49] M. Leonelli, “Simulation and Modelling to Understand Change,” 4 2021.

[50] T. Ashuri, J. R. R. A. Martins, M. B. Zaaijer, G. A. M. van Kuik, and G. J. W. van Bussel, “Aeroservoelastic design definition of a 20 MW common research wind turbine model,” *Wind Energy*, vol. 19, pp. 2071–2087, 11 2016.

[51] IRENA, “Future of wind: Deployment, investment, technology, grid integration and socio-economic aspects (a global energy transformation paper), international renewable energy agency,” tech. rep., Abu Dhabi, 2019.

[52] W. Musial, P. Spitsen, P. Duffy, P. Beiter, M. Marquis, R. Hammond, and S. Matt, “Offshore Wind market Report: 2022 edition,” Tech. Rep. DOE/GO-102022-5765, Office of Energy Efficiency & Renewable Energy, Washington, DC, 2022.

[53] “V236 - 15.0 MW prototype.” https://www.vestas.com/en/products/offshore/V236-15MW/prototype. Accessed: 13-04-2023.

[54] “Construction and Heavy Maintenance Intelligence Database.” https://www.4coffshore.com, 2022. Accessed: 2023-5-15.

[55] “Video: Siemens Gamesa installs 14 MW wind turbine prototype.” https://www.projectcargojournal.com/construction/2021/11/16/video-siemens-gamesa-installs-14-mw-wind-turbine-prototype/, 2021. Accessed: 13-04-2023.

[56] Eize de vries, “Haliade-X uncovered: GE aims for 14MW.” https://www.windpowermonthly.com/article/1577816/haliade-x-uncovered-ge-aims-14mw, 2019. Accessed: 13-04-2023.

[57] J. Peeringa, O. Ceyhan, W. Engels, G. De Winkel, and R. Brood, “Upwind 20mw wind turbine pre-design. blade design and control,” Tech. Rep. ECN-E-11-2017, ECN, Dec 2011.

[58] P. Chaviaropoulos and A. Milidis, “20 mw reference wind turbine aeroelastic data of the onshore version,” Tech. Rep. Deliverable D 1.25 (a), INNWIND, April 2016.

[59] J. Jonkman, S. Butterfield, W. Musial, and G. Scott, “Definition of a 5-MW reference wind turbine for offshore system development,” *Contract*, no. February, 2009.

[60] C. Bak, F. Zahle, R. Bitsche, T. Kim, A. Yde, L. Henriksen, M. Hansen, J. Blasques, M. Gaunaa, and A. Natarajan, “The dtu 10-mw reference wind turbine,” 2013. Danish Wind Power Research 2013 ; Conference date: 27-05-2013 Through 28-05-2013.

[61] Bart Ummels, 2023. Personal conversation.

[62] Y. Kikuchi and T. Ishihara, “Upscaling and levelized cost of energy for offshore wind turbines supported by semi-submersible floating platforms,” *Journal of Physics: Conference Series*, vol. 1356, no. 1, p. 012033, 2019.

[63] G. Sieros, P. Chaviaropoulos, J. D. Sørensen, B. H. Bulder, and P. Jamieson, “Upscaling wind turbines: theoretical and practical aspects and their impact on the cost of energy,” *Wind Energy*, vol. 15, pp. 3–17, 1 2012.

[64] E. Loth, M. Kaminski, C. Qin, and L. J. Fingersh, “Gravo-aeroelastic scaling for extreme-scale wind turbines,” 2017.

[65] Erik Snijders, 2023. Personal conversation.

[66] “Dutch Offshore WInd Innovation Guide,” tech. rep., Netherlands Enterprise Agency, The Hague, 2023.

[67] M. Perry, M. Georgieva, M. Quah, and K. Foo, “Rapid development in offshore wind and the need for jackup installation vessel evolution,” in *The Seventeenth International Conference the JACK-UP PLATFORM*, City University London, September 2019.

[68] D. W. Rabaut and M. M. Bertels, “Floatable structure comprising a mooring system for mooring a second floating structure, and method for mooring the second floating strcuture,” Julyl 2021.

[69] J. D. Stroo, S. J. Jiskoot, and E. J. B. Snijders, “Self-propeller jack-up vessel,” April 2018.

[70] U. D. . solutions B.V., “J102 zero emission.” https://ulstein.com/vessel-design/j102-1. Accessed: 21-04-2023.

[71] Z. Jiang, Z. Gao, Z. Ren, Y. Li, and L. Duan, “A parametric study on the final blade installation process for monopile wind turbines under rough environmental conditions,” *Engineering Structures*, vol. 172, 2018.

[72] Temporary Works Design, “Concept design Vineyard WTG SF,” 2022. Document provided under disclosure.

[73] R. Wiser, M. Blonger, M. D. Hoen, Ben and, J. Rand, G. Barbose, N. Dargouth, W. Gorman, S. Jeong, and B. Paulos, “Land-Based Wind Market Report: 2022 edition,” tech. rep., Lawrence Berkely National Lab, Berkely, CA, 2022.

[74] International Maritime Organization (IMO), “IS-Code - Code on Intact Stability by IMO instruments (IS Code 1998) - ships constructed before 1-7-2010,” 2008.

[75] Wesley de Groot, 2023. Personal conversation.

[76] C. Maritime, “CROWLEY SHIPPING - TUGS AND BARGES.” `https://www.crowley.com/shipping/offshore/tugs-barges/`. Accessed: 2023-24-8.

[77] M. M. Service, “ABS OCEAN BARGES.” `https://www.mcdonoughmarine.com/ocean-barges.html`. Accessed: 2023-24-8.

[78] B. Master, “Motion compensated platform - BM-Feeder.” `https://www.barge-master.com/products/feeder/`. Accessed: 2023-10-05.

[79] Seaqualize, “The Seaqualize Heave Chief.” `https://www.seaqualize.com/`, 2023. Accessed: 2023-10-18.

[80] US Maritime Intelligence, “Memphis Bridge.” `https://intelligence.marinelink.com/vessels/vessel/memphis-bridge-338875`, 2023. Accessed: 2023-11-06.

[81] ITTC, “Estimation of Roll Damping. Recommended Procedure 7.5-02-07-04.5.,” *International Towing Tank Conference*, June 2021.

[82] Det Norske Veritas, “DNV-RP-205 Environmental conditions and environmental loads,” 2021.

[83] DEME offshore, “MOTION ANALYSIS ”American Trader Barge” for transporting WTG components in the project Vineyard Wind,” 2022. Document provided under disclosure.

[84] A. Voogt and A. Sreenivasan, “Project 107: Final report comparative operability of floating feeder solutions (m1.1),” Tech. Rep. 107 (M1.1), MARIN USA inc, Houston, TEXAS, December 2021.

[85] S. Wang, W. Huang, and Q. Yu, “Project 107: Consensus-based guidance (m2.1), guidance on operability analysis of floating feeder solutions,” Tech. Rep. 107 (M2.1), ABS, Houston, TEXAS, February 2022.

[86] A. Sreenivasan and A. Voogt, “Numerical Simulations to Determine Comparative Operability of Floating Feeder Solutions,” in *SNAME Maritime Convention, SMC 2022*, 2022.

[87] Joost Hogerheide, 2023. Personal conversation.

[88] Bill White, “New Bedford Marine Commerce Tarrif Schedule No.1 april 2016).” `https://files.masscec.com/Marine%20Commerce%20Terminal%20Tariff%20Schedule%20No.%201.pdf`, april 2016. Accessed: 2023-08-02.

[89] Det Norske Veritas, “DNVGL-RP-N103: Modelling and Analysis of Marine Operations,” 2021.

[90] Edwin van Hassel, “Small River Barges innovatief concept van het gebruik van de kleine vaarwegen,” Master’s thesis, Delft University of Technology, Delft, Juli 2008.

[91] S. Lang, T. Reggelin, M. Müller, and A. Nahhas, “Open-source discrete-event simulation software for applications in production and logistics: An alternative to commercial tools?,” in *Procedia Computer Science*, vol. 180, 2021.

[92] Ruud van der Ham, *salabim*, 2023. Accesed on: 2023 - 19 - 06.

[93] J. Lerche, S. Lindhard, P. Enevoldsen, H. H. Neve, D. E. Møller, E. L. Jacobsen, J. Teizer, and S. Wandahl, "Causes of delay in offshore wind turbine construction projects," *Production Planning and Control*, 2022.

[94] C2WIND, "16021-50-1 DHI local model hindcast data delivery," 2018. Confidential document provided by TWD, not publicly accessible.

[95] Jim Koppenol, 2023. Personal conversation.

[96] Seaqualize, "20230104 Results VW fastlift rehit Rev0," 2023. Document provided under disclosure.

[97] TIDEWATER, "SAVOY TIDE GHSI 7,150 BHP Anchor Handling Tug." https://www.tdw.com/wp-content/uploads/2021/07/Savoy-Tide-Brochure-3108-1.pdf, 2022. Accesed on: 2023 - 26 - 10.

[98] TIDEWATER, "ALLISON TIDE Remontowa 10,000 BHP Anchor Handling Tug." https://www.tdw.com/wp-content/uploads/2016/08/Allison-Tide-Brochure-2385-R1.pdf, 2022. Accesed on: 2023 - 26 - 10.

[99] TIDEWATER, "MARTY QUIST TIDE." https://www.tdw.com/wp-content/uploads/2016/08/Marty-Quist-Tide-Brochure-2394-R1.pdf, 2022. Accesed on: 2023 - 26 - 10.

[100] TIDEWATER, "COXON TODE 180T BP Anchor Handling Tug." https://www.tdw.com/wp-content/uploads/2016/08/Coxon-Tide-Brochure-1664-2.pdf, 2021. Accesed on: 2023 - 26 - 10.

[101] Interreg North Sea Region, "Comparison of Various Logistic Configurations." https://northsearegion.eu/media/17710/20210524154702_results_wp5comparisonoflogisiticconfigurations.pdf, 2019. Accesed on: 2023 - 08 - 03.

[102] Fred. Olsen Windcarrier, "SPECIFICATIONS: JACK-UP INSTALLATION VESSEL BLUE TERN." https://windcarrier.com/media/gdhexjgm/blue-tern-29102021.pdf, 2020. Accesed on: 2023 - 08 - 03.

[103] R. G. Sargent, "Verification and validation of simulation models," *Journal of Simulation*, vol. 7, no. 1, 2013.

[104] 4COffshore, "NG-20000X Heavy Maintenance and Construction." https://www.4coffshore.com/vessels/vessel-ng-20000x-vid2304.html, 2023. Accessed: 2023-11-23.

[105] M. Hertel, C. Hooper, and A. Mohtat, "Nowrdc agreement 103, technical validation of existing u.s. flagged barges as a feeder solution for the u.s. offshore wind industry: Weather downtime based on metocean data and frequency domain motions final technical report," Tech. Rep. 103-213025-NOCM5.5, NYSERDA, Seattle, WA, December 2022.

[106] Jason Fernando, "What Are Stakeholders: Definition, Types, and Examples." https://www.investopedia.com/terms/s/stakeholder.asp, 2023. Accessed: 05-04-2023.

[107] E. G. Carayannis and D. F. Campbell, "'Mode 3' and 'Quadruple Helix': Toward a 21st century fractal innovation ecosystem," 2009.

[108] F. Ackermann and C. Eden, "Strategic Management of Stakeholders: Theory and Practice," *Long Range Planning*, vol. 44, pp. 179–196, 6 2011.

[109] V. Spielmann, T. Brey, J. Dannheim, J. Vajhøj, M. Ebojie, J. Klein, and S. Eckardt, "Integration of sustainability, stakeholder and process approaches for sustainable offshore wind farm decommissioning," *Renewable and Sustainable Energy Reviews*, vol. 147, 2021.

[110] R. Davidson, “Pentagon objects to US offshore wind leasing areas over military training.” https://www.windpowermonthly.com/article/1819907/pentagon-objects-us-offshore-wind-leasing-areas-military-training, 2023. Accessed: 2023-5-8.

[111] Delft University of Technology, “TU Delft Strategic Priorities 2022-2024.” https://www.tudelft.nl/over-tu-delft/strategie, May 2023. Accessed: 07-04-2023.

[112] “Maersk Supply Service to construct pioneering wind installation vessel for Equinor and bp to operate in the U.S. market.” https://www.maersksupplyservice.com/2022/03/29/maersk-supply-service-to-construct-pioneering-wind-installation-vessel/, 2022. Accessed: 2023-4-20.

[113] A. Memija, “US and German Firms Unveil Jones Act-Compliant Offshore Wind Farm Installation Solution.” https://www.offshorewind.biz/2022/09/27/us-and-german-firms-unveil-jones-act-compliant-offshore-wind-farm-installation-solut 2022. Accessed: 2023-4-20.

[114] D. Foxwell, “Semi-sub and feeder ships put Havfram in the frame for Jones Act market.” https://www.rivieramm.com/news-content-hub/news-content-hub/semi-sub-and-feeder-ships-put-havfram-in-the-frame-for-jones-act-market-63506, 2021. Accessed: 2023-4-20.

[115] A. Memija, “BargeRack design said to improve offshore wind turbine installation.” https://www.offshore-mag.com/renewable-energy/article/14205387/bargerack-design-said-to-improve-offshore-wind-turbine-installation, 2021. Accessed: 2023-4-20.

[116] J. H. EVANS, “BASIC DESIGN CONCEPTS,” *Journal of the American Society for Naval Engineers*, vol. 71, no. 4, 1959.

[117] H. Hopman, “From Evans Design Spiral to Systems Engineering, MT44035 Design of Complex specials,” 9 2021. not publically accessible.

[118] D. J. Singer, N. Doerry, and M. E. Buckley, “What is set-based design?,” *Naval Engineers Journal*, vol. 121, no. 4, 2009.

[119] E. A. E. Duchateau, *Interactive Evolutionary Concept Exploration in Preliminary Ship Design.* 2016.

[120] A. Kossiakoff, W. N. Sweet, S. J. Seymour, and S. M. Biemer, *Systems Engineering Principles and Practice: Second Edition*. 2011.

A

Scatter Plot

Tp /Hs	0-0,5	0,5 - 1	1 - 1,5	1,5 - 2	2 - 2,5	2,5 - 3	3 - 3,5	3,5 - 4	4 - 4,5	4,5 - 5	5 - 5,5	5,5 - 6	6 - 6,5	6,5 - 7	7 - 7,5	7,5 - 8	8 - 8,5	8,5 - 9	9 - 9,5	9,5 - 10	10 - 10,5	10,5 - 11	11 - 11,5
20	3	9	9	11	15	4	3	2	1	0	0	0	0	0	0	0	0	0	0	0	0	0	0
19	43	147	28	39	38	29	11	4	2	1	0	0	0	0	0	0	1	1	0	0	0	0	0
18	8	13	22	25	22	25	11	5	1	5	2	0	0	1	1	2	0	0	1	0	1	1	2
17	201	662	162	116	117	79	79	27	11	9	13	2	3	2	4	1	2	0	0	2	0	3	1
16	27	238	152	166	167	90	76	21	4	1	2	7	5	7	4	8	1	4	2	0	0	0	0
15	231	1420	446	370	240	155	121	47	17	18	21	11	5	12	1	2	0	4	1	0	0	0	0
14	106	741	669	456	260	154	92	65	88	39	34	25	19	2	5	4	4	2	0	0	0	0	0
13	337	2005	1320	919	509	349	389	466	308	194	99	47	39	21	12	1	0	0	0	0	0	0	0
12	132	1458	1563	1104	667	638	709	416	201	111	60	38	20	9	6	0	0	0	0	0	0	0	0
11	608	4649	3978	2696	2275	2200	1355	648	339	185	143	99	26	7	0	0	0	0	0	0	0	0	0
10	1066	7450	7725	5904	3639	1897	1141	784	608	376	175	34	1	0	0	0	0	0	0	0	0	0	0
9	1347	11778	12749	6035	2991	2263	2240	1830	700	126	40	23	3	1	0	0	0	0	0	0	0	0	0
8	1279	18524	14688	6564	6266	6797	3047	747	187	52	17	2	0	0	0	0	0	0	0	0	0	0	0
7	1198	19352	13658	14272	11222	2924	613	119	4	1	0	0	0	0	0	0	0	0	0	0	0	0	0
6	572	14591	21576	15265	2314	98	1	0	0	0	0	0	0	0	0	0	0	0	0	0	0	0	0
5	587	18454	19708	1358	5	0	0	0	0	0	0	0	0	0	0	0	0	0	0	0	0	0	0
4	968	9320	271	0	0	0	0	0	0	0	0	0	0	0	0	0	0	0	0	0	0	0	0

Figure A.1: Vineyard Scatter plot [94]

B
Stakeholder analysis

Several stakeholders are involved in the development of a US offshore wind farm. A stakeholder is defined as *a party that has an interest in a company and can either affect or be affected by the business.* [106]. Depending on their level of influence, they can play a significant role in the development of, and decisions made for the project. This section introduces the stakeholders and discusses their interests.

B.1. Stakeholder mapping

Stakeholders of an offshore wind farm belong to the groups as described by the quadruple helix model of Carayannis and Campbell [107]. The quadruple helix model describes interactions between academia, industry, government and civil society within an knowledge economy and builds on the 'triple helix model of knowledge' by adding the civil society as an additional helix. Each group is represented by a helix, overlapping an intertwining with the other helices. Within and on the edge of these groups, several stakeholders groups are identified. Stakeholders involved in the installation phase of the project differ from the total OWF as the interest of some stakeholders does not apply to the installation phase. For the remainder of this research only the stakeholders of the installation phase will be taken into account.

Stakeholders are categorized according to the method described by Ackermann and Eden [108] to analyze their influences on the installation phase. According to their two-by-two matrix, stakeholders are categorized in four groups: players, subjects, context setters and crowd. Players have high interest and high power to influence the activities. Subjects have high interest but low power but can become players if they gain power. They should be kept informed and monitored closely during the activities. Context setters have high power and low interest on the project as long as their requirements are fulfilled. These stakeholder should therefore be kept satisfied during the activities. Finally there are the 'crowd' stakeholders who have low interest and low power. Therefore minimal effort should be put into managing these stakeholders.[109] Figure B.1 shows this stakeholder matrix

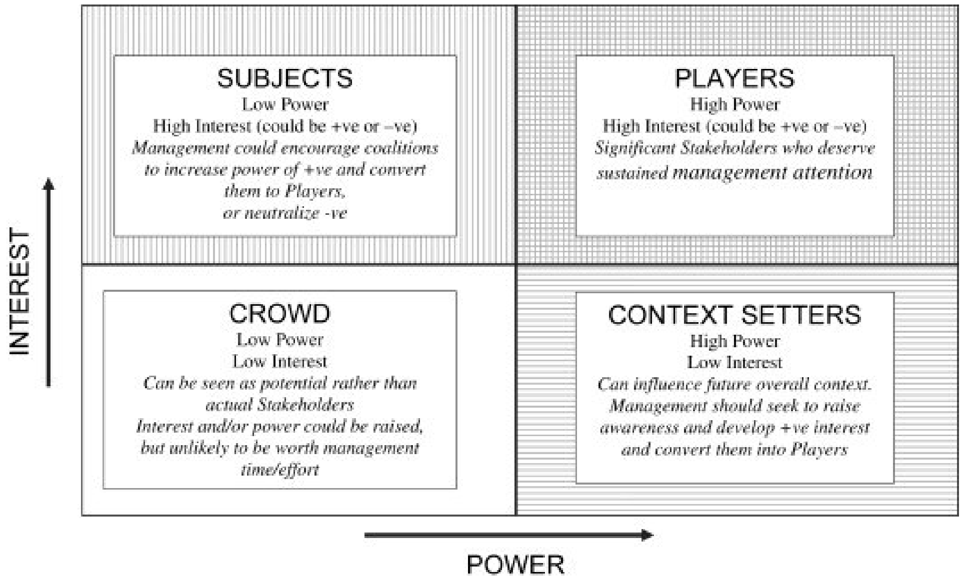

Figure B.1: Stakeholder matrix [108]

B.2. Stakeholder identification

This section discusses the stakeholders, including their concerns and interests, that should be managed for the installation phase. Only players, context setters and subjects will therefore be identified and discussed. The following stakeholders are identified:

- OWF Developers
- contractors
- turbine suppliers
- vessel spread owners
- port facilities
- engineering companies
- US government
- shipbuilders
- Delft University of Technology

B.2.1. OWF developers

OWF developers are one of the key stakeholders. They oversee all installation strategies, drive offshore wind technology and control the business as they are the ones demanding the need for turbines, installation and all other OWF related activities. Developers determine what happens and are recognized as players. Their interest lies in seeing a high return on their investments and minimizing risk. Regarding the installation phase, higher return on investments can be realized by either lower installation costs or a shorter installation time. Lower installation costs lead to lower investments. Given that the return is equal, their ROI will be higher. A shorter installation time allows a developer to operate the OWF earlier in time, leading to increased return and consequently a higher ROI. For a developer, risk can be minimized by having more certainty regarding the costs and duration of the installation.

B.2.2. Contractors

Contractors are the parties actually constructing an offshore wind park. Their interest lies in winning construction contracts. A contractor wins these contracts by supplying the developer's needs: a fast installation with low costs and risks regarding the duration of installation and costs. A contractor's interest can therefore be fulfilled by the same efforts as those necessary for fulfilling a developer's interest. Contractors own the vessels required for installation and therefore partially determine what is possible in terms of WTG installation. Contractors have high power and interests and are thus recognized as players during the installation phase. Although their interest might seem the same as the OWF developers, the installation might come at a cost a developer is not willing to pay, resulting in a possible conflict that is more present in free-market situations.

B.2.3. Turbine suppliers

A turbine supplier's main interest is winning contracts for supplying WTGs to an OWF. They don't have a real interest in the installation phase. However, turbine suppliers shape the market for wind energy and the turbine characteristics determine the method with which a WTG can or must be installed. Their influence on the installation phase is therefore big. Turbine Suppliers are recognized as context setters.

B.2.4. Vessel spread owners

Vessel spread owners are considered as the owners of vessels that are required during the installation phase in addition to the contractor's installation vessel. Their interest is to charter their vessels to a contractor or developer during the installation phase. The characteristics of their fleet determine which level of support can be provided during the installation phase. When specifically looking at barge or feeder vessel owners, their fleet characteristic is an essential factor during the installation phase. Therefore, they have high interest and high power and are thus recognized as a player. However, their level of power and interest is lower in comparison to a contractor or developer.

B.2.5. Port facilities

Port facilities are constantly used by developers, contractors and vessel owners during the installation phase. Port facilities are used to store WTG components and transfer them to vessels. A suitable port must be chosen for ensuring effective and efficient installation activities. The distance between the port and the OWF and the quality of the offered facilities are key factors in selecting a suitable port. Port facilities have a big influence on the vessels which can be used and the distance that must be covered. They also have high interest as they are used for the complete installation phase and could also be used for the O&M phase of a wind farm. Port facilities are therefore also considered players, especially in the long term. It must be stated that choices made by a port facility to upgrade facilities or improve accessibility takes time. This might surpass the duration of the installation phase decreasing their interest. In the short term, port facilities are consequently more considered as context setters.

B.2.6. Engineering companies

Engineering companies provide solutions to engineering challenges and help contractors with realizing their goals, in this case realizing OWFs. Their solutions determine the way in which OWFs can be realized. Engineering companies are therefore considered as players as they both have high interest and high power. TWD is an engineering company and helps clients in realizing their goals by offering innovative design solutions to their clients in the offshore wind and heavy civils industry. Since they help clients reaching their goals, their interests for the solutions they offer are equal. Engineering companies also experience stakeholder conflicts. The services they provide might come at a price that a client is not willing to pay.

B.2.7. US Government

The US government is a player in terms of the whole OWF project. Their BOEM department is responsible for leasing and management of wind energy areas. [10] Also, they have high interest in OWF development for reaching their 30 by 30 goal. Besides external parties, the U.S. government must also manage its internal stakeholders, as they have interfering conflicts. This is stressed by the recent conflict between the BOEM department and the Pentagon regarding the overlap of wind energy lease sites and military training grounds. [110] Regarding the installation phase, they have little interest in the actual WTG installation. However, due to the Jones Act, they literally set the context for WTG installation by having an enormous impact on the installation method and allowable installation and spread vessels. The US government is therefore recognized as a key context setter during the installation phase. The U.S. Government's interests conflict with those of the foreign contractors, as they don't allow the transportation of goods by their installation vessels. They are therefore forced to come up with alternative solutions, such as feedering, to win construction contracts.

B.2.8. US Shipbuilders

US shipbuilders have great interest in the installation phase for US OWFs as they could provide and construct the necessary installation vessels. However, they are currently not able to deliver the necessary installation vessels and lack influencing power. They are therefore recognized as subjects but could become key players in the near future if they are able to deliver the required vessels. A critical note is that building and engineering US installation vessels may come at a cost that contractors and subsequently developers are not willing to pay.

B.2.9. Delft University of Technology

Delft University of Technology (DUT) is an external stakeholder. DUT aims to contribute to solving global challenges by educating new generations of socially responsible engineers and expanding the frontiers of engineering sciences. They do this by, among others, performing world-class research by combining science, engineering and design in a socially responsible manner. Thus, they advance and share the benefits of technology.[111] DUT supports this study which contributes to the feasibility of successfully constructing OWFs in the U.S. and thus the transition towards cleaner energy, solving a global challenge.

B.3. Applicable stakeholders

This report aims to provide an understanding of the feedering installation method for future 20 MW WTGs and to optimize the feedering process for this future operation, contributing to the feasibility of successfully constructing OWFs in the U.S. OWF developers and contractors are the main stakeholders engaged with successful WTG installation. This report therefore focuses on their interests while not forgetting the power and influence of the other stakeholders.

C

Feedering methods

This appendix describes the different feedering methods present in literature and industry including their advantages, disadvantages and applicability.

C.1. Base-port method

Ait Alla et al. [18] first modeled and described a feedering installation method in 2017, which is the base-port method. In this work, the base-port method is described, modeled and compared to the conventional installation method. For the base-port feedering method, a feedering vessel collects components at the component productions site and transports them to a base port, which is as safe/sheltered area with favourable lifting conditions where the components are directly transferred to the installation vessel. The installation vessel then sails to the installation site and installs the WTG components. For this installation method, no storage port is required. The feedering vessel only sails between production sites and the base port and the installation vessel only sails between the base port and the installation site.[18]. This method is visualized in figure C.1 In this case the installation vessel still transports WTG components, therefore this is not a suitable method for a Jones Act regulated market.

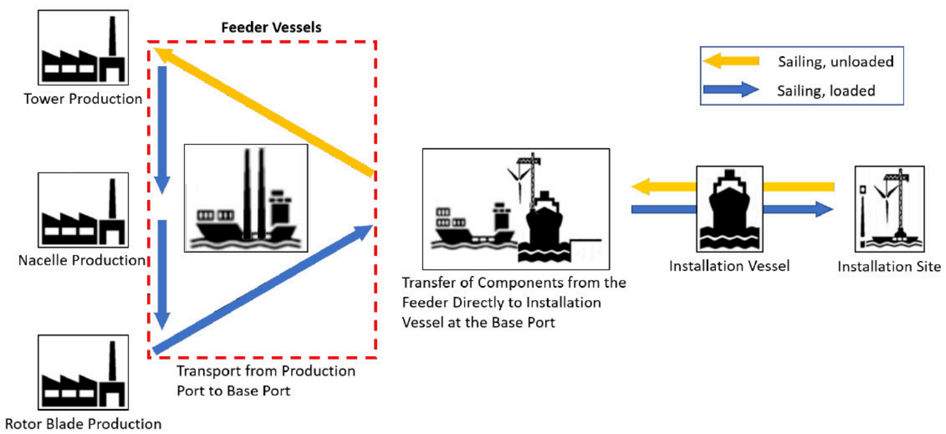

Figure C.1: Base-Port feeder method visualized by Ait Alla et al. [18]

C.2. Offshore feeder-ship method

Ait Alla et al. [18] also described the offshore feeder-ship method which is modeled in the follow-up research by Oelker et al. [19]. For the Feeder-ship method, a feeder vessel collects the WTG components at the production locations and transports them directly to the installation vessel which is located and jacked up at the installation site. The feeder vessel sails back to the production sites when it no longer has any WTG components to repeat the cycle. This method is visualized in figure C.2. Oelker et al. also investigated the possibility of using multiple feeder vessels. Using multiple feeder vessels allows the WTIV to constantly install components by having a constant component supply. This method allows for a more efficient installation vessel since the WTIV does not have to transport any components and waiting time is eliminated by using multiple feeder vessels. Since the WTIV does not transport any WTG components, this method is suitable for Jones Act regulated markets. A disadvantage to this method is the requirement of an offshore component transfer which contains high risks as pointed out by Haselsteiner et Al. [22]. Such a lift can only be performed in the right conditions, potentially causing delays for the entire project. This can be counterbalanced by using specialized lifting tools which can increase the range in which a lift can be executed and thus decreases the chance for potential delays.

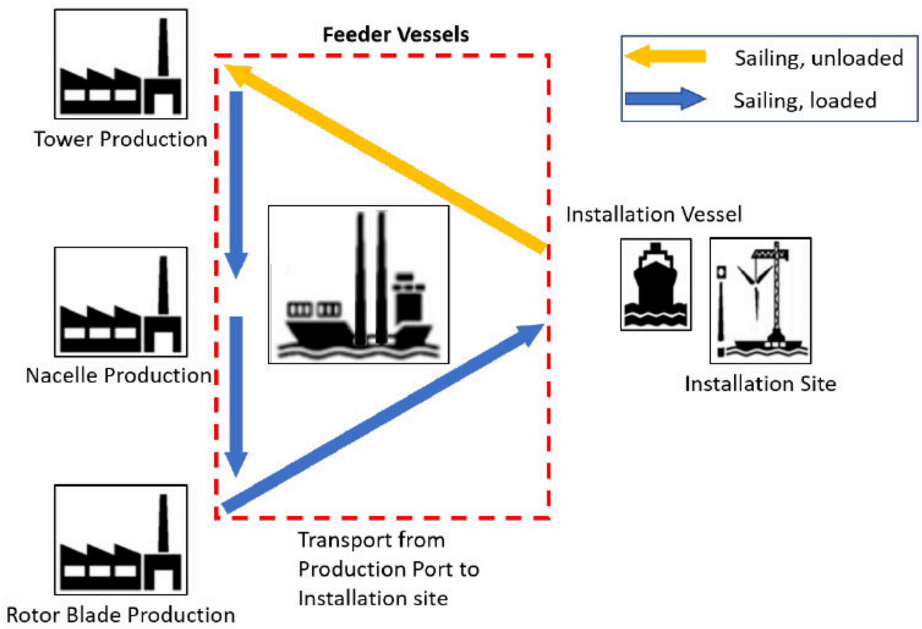

Figure C.2: Offshore feeder-ship method visualized by Ait Alla et al. [18]

C.3. Practical feeder-ship method

Smorenberg and Maloney et al. describe an alternative to the feeder-ship method [21] [20]. Smorenberg defines this as the practical feeder-ship method. This is also the considered method by TWD. This method only focuses on feedering between the base port and the installation site and WTG installation. In contrary to the base-port feedering method, the base port is always an actual port where the WTG components are stored on land. At this port, a feeder vessel picks up the WTG components and sequentially transports them to the installation site where an installation vessel is jacked-up and ready to install the WTG components. The transportation processes from production sites to the base port are not taken into account. This method is visualized in figure C.3. As for the offshore feeder-ship method, this method allows for an efficient installation vessel, since it does not transport any WTG components and waiting time can be eliminated by using multiple feeder vessels. Just as the offshore feeder-ship method, this method is also suitable for Jones Act regulated markets but requires an offshore component transfer which contains high risks.

C.4. Hybrid feeder method

The last described hybrid feeder method is shortly introduced by Smorenberg [21]. This method is a combination between the practical feeder-ship method and the conventional shuttling method. Here, the WTIV transports the first WTG components to the installation site. Once the WTIV is at the installation site, it will be resupplied by feeder vessels. This would make for an even more efficient WTIV since

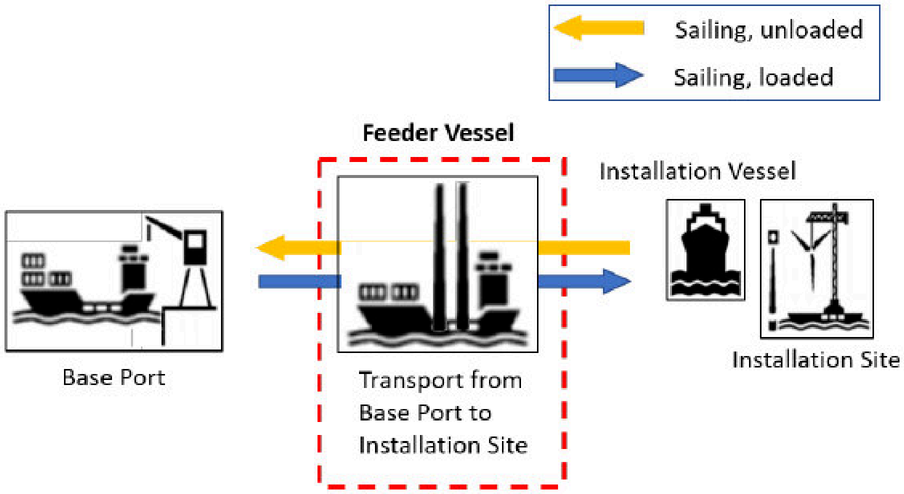

Figure C.3: Practical feeder-ship method visualized by Smorenberg [21].

its transport capacities are used as well. This method is not suited for a Jones Act regulated market. However, this could be a promising method for the European offshore wind market.

Since this research only focuses on the U.S.-market, hybrid and base-port feedering will not be considered further. In practice, it turns out that the offshore feeder-ship method is not viable. Production ports might be spread across a large distance, which would cause the feeder vessel to sail for an extremely long time. Besides, contracts may require the usage of a base port, which would make it impossible to implement the feeder-ship method [21]. For the remainder of this research, the scope is limited to the practical feeder-ship method where only the installation and transportation between the base port and installation site are considered. Table C.1 provides a summarized overview of the described feedering methods.

Table C.1: Feedering method overview

	Base-port	**Feeder-ship**	**Practical feeder ship**	**Hybrid feeder method**
Offshore transfer	No	Yes	Yes	Yes
Production ports included	Yes	Yes	No	No
WTIV efficiency	Medium	High	High	Very high
Suitable for US	No	Yes	Yes	No

D

Example Feeder - WTIV Gantt

ID	Task Mode	Task Name	Duration	Predecessors
1		**Installation vessel**	**93 hrs**	
2		**1st WTG**	**31 hrs**	
3		Feeder 1 mooring	1 hr	25SS
4		Transfer 1	10 hrs	3
5		Feeder 1 departure	1 hr	4
6		WTG 1 installation	14 hrs	5
7		WTIV relocation	5 hrs	6
8		**2nd WTG**	**31 hrs**	
9		Feeder 2 mooring	1 hr	36SS
10		Transfer 2	10 hrs	9
11		Feeder 2 departure	1 hr	10
12		WTG 2 installation	14 hrs	11
13		WTIV relocation	5 hrs	12
14		**3rd WTG**	**31 hrs**	
15		Feeder 1 mooring	1 hr	47SS
16		Transfer 3	10 hrs	15
17		Feeder 1 departure	1 hr	16
18		WTG 3 installation	14 hrs	17
19		WTIV relocation	5 hrs	18
20		**Feeder 1**	**44 hrs**	
21		Port Transfer	12 hrs	
22		Leaving Port	0 hrs	21
23		barrier transit	0 hrs	22
24		Loaded Offshore transit	10 hrs	23
25		Offshore approach	1 hr	24
26		Offshore transfer	10 hrs	25
27		Offshore departure	1 hr	26
28		Unloaded Offshore transit	10 hrs	27
29		Barrier arival	0 hrs	28
30		Port arrival	0 hrs	29
31		**Feeder 2**	**44 hrs**	
32		Port Transfer	12 hrs	
33		Leaving Port	0 hrs	32
34		barrier transit	0 hrs	33
35		Loaded Offshore transit	10 hrs	34
36		Offshore approach	1 hr	7;35
37		Offshore transfer	10 hrs	36
38		Offshore departure	1 hr	37
39		Unloaded Offshore transit	10 hrs	38
40		Barrier arival	0 hrs	39
41		Port arrival	0 hrs	40
42		**Feeder 1**	**44 hrs**	
43		Port Transfer	12 hrs	30
44		Leaving Port	0 hrs	43
45		barrier transit	0 hrs	44
46		Loaded Offshore transit	10 hrs	45
47		Offshore approach	1 hr	46;13
48		Offshore transfer	10 hrs	47
49		Offshore departure	1 hr	48
50		Unloaded Offshore transit	10 hrs	49
51		Barrier arival	0 hrs	50
52		Port arrival	0 hrs	51

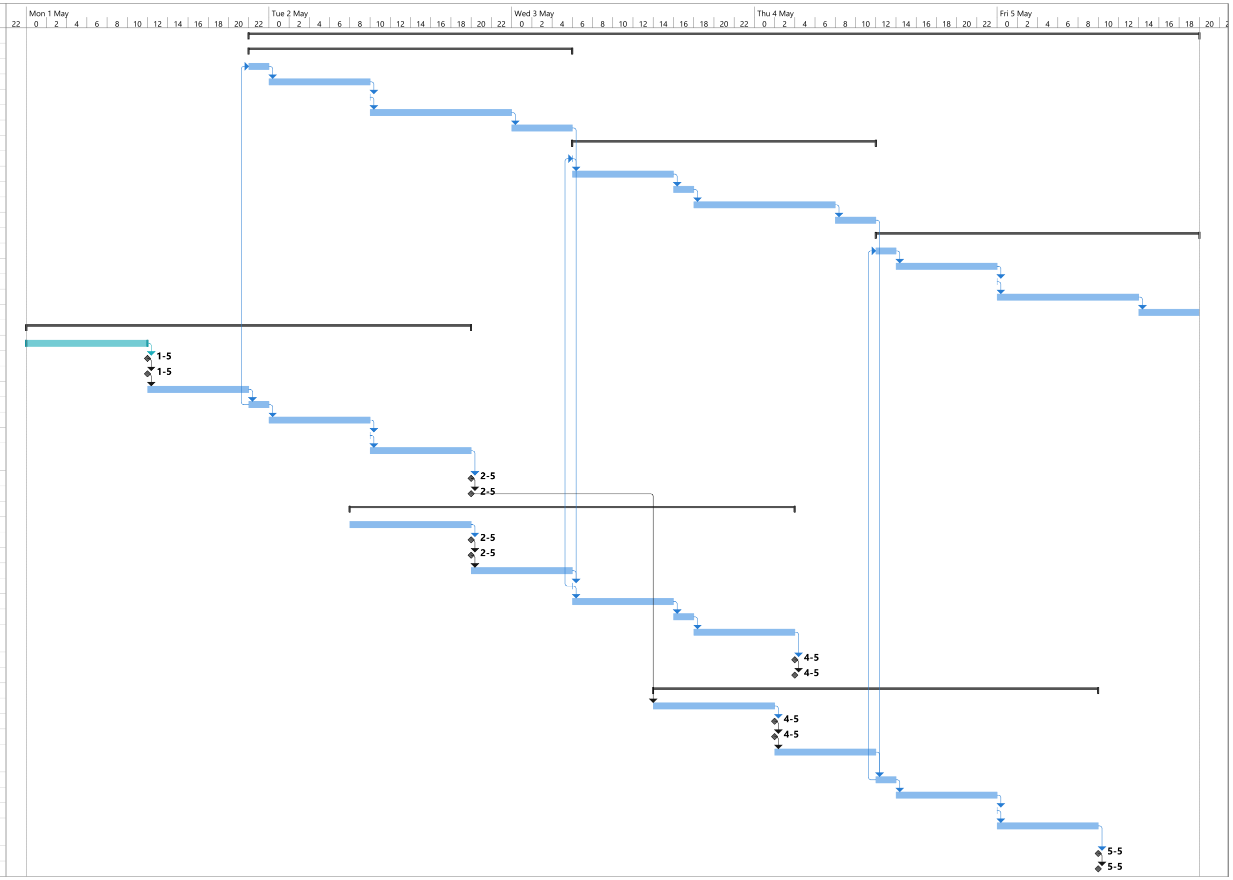

E

DSM

/	No of WTG	Distance to shore	Inner array distance	WTG characteristcs	Installation strategy	Type of vessel	No of vessel	Type of equipment	no of equipment	Mobilisation distance	Insurance	Weather
No of WTG												
Distance to shore												
Inner array distance												
WTG characteristcs												
Installation strategy				Possible installation strategy		Availability limits possible strategies		Availability limits possible strategies				
Type of vessel		Transit performance of vessels		capacity, crane, strength, spatial requirement	strength, crane, stability, spatial requirements							
No of vessel		No of feeders			No of feeders							
Type of equipment				Strength, size, capacity, & type	Strength, size, capacity, type	capacity of MC equipment						
no of equipment							No of equipment needed					
Mobilisation distance												
Insurance						Amount to be insured	no of insurances	Amount to be insured				
Weather												

F Jack-up database

Table F.1: Jack-up vessel database [54]

Vessel Name	Vessel status	Year Built	Max. Water depth (m)	Max Lift (t)	Max. Crane hook height (m)	Max Hook height WRT seabed
Cadeler NG-20000X-G 1	Under construction	2024	80	2000	181	291
Cadeler NG-20000X-G 2	Under construction	2025	70	2000	181	281
Eneti WTIV 2	Ordered	2025	65	2600	185	280
Voltaire	Under construction	2022	80	3000	163	273
Van Oord New Build 1	Ordered	2024	70	3000	163	263
OIM BT-220IU	Ordered		67	2600	165	262
OIM BT-220IU 2	Pre-order		67	2600	165	262
Triumph 1	Pre-order		65	2500	166	261
Eneti WTIV	Ordered	2023	65	2600	162	257
Shimizu Corporation SEP	Under construction	2019	65	2500	161	256
Seaway Ventus	Under construction	2023	65	2500	156	251
VIND 2	Pre-order	2023	65	2500	156	251
Bold Tern	Active in sector	2013	60	1600	158	248
Havfram - VARD	Pre-order	2024	60	1000	150	240
Apollo	Active in sector	2018	70	800	140	240
Charybdis	Under construction	2023	65	2200	144	239
Hai Long Xing Ye Hao	Active in sector	2019	60	1200	145	235
Seajacks Scylla	Active in sector	2015	65	1500	132	227
Wind Osprey	Active in sector	2012	55	1150	132	217
CIMC Raffles 3060 tbn	Ordered	2023	65	2200	120	215
INNOVATION	Active in sector	2012	65	1500	120	215
Brave Tern	Active in sector	2012	60	800	122	212
Triumph 2	Pre-order		65	2500	116	211
San Hang Feng He	Active in sector	2019	50	1200	130	210
SEA CHALLENGER	Active in sector	2014	55	900	121	206
Hai Yang Feng Dian 79	Active in sector	2021	50	1200	125	205
Long Yuan Zhen Hua 3	Active in sector	2018	50	2000	120	200
Vole au Vent	Active in sector	2013	50	1500	120	200
Tie Jian Feng Dian 01	Active in sector	2019	50	1300	120	200
Blue Tern	Active in sector	2012	65	1200	105	200
KOE-02	Under construction		60	1200	110	200
Wind Orca	Active in sector	2012	70	1200	97	197

G

Feeder concepts

Due to the challenge of the component transfer, alternative concepts for feeder and installation concepts have been developed as well. These are all bespoke solutions focussed on coping with glsus Jones Act limitations and eliminating the motions between the feeder and installation vessel. Development and construction costs for these bespoke vessels are often high, resulting in higher dayrates, which brings in risk when dayrates of concurring vessels come down. However, as long as the installation vessel supply is short, there may be room for these future conceptual vessels.

Appendix G highlights the future concepts to provide an overview of what future concepts could look like. All existing concepts eliminate the floating-to-fixed transfer phase, by fixing the feeder vessel to the installation vessel in a rigid way. This eliminates the need for a critical transfer phase, and therefore saves net project time. The ‘approach’ and ‘departure’ phases where the feeder will be fixed or detached from the vessel could take more time and the limits could be more stringent due to the fixed connection.

Maersk Supply Service developed a concept where a barge sails into a U-shaped WTIV. The barge is stabilized and locked after sailing into its ‘slot’, creating a fixed-to-fixed transfer solution. The WTG components are stored on a tray on the barge, which is completely lifted up by the vessel until it sits flush with the vessel’s deck. The locking system is then retracted and the barge is released after which the WTG components can be installed. This feeder solution requires Jones Act compliant tugs, and newbuild barges that are compatible with the installation vessel [112].

Feederdock’s concept follows the lines of the Maersk concept with the exception that the barge stays docked in the installation vessel, and is lifted out of the water during the entire WTG installation. After the WTG is installed and the installation vessel jacks down, the barge is released and ready to be picked up by a tug. This concept removes the need for the critical transfer phase, saving net project time [113].

Havfram presents a more unorthodox concept with a semisubmersible jack-up including a float–over feeder barge. When submerged, the feeder barge is brought into position over the main deck, the installation vessel then jacks up and lifts the barge out of the water. This concept eliminates the transfer phase as well. Positioning of the barge still faces challenges as the tugs should be away from the vessel as they cannot be lifted out of the water and a self-propelled barge introduces issues regarding damaging of the thrusters at the instant of lifting. [114].

Friede & Goldman’s Bargerack design lifts the feeder barge and its cargo out of the water by using a gigantic ‘forklift’ also creating a fixed-to-fixed transfer solution. After lifting the barge, the components can directly be installed from the feeder vessel thus eliminating the transfer phase as well [115].

Most concepts are more costly and require significant investments compared to the more simple tug-barge combination and this will reflect in the dayrate of such vessels. On the other side, these concepts should be able to shorten the cycle time for the installation of one WTG as the transfer phase, which takes about 10 hours, is eliminated. This opens up the opportunity for those methods to be potentially more cost-effective due to a shorter installation timespan.

A limiting factor to these installation methods is the limited flexibility. All solutions seem to rely on purpose-built combinations of installation vessels and feeder barges, whereas the feeder-barge method can be executed with locally available barges and tugs and can supply any WTIV capable of installing 20 MW WTGs. A second disadvantage to these methods is that they rely on creating a fixed-to-fixed connection. Such operations can only be executed up a limited H_s creating a potential bottleneck operation in the operational sequence. Maersk's concept is the only concept being built and is scheduled for delivery in 2025.

Figure G.1: Feeder concepts clockwise from top left: Maersk concept [112], Feederdock concept [113], Havfram concept [114] and Bargerack concept [115]

H

Design Methods

This appendix presents an overview of design methods used for ship design. This provides a basis for the proposed solving framework to answer the main research question.

H.1. Design Spiral

The design spiral by Evans [116] is one of the best-known design methods to structure ship design. This method clearly shows the iterative process necessary due to the complex nature of ship design. In the first instance, educated guesses regarding principle dimensions are made according to the requirements. Initial guesses are often based on similar vessels. Principle dimensions and ship characteristics are modified after each iteration when more detailed information is known. With each iteration, the ship design progresses towards a converged solution. The ship design spiral by Evans is presented in figure H.1

However, this method deals with the synthesis of ship design and not with optimization. A converged solution may be attained, and a ship is designed in the 'right' way. However, it may not be the 'right' ship that is designed for attaining its requirements. As each step is input for the next step, the initial starting point is critical and constrains the design space rapidly. The design spiral is therefore a tool to make the initial direction work and not to attain an optimal design. [117]

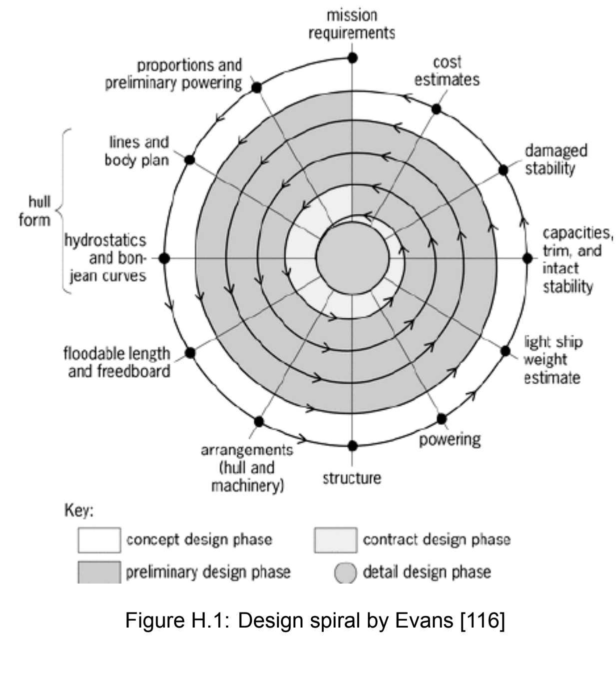

Figure H.1: Design spiral by Evans [116]

H.2. Set Based Design

SBD can be used to attain optimized designs. SBD focuses on delaying design decisions until trade-offs are fully understood. [118] This opens up the opportunity to save time and costs and to boost quality. At the start of a project, little details regarding the design or problem are known or well understood. Decisions made at this stage are project-defining but often hard, due to incomplete data. As the project matures, knowledge increases and making decisions will be easier as it becomes easier to understand their implications.

SBD uses a large set of designs covering a broad area of the design space. This allows a designer to analyze trade-offs and helps to increase the knowledge regarding the project. By delaying design decisions, SBD reduces committed costs related to an initial design direction. Delaying decisions also allows for flexibility in the design when new information comes to light. Figure H.2 presents these shifts in costs, knowledge and design freedom with respect to conventional design method.

SBD is implemented by three principles. First, generate a broad set of concept solutions covering varying design options to populate and understand the design space. Then, divide this design space into specialist areas or disciplines and allow specialists to consider the area from their perspective, identifying key parameters for each area and gaining problem insight. Finally, use the overlap of the specialist areas to optimize a solution. In this way, feasibility is established before commitment to a certain design is made. By integrating more specialist areas and gradually narrowing sets with increasing detail, a small set of unified global concepts is created. Figure H.3 visualizes this design process.

During this process, only concepts that are not Pareto-dominated are communicated and selected. The unified global concepts shall therefore represent the Pareto front since infeasible concepts are never selected. Applying these principles thus enables the development of conceptually robust concepts and promises a capacity to adapt quickly to changing requirements and design discoveries.

Set Based Design is best suited for projects characterized by a large number of design variables, coupling between variables, conflicting or flexible requirements and design problems that are not yet well understood. Therefore it is most valuable in early-stage design, where a solution is to be found within a defined design space with an increasing level of modeling detail.

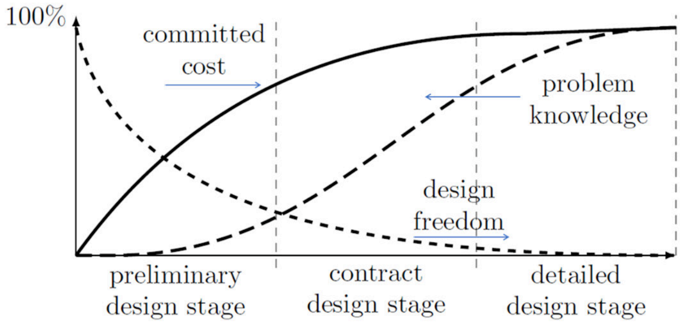

Figure H.2: Effects of Set-Based Design [119]

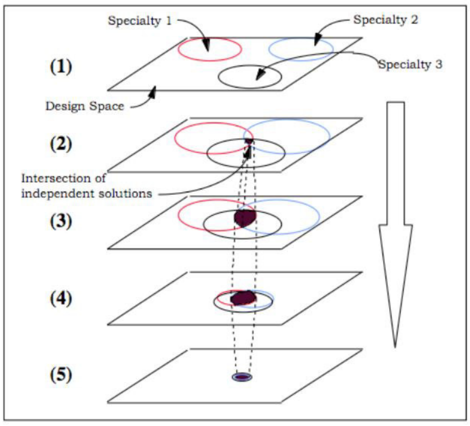

Figure H.3: Visualization of Set-Based Design [118]

H.3. Systems Engineering

Systems engineering is a holistic design method focused on guiding the engineering of complex systems. A system is defined as a set of interrelated components working together towards a common objective. [120] Complex engineered systems are composed of a multiplicity of intricately interrelated diverse elements and require systems engineering to lead the development. The evolution of a system, from the time when a need for it is recognized to its introduction into operational use, is a complex effort, which is referred to as the 'system development process'. This process can be divided into three stages: concept development, engineering development and postdevelopment.

The concept development stage defines and formulates a system that is perceived to best satisfy a valid need. Engineering development translates the concept into a validated and physical system design meeting the operational, cost and schedule requirements. The postdevelopment stage beholds production, deployment, operation and support throughout the system's life. This research focuses on a holistic concept and will not provide detailed engineering and production. The concept development stage will be further elaborated. This phase is graphically represented in figure H.4.

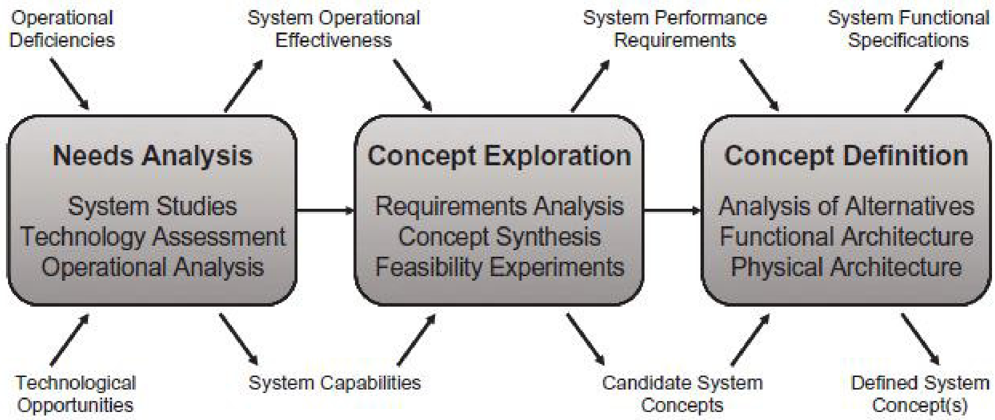

Figure H.4: Concept development phases by Kossiakoff [120]

The concept development stage considers four main objectives which are attained in three different phases. The first objective is to establish a valid need for a system that is technically and economically feasible. Following this needs analysis, the second objective is to set-up performance requirements and explore potential system concepts. The third objective is to select the most attractive system, define its functional characteristics and develop a plan for engineering, production and operational deployment. The final objective is to develop new technology required for the system concept and validate the system's capability to meet the requirements from the second objective. The consecutive phases of concept development are: needs analysis, concept exploration and concept definition.

The needs analysis attains the first objective. It answers the question: is there a valid need for a new system and is there a practical approach in satisfying such a need? The output of this phase is a description of a system's capabilities, what must the system do, and its operational effectiveness, what are the requirements to satisfy the need.

The concept exploration stage answers the questions which performance is required to satisfy the perceived need and whether there is a feasible approach to achieving this performance at an affordable cost. It thereby satisfies the second objective. The output of this system is a requirements set and a set of candidate systems. To explore the possibilities, it is crucial to have at least more than one alternative system concept. These outputs require a variety of tools to be realized ranging from process methods to mathematical based or expert judgment. The initial set of concepts can be large but quickly reduces to a manageable set of alternatives. The feasibility of the final concept set must be understood and proved before it becomes an input to the next phase.

The concept definition phase selects the preferred concept. This defines the key characteristics of a system concept that achieves the most beneficial balance between capability, operational life and cost. The result of this phase is a set of specifications that describes what the system must do, and how well it performs, validating the requirements from the needs analysis phase.

The system engineering principles that are employed in the concept development stage as described, are also present in the other stages and can be seen as the systems engineering method. This can be thought of as the systematic application of a method to the engineering of a complex system. It consists of four successively applied activities as depicted in figure H.5.

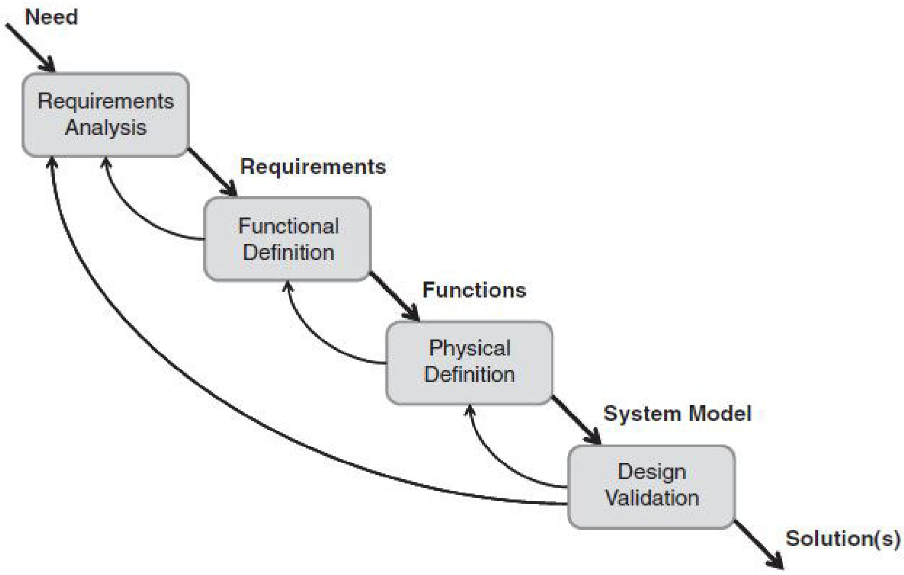

Figure H.5: System engineering flow method [120]

I

20 MW scaling

The commercial 20 MW WTG is not yet defined. To obtain a clear input for the requirements for the feedering method, the characteristics of 20 MW WTG components must be known. These are obtained through a scaling assessment.

I.1. General dimensions

. The commercial WTGs from table 3.1 provides an average power density of 357,63 W/m^2. Commercial 20 MW WTGs will have a comparable density [61], leading to a rotor diameter of 266,8 m. Equation I.1 presents the used formula to relate the rated power to the rotor diameter.

$$\text{Power Density} = \frac{\text{Rated power}}{\text{Rotor Area}} = \frac{P}{\frac{1}{4}\pi D_{\text{rotor}}^2} \tag{I.1}$$

Where:
D_{rotor} = Rotor diameter

The hub is expected to scale with the rotor diameter. From the commercial turbines, the average hub-to-rotor diameter ratio is 0,0252. This results in a hub diameter of 6,7 meter and a blade length of 130,06 m. This relation is provided by equation I.2.

$$l_{\text{Blade}} = \frac{D_{\text{Rotor}} - D_{\text{hub}}}{2} \tag{I.2}$$

Where:
D_{hub} = Hub diameter

Section 3.1.3 concludes that the RNA mass scales with D^2 so linearly with the rated power power. In order to remain competitive, the RNA mass will remain the same per outputted power as for the current WTGs [61]. With a specific RNA density of 64,2 t/MW, leading to a RNA mass of 1283,9 t.

The blade mass can be determined through the relationship provided by Loth et al. [64] and the blade mass of commercial WTGs. Loth et al. conclude that blade mass scales with $\lambda^{2,1}$, where λ represents the scaling factor based on characteristic length. Blade mass is consequently determined by calculating the average blade mass constant for the commercial blades, and applying this constant for the 20 MW blade resulting in a blade mass of 90,82 t. This relation is depicted in equation I.3. Nacelle-hub mass is then acquired by subtracting three times the blade mass from the RNA assembly mass. The COG of several blades is provided confidentially. The dimensionless lengthwise location of the blade COG fluctuates between 0,257 and 0,278, measured from the root end. The COG location can be described by the relation provided in equation I.4. This results in a longitudinal blade COG at 34,6 m from the blade root.

$$m_{\text{Blade}} = c_{\text{bm}} * l_{\text{blade}}^{2,1} \tag{I.3}$$

Where:
m_{Blade} = Blade mass
c_{bm} = Blade mass constant
l_{blade} = Blade length

$$x_{\text{COG}} = 0,2659 * l_{\text{blade}} \tag{I.4}$$

Where:
x_{COG} = x position of COG

The ground clearance of the turbine remains the same. This ranges between 20 and 30 meters. A value of 30 meters is taken as the clearance between the blade tip and the sea surface, resulting in a hub height of 163,4 m. With the transition piece assumed to be 20 m above the water surface and the hub height 7,05 m from the nacelle bottom, this results in a tower height of 136,4 m.

Tower designs differ per manufacturer and installation site. Depending on the tower design, the tower can be divided into multiple sections with each section having its own characteristics in terms of dimensions, weight and COG. For this research, a generic tower design with an equal taper from top to bottom is used to capture the tower characteristics of a 20 MW WTG. Multiple towers are assessed to provide an estimate for the order of magnitude in terms of weight and COG. The data of these towers are confidentially provided by several turbine manufacturers to TWD. From these towers, the weight can be estimated with the function depicted in equation I.5. Resulting in a tower weight of 1233 t. The dimensionless height of the COG for the different towers varies between 0,367 and 0,427 with its average at 0,410 and no trend observed for increasing tower height. The dimensionless COG height of the complete tower is therefore taken as 0,410. Table I.1 presents an overview of the characteristics of a commercial 20 MW WTG

$$m_{\text{tower}} = 0,0217 * h_{\text{tower}}^{2,2273} \tag{I.5}$$

Table I.1: 20 MW WTG characteristics

Parameter	Value	Unit
Capacity	20	MW
Power Density	357,3	W/m^2
Rotor area	55923,9	m^2
Diameter	266,8	m
Hub height	163,4	m
Blade length	130,1	m
Blade mass	90,82	t
Blade COG	34,6	m
Nacelle mass	1011	t
TP height	20	m
Tower height	136,35	m
Tower mass	1233	t
Tower COG	55,9	m
Tower diameter bottom	10	m

Prevention of re-hits between the barge and the blade rack appears to be the most limiting criterion for the transfer operations. To assess re-hits by the blade rack, the blade rack dimensions are crucial. The blades are supported by a root and a tip frame as depicted in figure I.1. The spacing between the two frames is defined as the blade rack length. This length is determined by performing a trend analysis on blade rack lengths for 5 blade types ranging from 80 to 135,2 m. Blade rack length is subsequently determined by equation I.6 resulting in a blade rack length of 73,5 m

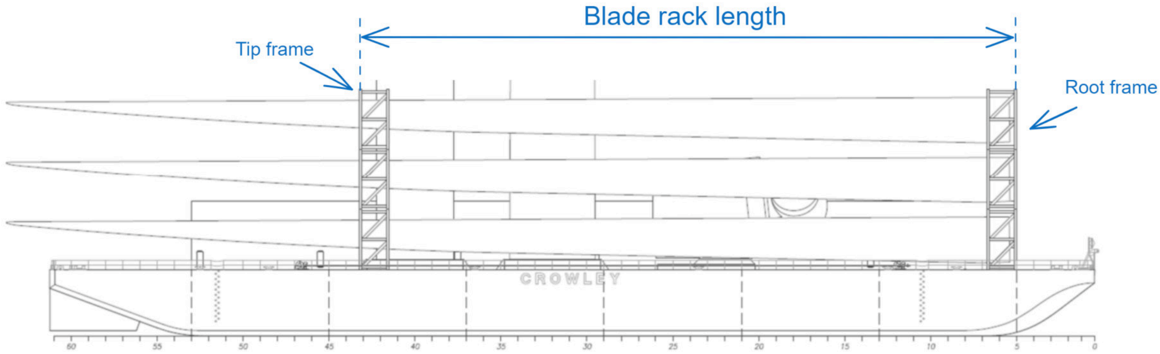

Figure I.1: Side view of a loaded blade rack on a barge. Original drawing by NYSERDA [105].

$$l_{\text{blade rack}} = 0,5648 * l_{\text{blade}} \tag{I.6}$$

I.2. Inertia

The inertia scales by a mass and length relation, using radii of inertia. So linear scaling with mass and quadratic scaling with characteristic length. Equation I.7 shows this relation.

$$I_{20\text{ MW}} = I_{\text{reference}} * \frac{m_{20\text{MW}}}{m_{\text{reference}}} \cdot \lambda^2 \tag{I.7}$$

Where:
λ = Characteristic length based scaling factor

For the tower, not only the COG of the complete tower is important but also the COG from its separate components as the tower is split up into several sections for the different loading conditions. The tower is simplified as a constant tapered cylinder. The tower is split up into sections based on the capacity of the motion compensation platforms, which are discussed in depth in section 6.2.2. Figure I.2 shows the division of the tower. Regarding inertia, the tapered tower and tapered sections are simplified as straight hollow cylinders. The outer diameter of the cylinder is equal to the tower diameter at the height of the COG of the specific section or combination of sections. The thickness is consequently determined by setting the inner diameter such that the hollow cylinder has the same mass as the originally determined tapered tower section. The inertia of the hollow cylinder is given by formula I.8. This results in the tower properties tabulated in table I.2. This simplification is verified with the actual tower sections for Vineyard OWF and differs at a maximum of 2% from the actual inertias. The simplification is therefore accepted for the purpose of this study.

$$\begin{aligned} I_{xx} = I_{yy} &= \frac{m_{\text{section}}}{12}\left(3(R_1^2 + R_2^2) + h_{\text{section}}^2\right) \\ I_{zz} &= \frac{m_{\text{section}}}{2}(R_1^2 + R_2^2) \end{aligned} \tag{I.8}$$

Where:
m_{section} = Mass of the section

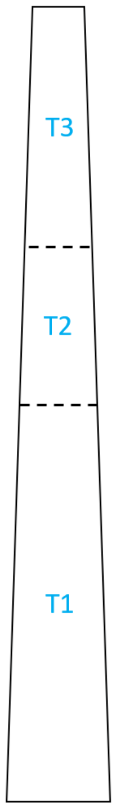

Figure I.2: Division of the WTG tower into its sections

R_1 = Inner radius
R_2 = Outer radius
h_{section} = Height of the section

Table I.2: Tower section properties

	Unit	Full Tower	T1	T2T3	T2	T3
Mass	[t]	1233	750,0	483,1	241,6	241,6
COG height	[m]	55,93	29,33	28,46	9,96	20,81
R1 at COG	[m]	4,180	4,570	3,626	3,898	3,373
Thickness	[m]	0,0441	0,0513	0,0382	0,0508	0,0315
Height	[m]	136,35	65,20	71,16	24,91	46,25
Density	t/m^3	7,85	7,85	7,85	7,85	7,85
I_{zz}	$[kg \cdot m^2]$	21315,67	15486,53	6286,068	3622,704	2723,344
I_{xx}	$[kg \cdot m^2]$	1921248	273400,3	206990,9	14299,61	44433,45

J Configuration overview

Configuration	1.A	1.B	1.C	2.A	2.B	2.C	3.A	3.B	3.C	4.A	4.B	4.C
Barge		Memphis Bridge			Barge 2			Barge 3			Barge 4	
Tower sections	1	2	3	1	2	3	1	2	3	1	2	3
L	122,76	122,76	122,76	140	140	140	160	160	160	180	180	180
B	30,4	30,4	30,4	35,7	35,7	35,7	40,8	40,8	40,8	45,9	45,9	45,9
H	6,55	6,55	6,55	8,47	8,47	8,47	10,22	10,22	10,22	11,97	11,97	11,97
T	2,82	2,92	3,01	2,37	2,46	2,52	2,1	2,16	2,21	1,89	1,94	1,99
GM [m]	13,52	16,38	16,13	31,84	33,53	32,93	53,44	54,48	53,36	80,41	80,51	78,48
Tn [s]	18	11,2	10,5	12,1	8,8	8,6	9,9	8	7,8	8,9	7,6	7,5
Transit time [h]	10	10	10	14	14	14	14	14	14	14	14	14
H_s min transit	4,46	3,13	2,83	2,67	2,68	2,69	2,3	2,95	2,89	2,45	3,43	3,32
H_s operational transit	3,89	2,62	2,41	2,27	2,09	2,1	1,94	2,52	2,47	2,07	2,95	2,85
H_s min lift	1,5	1,5	1,5	1,7	1,7	1,7	2,1	2,1	2,1	2,5	2,5	2,5
BP effective [t]	105,8	76,2	77,3	80,1	70,9	81,1	92,8	90,6	90,2	100,3	106,1	105,4
Tug efficiency	0,552	0,668	0,668	0,763	0,763	0,683	0,705	0,661	0,668	0,698	0,625	0,632
Static BP [t]	192	114	116	105	92,9	119	132	137	135	144	170	167

K

Bollard Pull calculations

Project:	**TWD-NL-2023-109, Provide project title here**
Author:	**RWE**
Revision:	**0**
Checked:	
Date:	**02-10-2023**

C-211, Bollard Pull Calculation

1 Introduction

This calculation determines the minimum required bollard pull (BP) of a tug towing a barge. The minimum required BP required is computed for zero forward speed (HOLDING condition). Furthermore, an assessment is made on the BP required with a forward speed in more moderate weather (SAILING condition).

2 References

[1] GL IV-6-4 - Industrial Services, Offshore Technology, Structural Design (2007)

[2] DNV-RP-C205 - Environmental conditions and environmental loads (2021)

[3] DNV-ST-N001 - Marine operations and marine warranty (2021)

[4] DNV-RP-N103 - Modelling and analysis of marine operations (Sep 2021)

3 Environmental conditions

3.1 General input

Air density	ρ_a	=	1.293	$\frac{kg}{m^3}$	[2]
Water density	ρ_w	=	1.028	$\frac{t}{m^3}$	[2]
Acceleration due to gravity	g	=	9.81	$\frac{m}{s^2}$	
Towing area		=	Other		[3]

3.2 Weather conditions

The BP is calculated against the following conditions acting simultaneously:

Holding

Design significant wave height	$H_{S,h}$	=	2.5	m
Design current speed	$V_{C,h}$	=	0.5	$\frac{m}{s}$
Design wind speed	$V_{W,h}$	=	15.0	$\frac{m}{s}$

Sailing

Design significant wave height	H_S	=	4.4	m
Design current speed	V_C	=	0.5	$\frac{m}{s}$
Design wind speed	V_W	=	15.0	$\frac{m}{s}$

4 Barge data

The input in this section is used to determine the wave drift force and current force acting on the barge.

Length of waterline	L	=	122.8	m
Breadth of waterline	B	=	30.4	m

Depth	D	=		6.6	m	
Mean draft	T	=		2.8	m	
Freeboard	f	=	$D-T$ =	3.7	m	
Frontal projected area of the submerged hull	A_{ch}	=	$B \cdot T$ =	86	m^2	
Target towing speed (ground speed)	V	=		6.0	kt	
Reflection coefficient	R	=		0.67		[4]
Drag coefficient of submerged hull	$C_{D,h}$	=		0.66		

5 Windage area

The cargo dimensions (dimensioned based on the reference given in Figure 5-1), are documented in table below and serve as input to determine the wind load on the barge and the items on deck. Height and shape coefficients are taken from [1] , Section 2, part B.

Item name	**Breadth** [m] b_i	**Height** [m] h_i	**Height coefficient** $C_{h,i}$	**Shape coefficient** $C_{s,i}$	**Product** [m^2] $b_i h_i C_{h,i} C_{s,i}$
Hull	30.4	3.7	1.00	1.0	113.4
Tower	8.0	146.5	1.72	0.5	1007.5
Blade Rack	10.0	24.0	1.23	1.5	441.5
				Total A_w	**1562.4**

The height coefficient is evaluated through the equation below and is equal to the calculated value when it is greater than 1; otherwise, the height coefficient of a cargo item is equal to 1.

$C_{h,i} = \left(\frac{z_i}{10\text{m}}\right)^{\frac{2}{10}}, z_i = f + h_i$

The total windage area is obtained through summing the product of the frontal area times the height and shape coefficients of each item as given in the equation below. No shielding effects are considered.

$A_w = \sum b_i h_i C_{h,i} C_{s,i}$

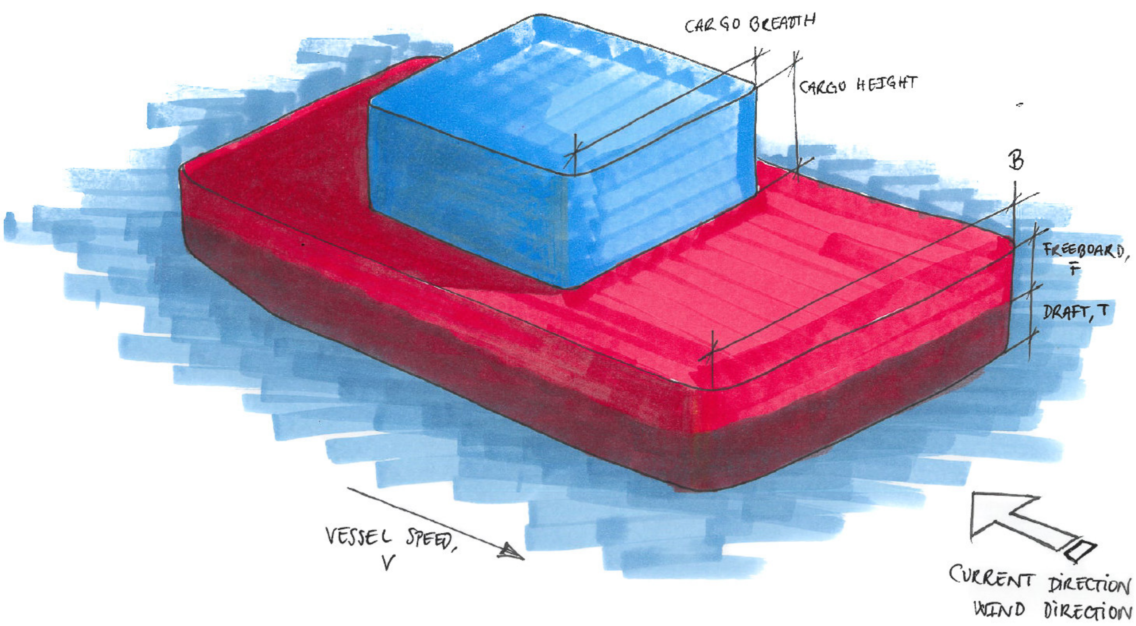

Figure 5-1, Reference for evaluating dimensions of windage areas.

6 Tug data

The data of the selected tug(s) is given below. The bollard pull of the tug (BPT) and the length of tug (LOA) are used to determine the tug efficiency. In accordance to [3], since the BPT exceeds the allowable value ($100t$), the BPT for efficiency calculation is set to $100t$.

Static continuous Bollard Pull of Tug	BPT	=			200	t	
BPT for efficiency calculation	BPT_e	=			100	t	[3]
Length of tug (for efficiency calculation)	$L_{\text{tug},e}$	=	L_{tug}	=	28.7	m	[3]
Number of tugs	n	=			1.00		

7 Bollard pull determination - holding condition

7.1 Total towline pull required

Wind resistance	$R_{W,h}$	=	$\frac{0.5 \cdot V_{W,h}^2 \cdot A_w \cdot \rho_a}{g}$	=	23.2	t	[2]
Current resistance	$R_{C,h}$	=	$\frac{0.5 \cdot A_{ch} \cdot V_{C,h}^2 \cdot C_{D,h} \cdot \rho_w}{g}$	=	0.7	t	[2]
Wave drift resistance	$R_{WD,h}$	=	$0.125 \cdot H_{S,h}^2 \cdot R^2 \cdot B \cdot \rho_w$	=	11.0	t	[2]
Total towline pull required	$R_{T,h}$	=	$R_{C,h} + R_{WD,h} + R_{W,h}$	=	34.9	t	

7.2 Capacity check

Total available static BP	BPT_T	=	$n \cdot \text{BPT}$	=	200	t	
Tug efficiency	$T_{e,h}$	=	$80\% - \left(18 - 0.0417 \cdot L_{\text{tug},e} \cdot \sqrt{\text{BPT}_e - 20}\right) \cdot (H_{S,h} - 1)\%$	=	69.0	%	[3]
Total effective BP	BPT_{eff}	=	$T_{e,h} \cdot \text{BPT}_T$	=	138	t	
Ratio of required and effective BP	UC_{hold}	=	$\frac{R_{T,h}}{\text{BPT}_{\text{eff}}}$	=	0.25		

7.3 Towing equipment

Minimum required towline breaking load	RTBL	=	$2 \cdot \text{BPT}$	=	400	t	[3]
Minimum breaking load shackles forming part of towline	MBL_{sh}	=	$1.3 \cdot \text{RTBL}$	=	520	t	[3]
Ultimate load capacity of towline connections (excluding shackles)	ULC_{con}	=	$\text{RTBL} + 40\,\text{t}$	=	440	t	[3]

8 Bollard pull determination - sailing condition

8.1 Total towline pull required

Wind resistance	R_W	=	$\frac{0.5 \cdot A_w \cdot \rho_a \cdot (V + V_W)^2}{g}$	=	33.7	t	[2]
Current resistance	R_C	=	$\frac{0.5 \cdot A_{ch} \cdot C_{D,h} \cdot \rho_w \cdot (V + V_C)^2}{g}$	=	38.1	t	[2]
Wave drift resistance	R_{WD}	=	$0.125 \cdot H_S^2 \cdot R^2 \cdot B \cdot \rho_w$	=	33.9	t	[2]
Total towline pull required	R_T	=	$R_C + R_W + R_{WD}$	=	105.8	t	

8.2 Capacity check

Tug efficiency	T_e	=	$80\% - \left(18 - 0.0417 \cdot L_{\text{tug},e} \cdot \sqrt{\text{BPT}_e - 20}\right) \cdot (H_S - 1)\%$	=	55.2	%	[3]
Total effective BP	BPT_{eff}	=	$T_e \cdot \text{BPT}_T$	=	110	t	
Ratio of required and effective BP	UC_{sail}	=	$\frac{R_T}{\text{BPT}_{\text{eff}}}$	=	0.96		

L

PFD

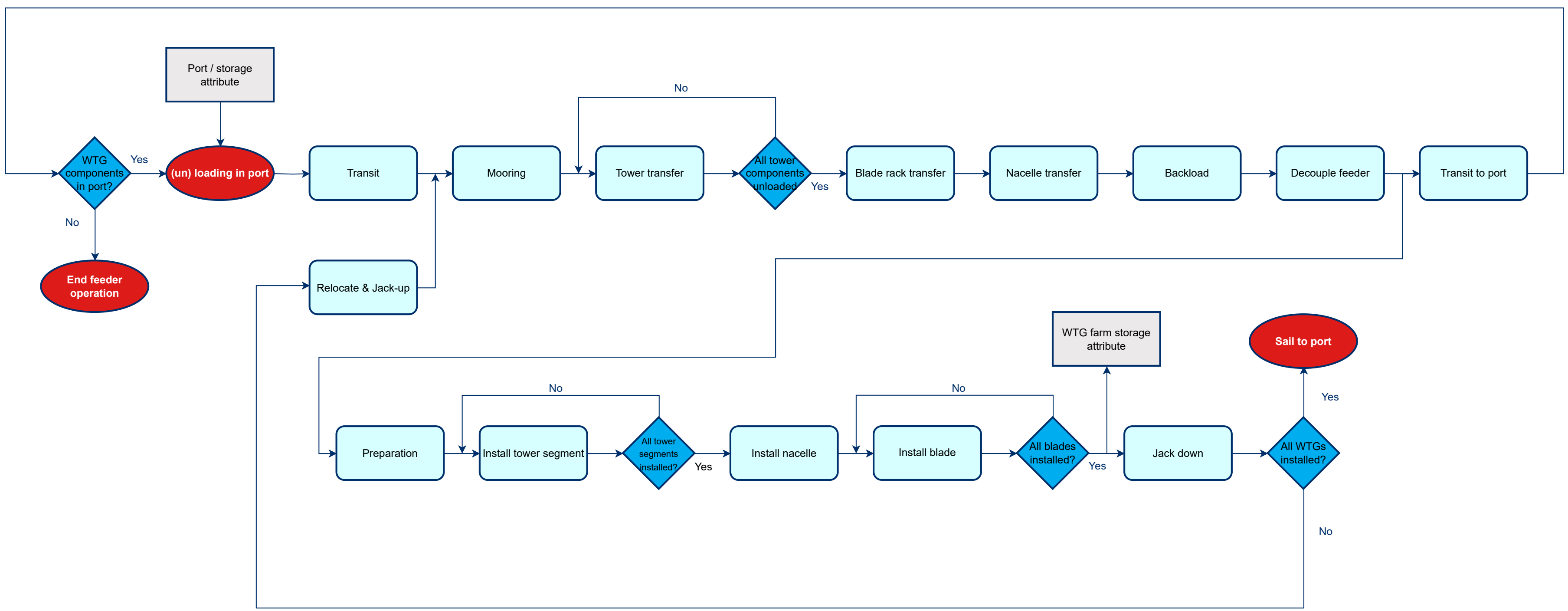

Figure L.1: Process Flow Diagram

M

Simulation base case characteristics

Table M.1: Operational characteristics for base case feedering simulation

Operation	Duration	Wave limit	Wind Limit at 10 mMSL	Operating mode WTIV	Operating mode tug
(un)loading in Port	12	5	16	-	Idle
Feeder transit	10	2,5	15	-	Sailing
Mooring	3	1,5	15	Idle	Operating
Tower transfer	2	2,5	14	Operating	Idle
Nacelle transfer	2	2,5	14	Operating	Idle
Blade rack transfer	3	1,5	12	Operating	Idle
Backload	1	1,5	12	Operating	Idle
Decouple feeder	1	1,5	15	Idle	Operating
Preparation	1	2,5	12	Positioning	-
Install tower segment	2	2,5	12	Operating	-
Install nacelle	6	2	12	Operating	-
Install blade	4	2	12	Operating	-
Jack down	1	2,5	20	Positioning	-
Relocate & jack-up	3	2,5	20	Positioning	-
Empty feeder transit	10	2,5	15	-	Sailing

Table M.2: Operational characteristics for conventional installation simulation

Operation	Duration	Wave limit	Wind Limit at 10 mMSL	Operating mode WTIV	Operating mode tug
(un)loading in Port	24	5	16	Idle	-
Transit	29	2,5	20	Sailing	-
Jack up & prepare	3	2,5	12	Positioning	-
Install tower segment	2	2,5	12	Operating	-
Install nacelle	6	2	12	Operating	-
Install blade	4	2	12	Operating	-
Jack down	1	2,5	20	Positioning	-
Relocate	1	2,5	20	Positioning	-
Empty transit	24	3,0	20	Sailing	-

N
Convergence tests

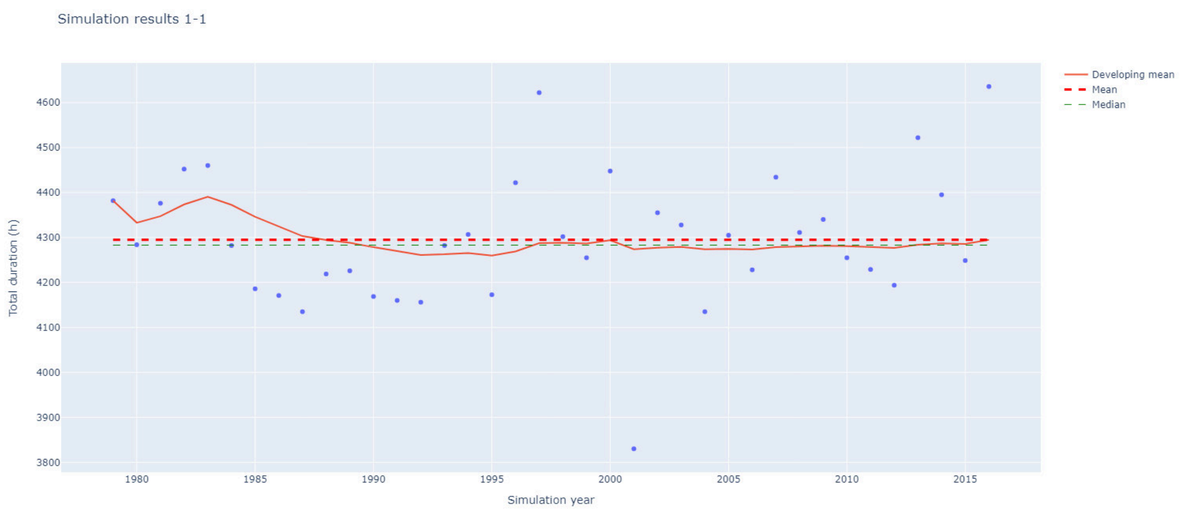

Figure N.1: Convergence test January

Figure N.2: Convergence test February

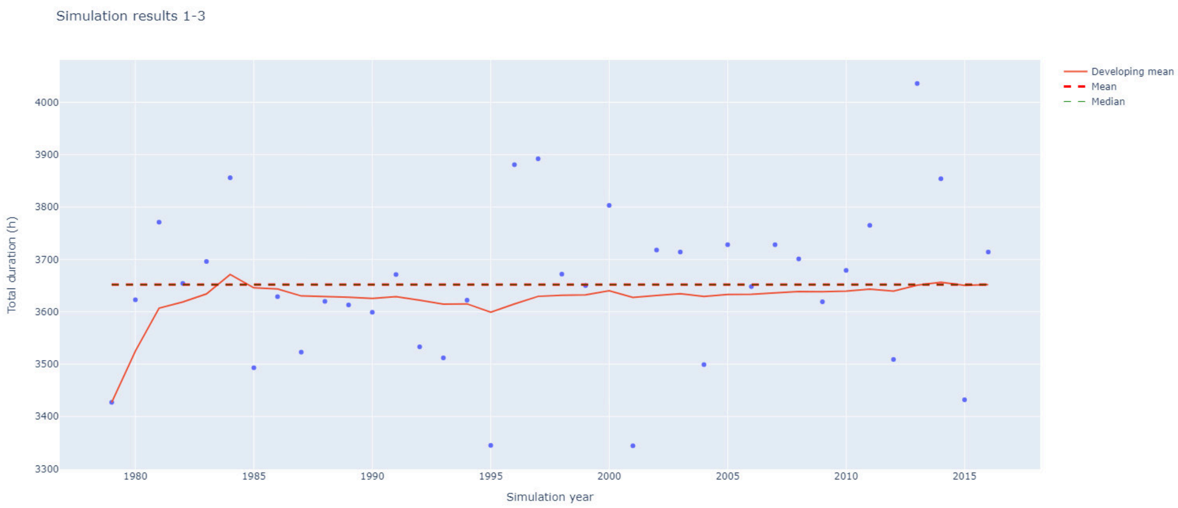

Figure N.3: Convergence test March

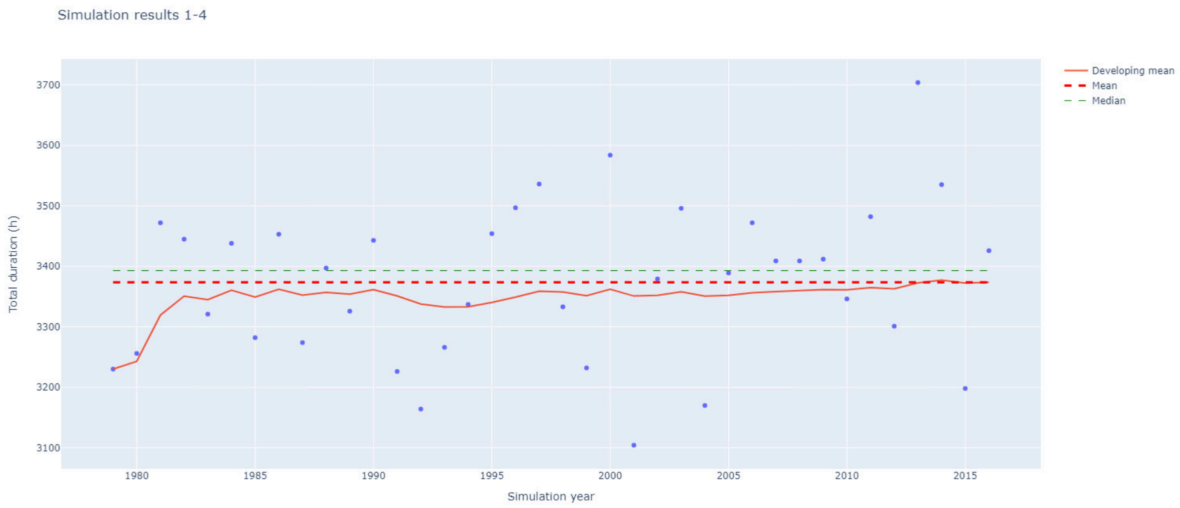

Figure N.4: Convergence test April

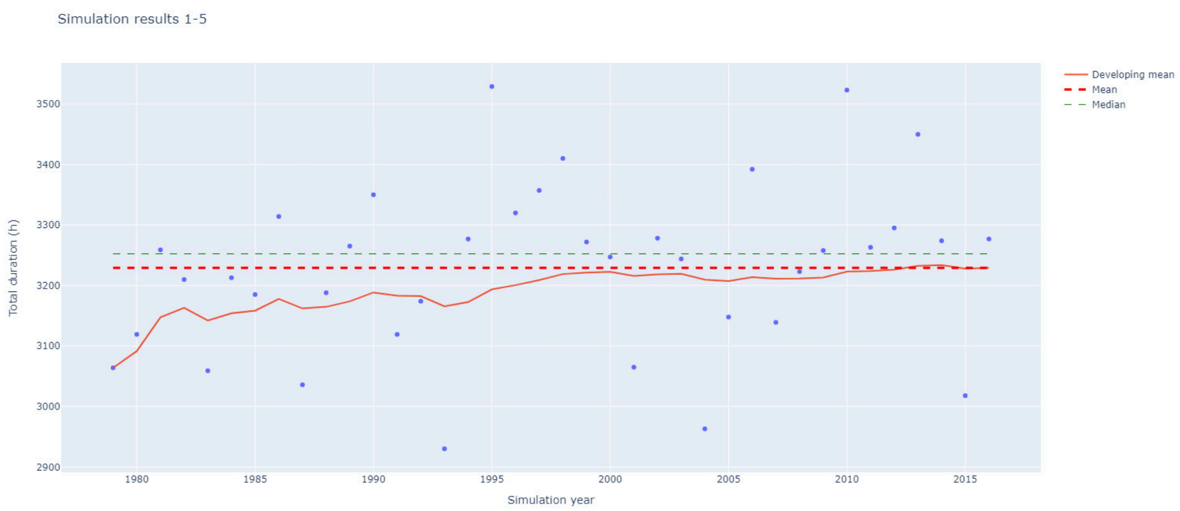

Figure N.5: Convergence test May

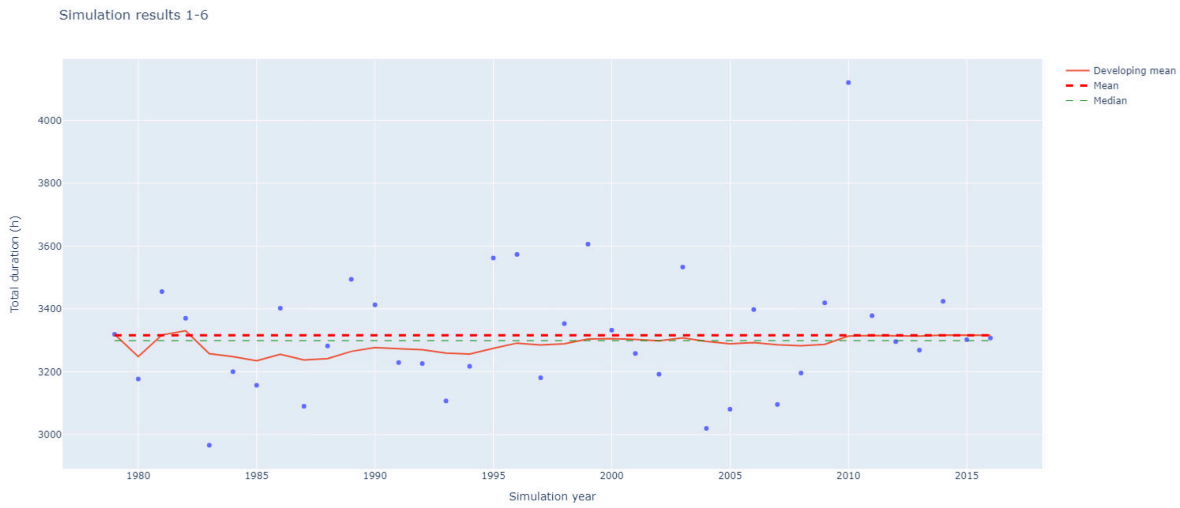

Figure N.6: Convergence test June

Figure N.7: Convergence test July

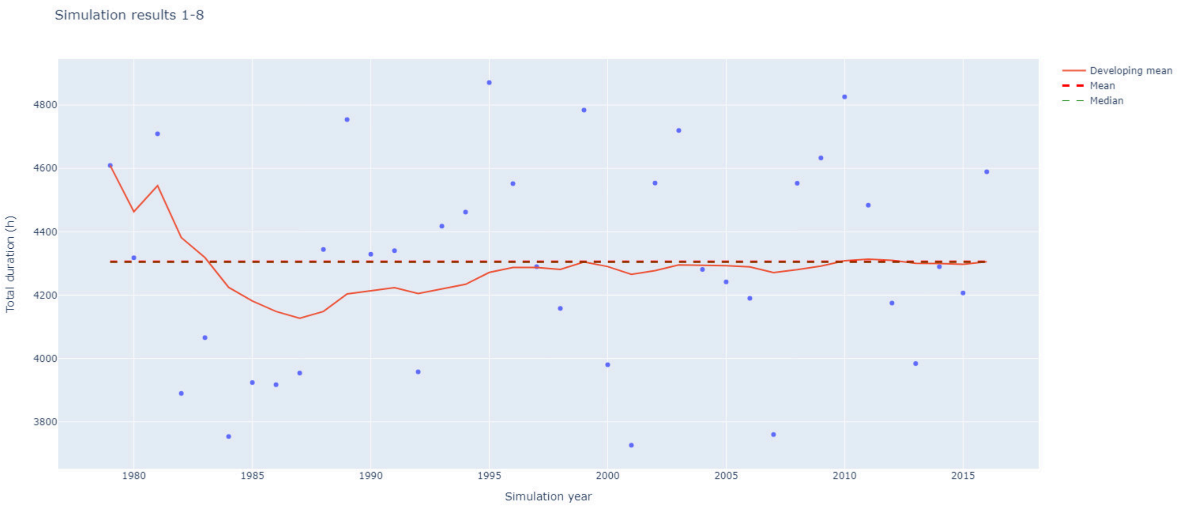

Figure N.8: Convergence test August

Figure N.9: Convergence test September

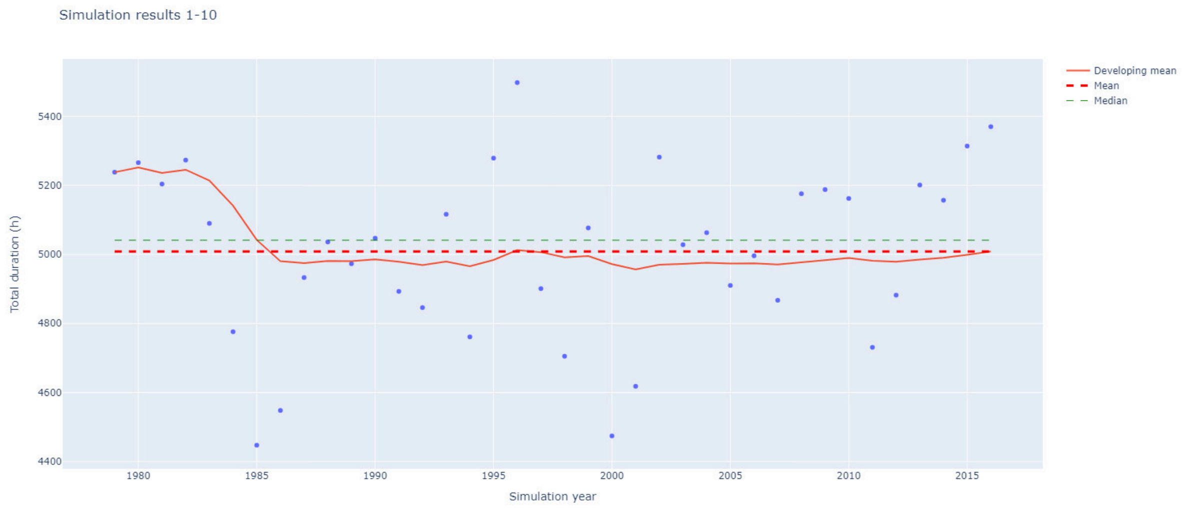

Figure N.10: Convergence test October

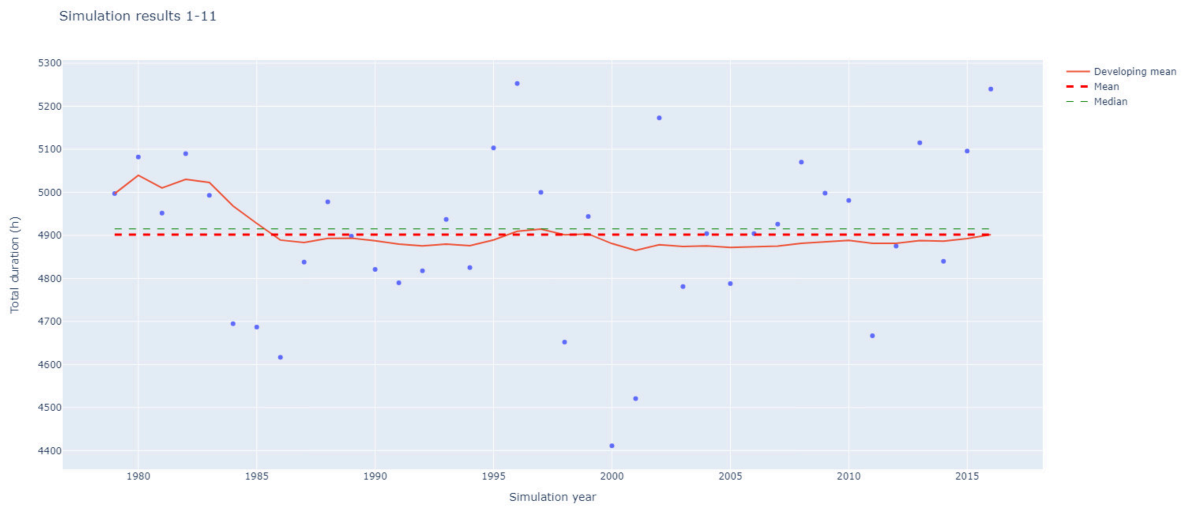

Figure N.11: Convergence test November

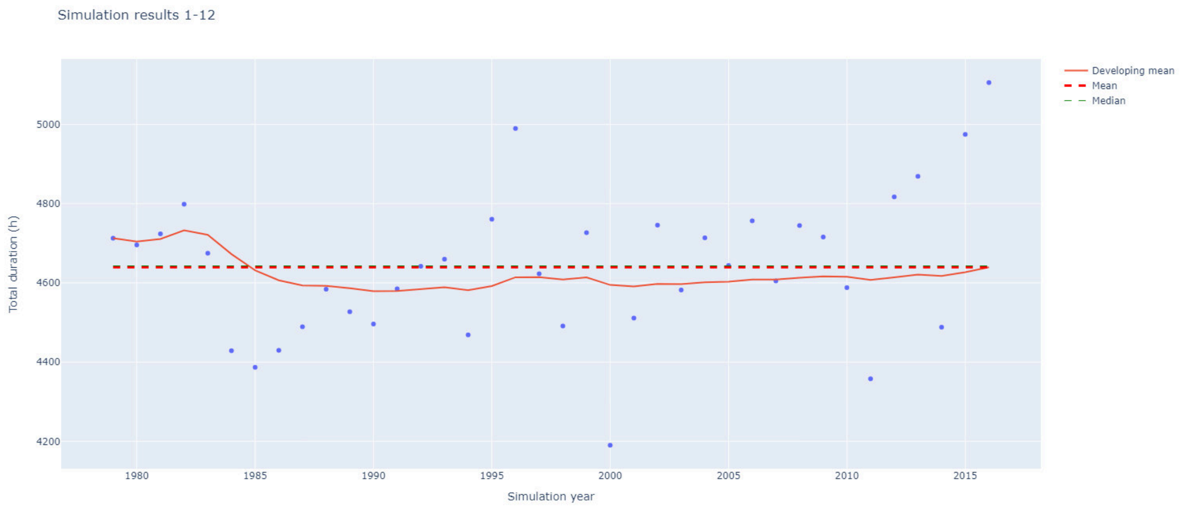

Figure N.12: Convergence test December

O

Model review minutes

MINUTES: ‘criticality of Tp for marine operations’

ATTENDEES: S. van den Munckhof, B. van Wuijckhuijse, P Kortekaas

Feasibility van concepten
Alle concepten lijken feasible, ook single-section installatie strategiën. Verifieer wel of de Memphis Bridge barge met de toren in één geheel naast GM ook voldoet aan minimale oppervlakte onder GZ-curve. Dit kan door middel van de stability booklets.

Hoe wordt Tp meegenomen in echte operaties, en hoe nemen we dit mee in de simulatie?
In operaties is je echte werkomgeving leidend, en wordt Tp volledig meegenomen. In de simulatie Tp dus ook volledig meenemen.

Wat betekent dit voor de resultaten?
Voor de resultaten betekent dit dat installatiemethode (1,2 of 3 secties) leidend is. De vershillende barges leiden amper tot een operationeel verschil. Dit gecombineerd met het feit dat contractors niet zullen investeren in barges, laat zien dat het belangrijk is om de huidige bottleneck (het aan- en afmeren) weg te nemen. De focus in conlusie en aanbeveling worden hierop gericht.

Overig
Hoisting van het blade rack wordt uitgevoerd met het lichtste blok. Dit betekent dat de hoisting speed hoger is dan 0.09 m/s er dus meer clearance wordt gecreëerd (minder re-hits). Met de huidige re-hit methode vergelijk je alles op relatieve basis. Daardoor zijn de resultaten met het huidige blok / hoisting speed wel bruikbaar.

P

Results

P.1. Results including period dependency

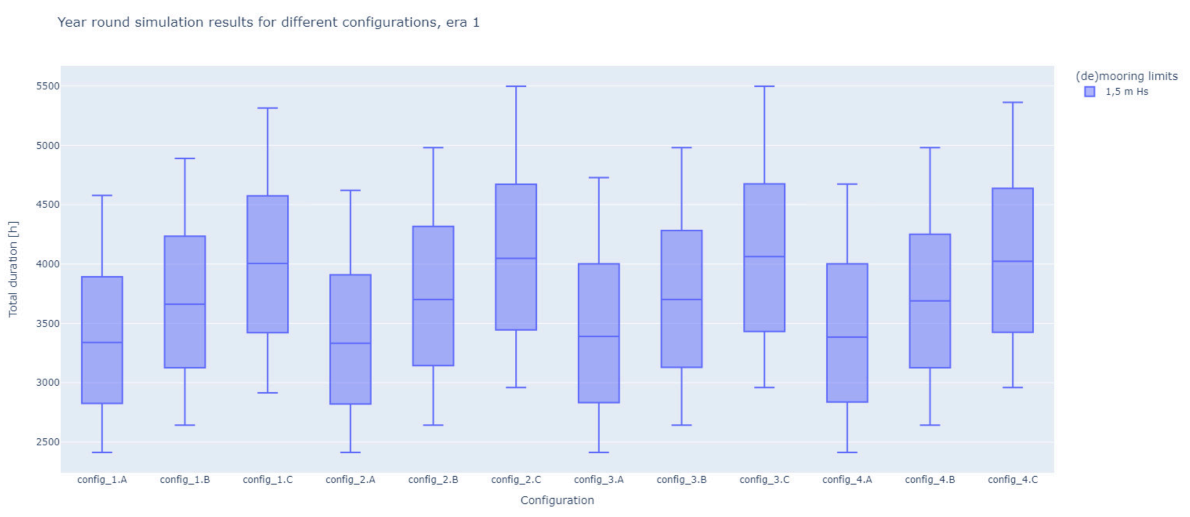

Figure P.1: Year-round duration for simulation era 1 including period dependency

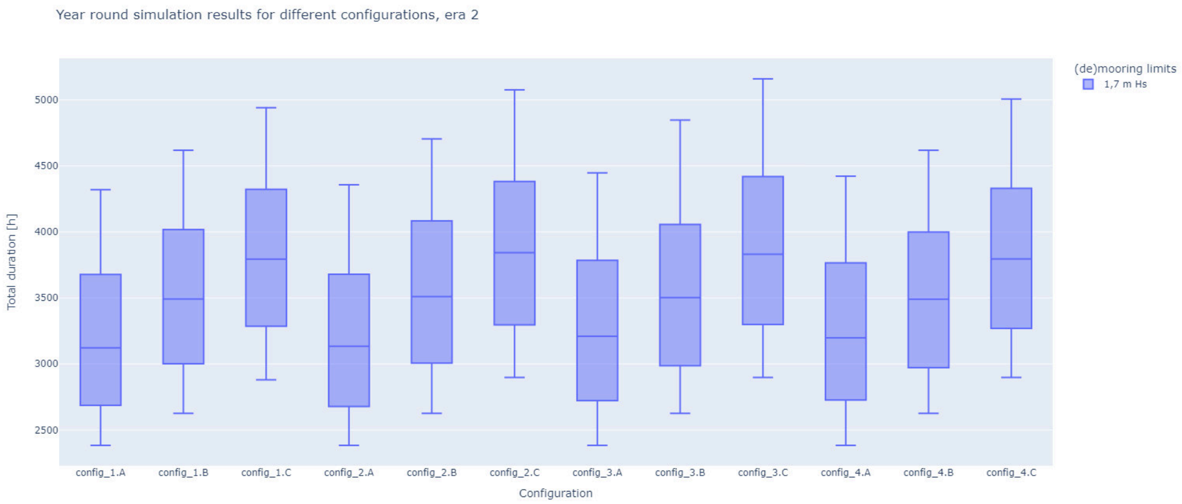

Figure P.2: Year-round duration for simulation era 2 including period dependency

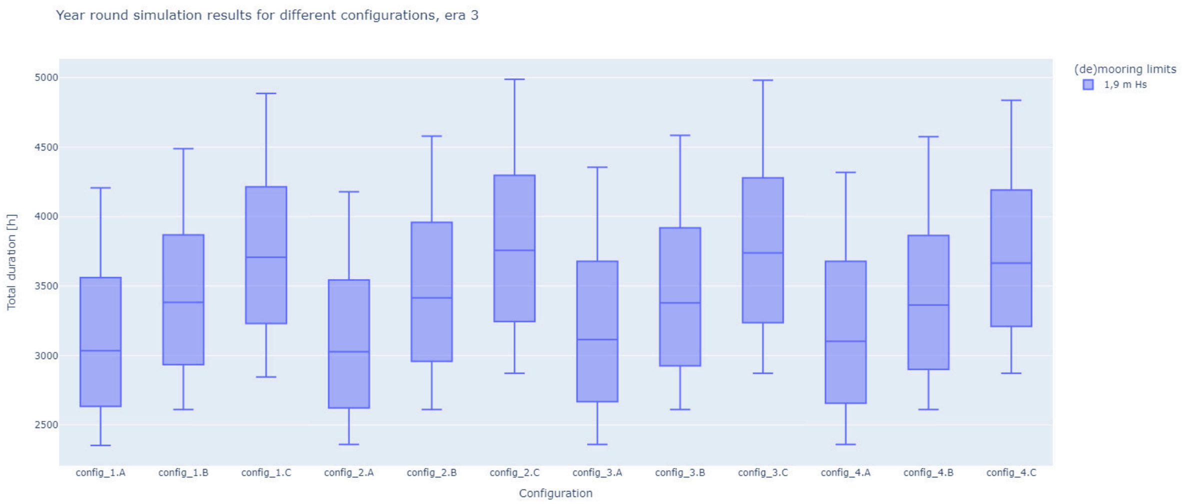

Figure P.3: Year-round duration for simulation era 3 including period dependency

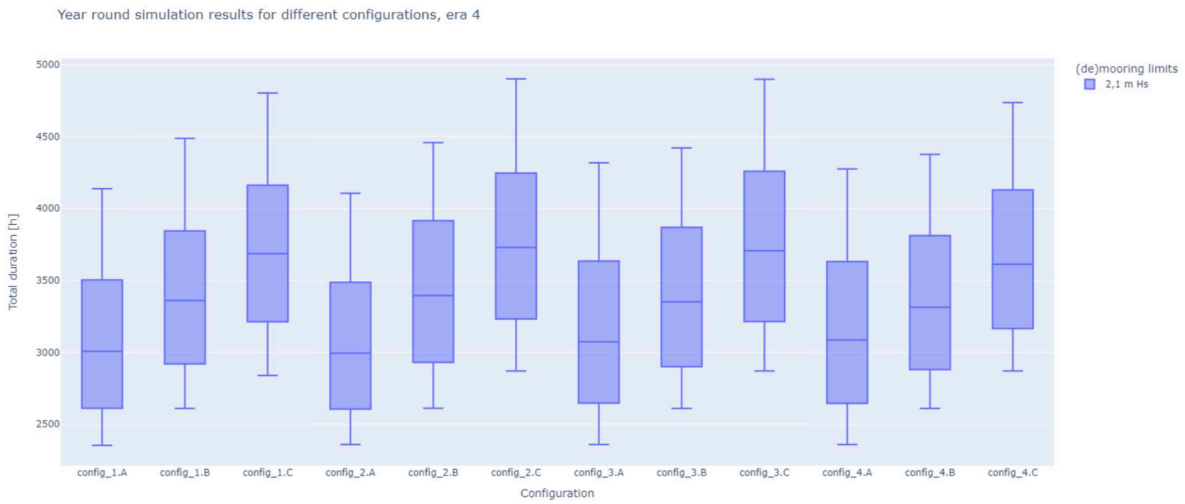

Figure P.4: Year-round duration for simulation era 4 including period dependency

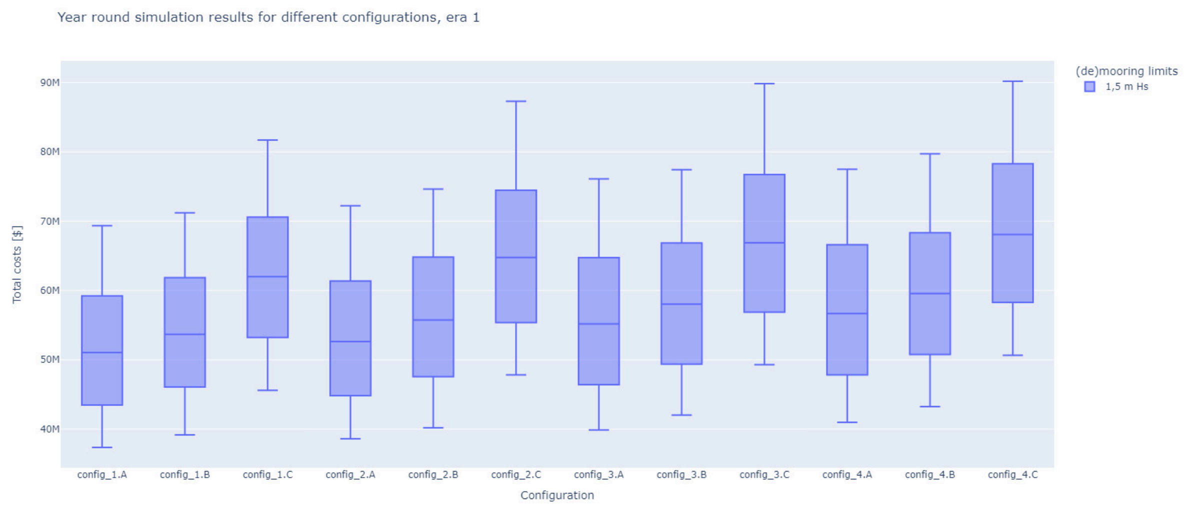

Figure P.5: Year-round costs for simulation era 1 including period dependency

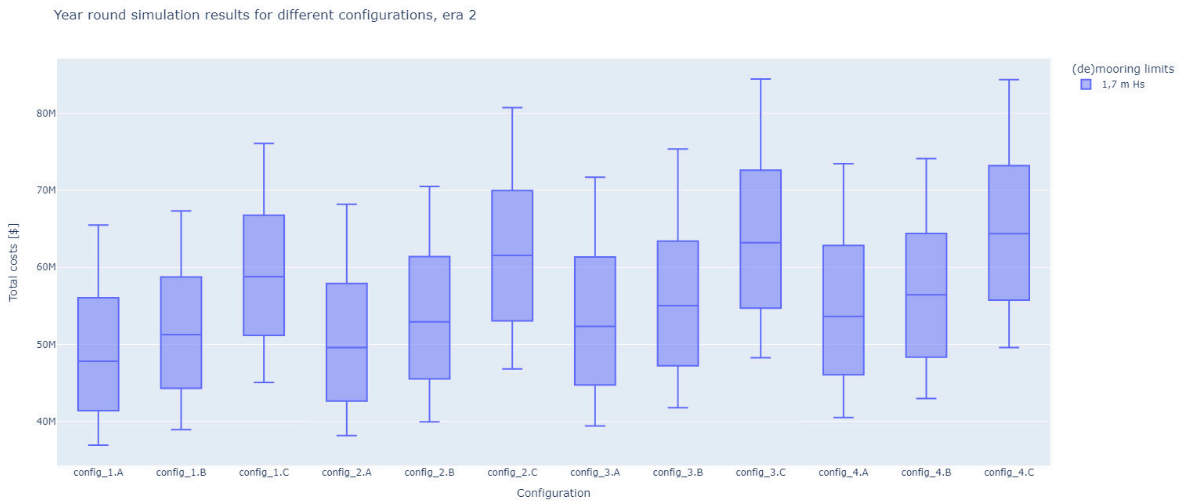

Figure P.6: Year-round costs for simulation era 2 including period dependency

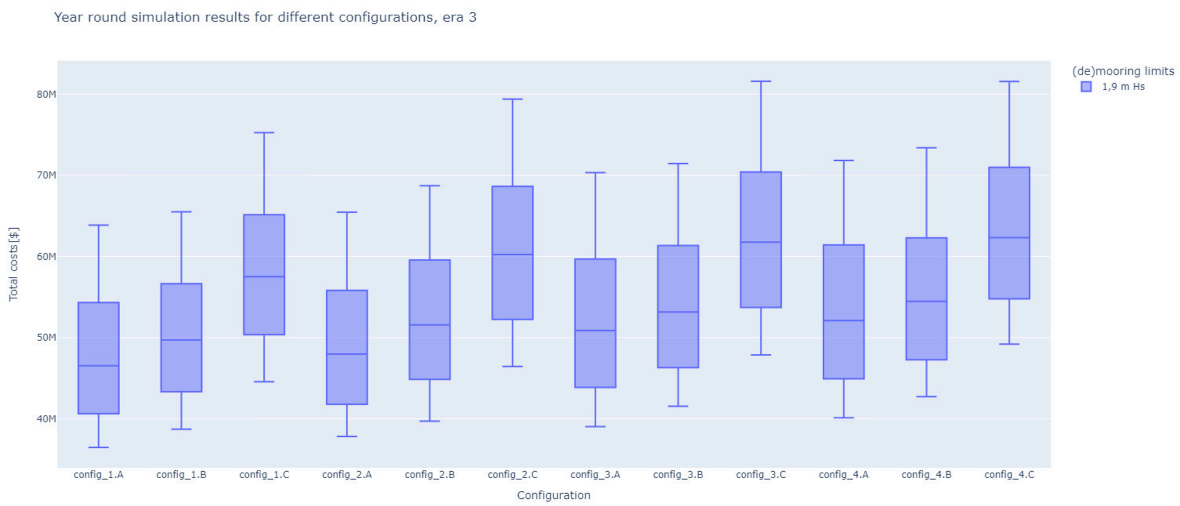

Figure P.7: Year-round costs for simulation era 3 including period dependency

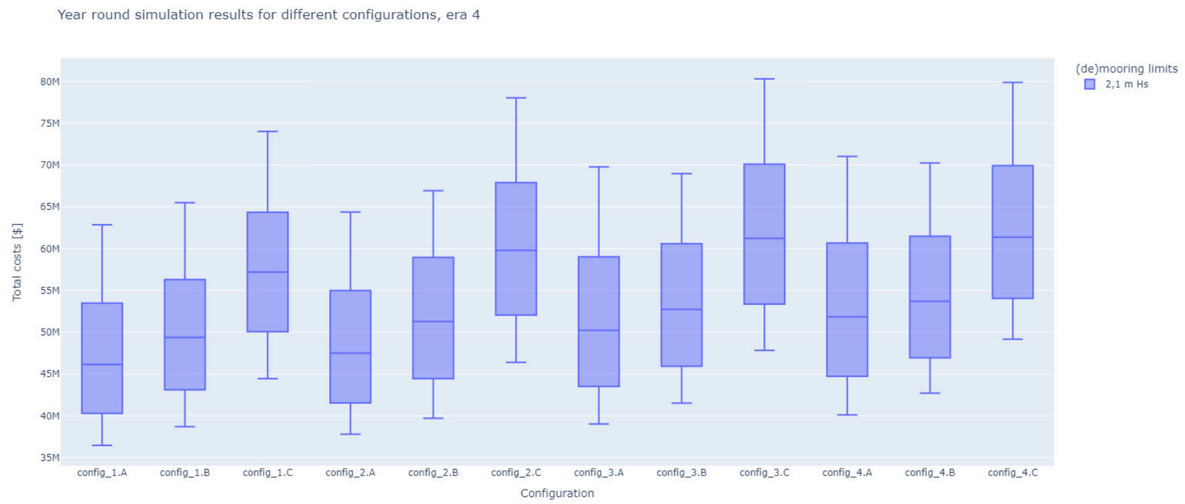

Figure P.8: Year-round costs for simulation era 4 including period dependency

P.2. Results excluding period dependency

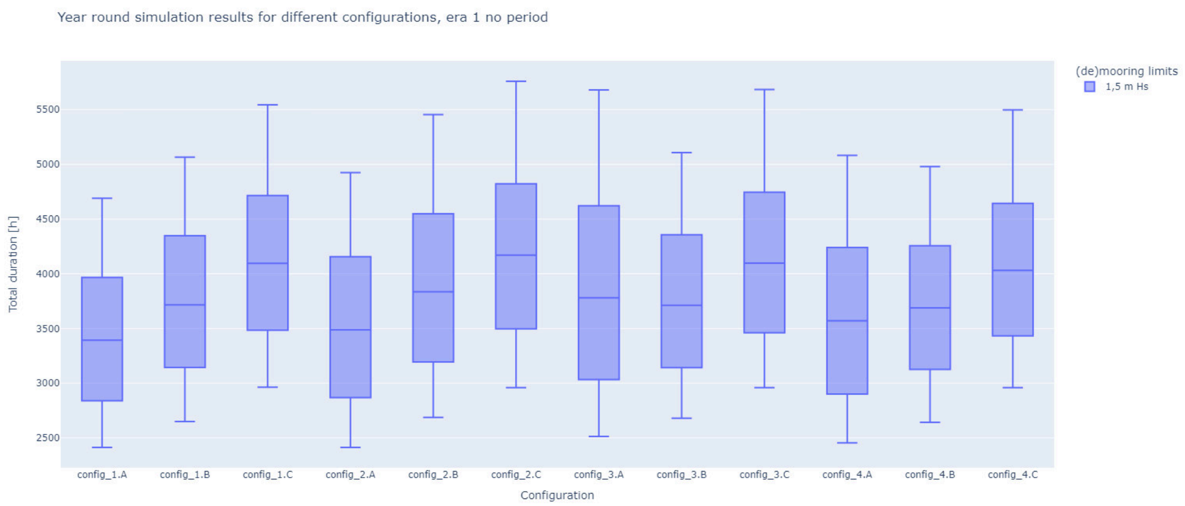

Figure P.9: Year-round duration for simulation era 1 excluding period dependency

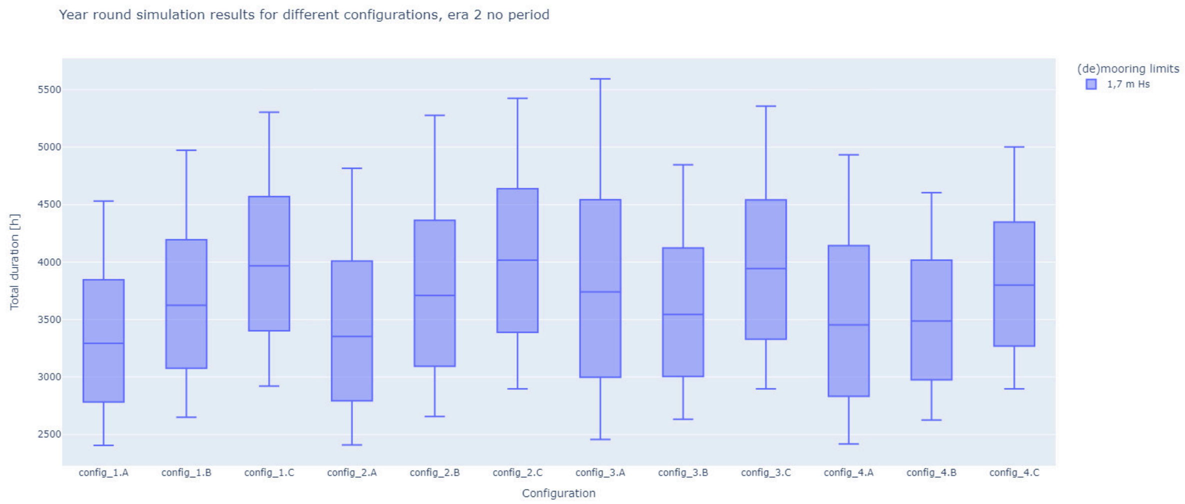

Figure P.10: Year-round duration for simulation era 2 excluding period dependency

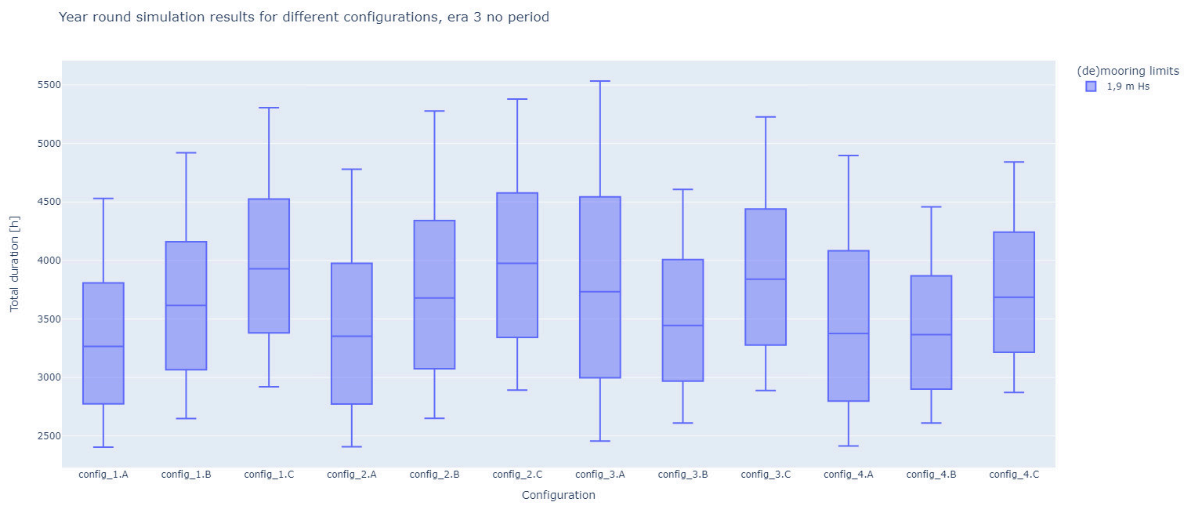

Figure P.11: Year-round duration for simulation era 3 excluding period dependency

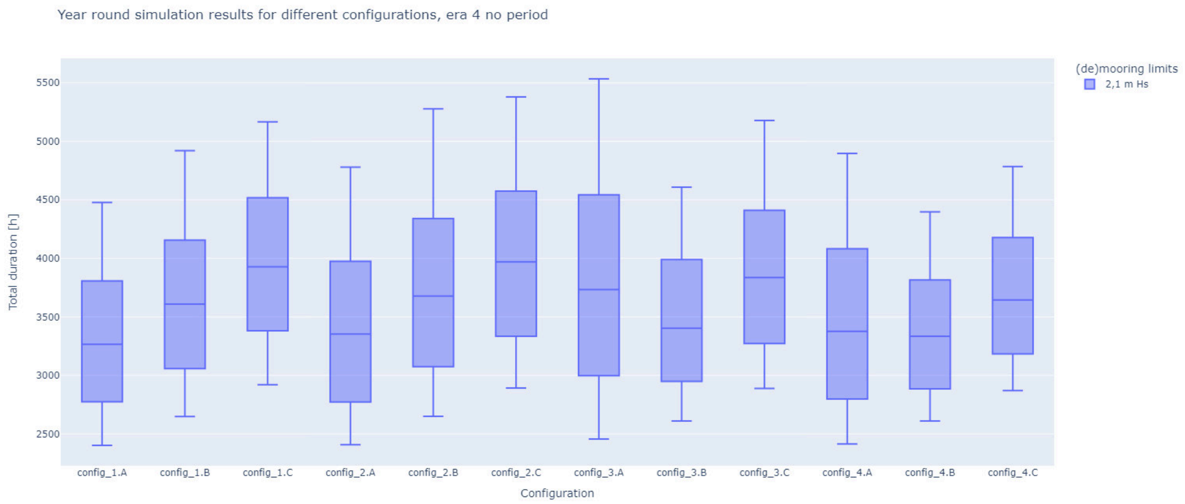

Figure P.12: Year-round duration for simulation era 4 excluding period dependency

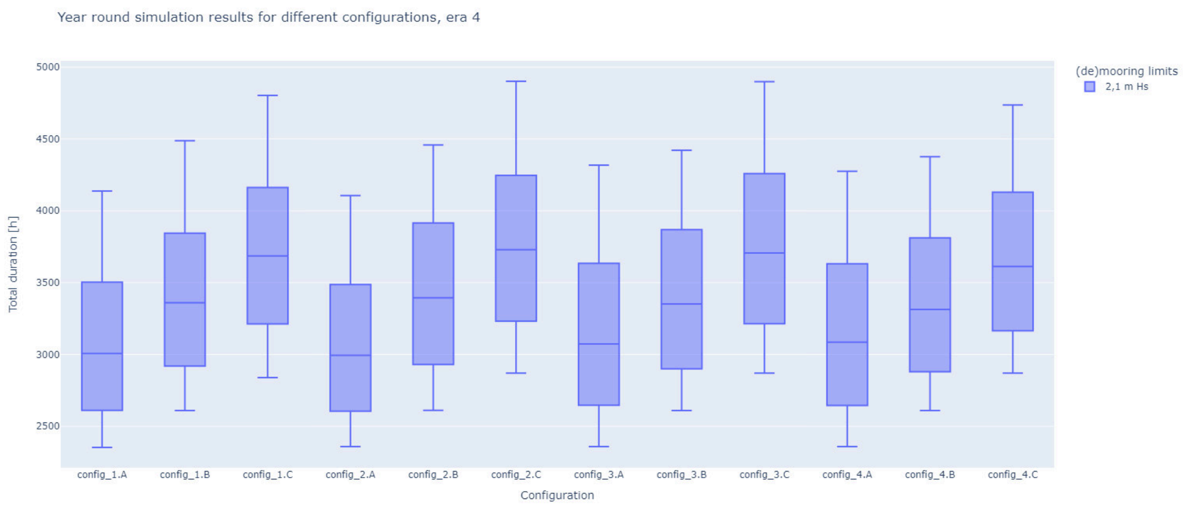

Figure P.13: Year-round costs for simulation era 1 excluding period dependency

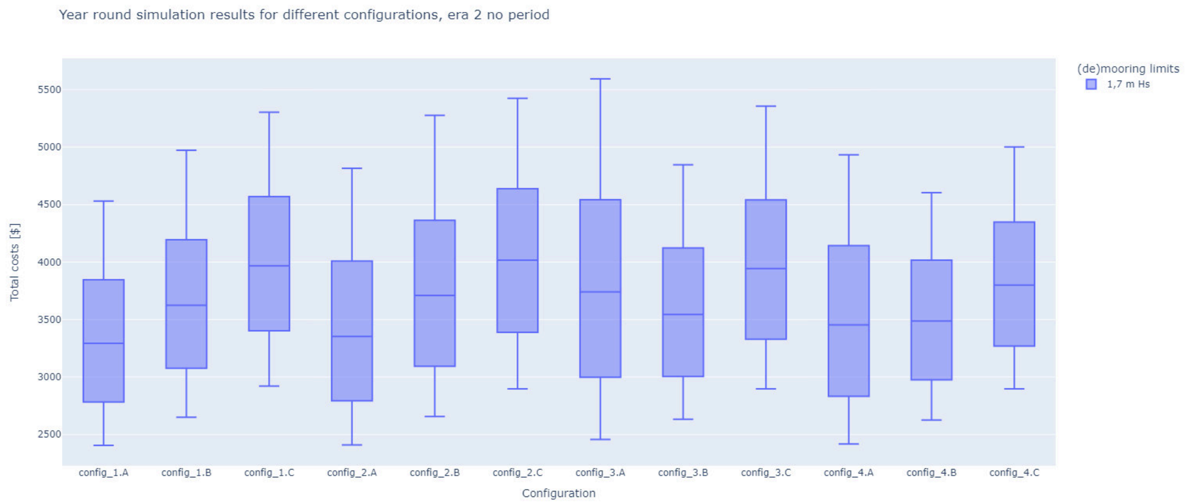

Figure P.14: Year-round costs for simulation era 2 excluding period dependency

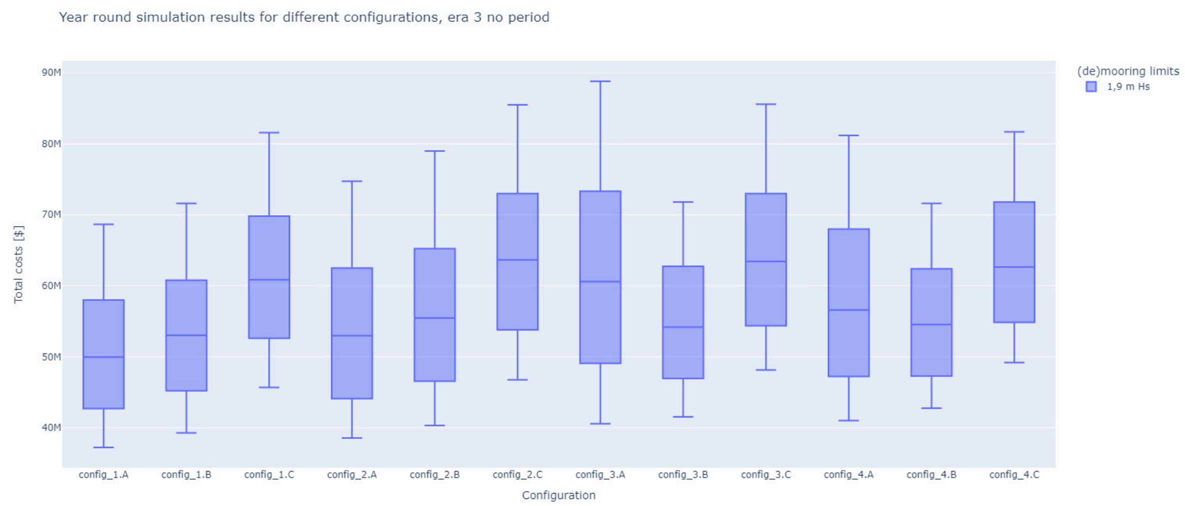

Figure P.15: Year-round costs for simulation era 3 excluding period dependency

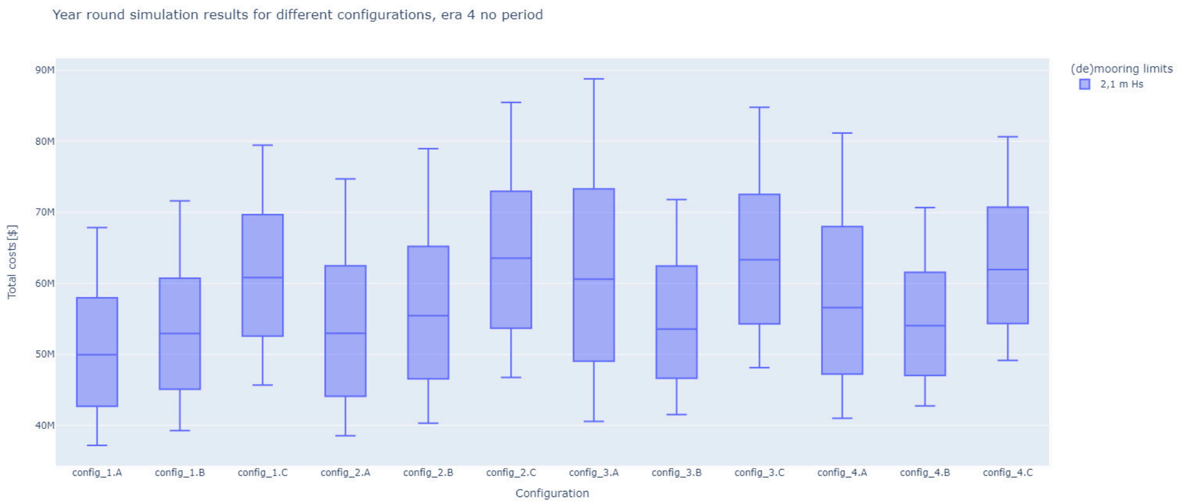

Figure P.16: Year-round costs for simulation era 4 excluding period dependency